Validation of a method for direct determination of glyphosate and AMPA in sugar beet root using hydrophilic interaction liquid chromatography and tandem mass spectrometry

Auteur : Salingros, Edouard
Promoteur(s) : Maesen, Philippe
Faculté : Gembloux Agro-Bio Tech (GxABT)
Diplôme : Master en bioingénieur : chimie et bioindustries, à finalité spécialisée
Année académique : 2019-2020
URI/URL : http://hdl.handle.net/2268.2/10188

LIÈGE université
Gembloux
Agro-Bio Tech

Validation of a method for direct determination of glyphosate and AMPA in sugar beet root using hydrophilic interaction liquid chromatography and tandem mass spectrometry.

SALINGROS EDOUARD

TRAVAIL DE FIN D'ÉTUDES PRÉSENTÉ EN VUE DE L'OBTENTION DU DIPLÔME DE MASTER BIOINGÉNIEUR EN CHIMIE ET BIO-INDUSTRIES

ANNÉE ACADÉMIQUE 2019-2020

Promoteur : Philippe MAESEN

[1] L'autorité académique est représentée par le promoteur membre du personnel enseignant de GxABT (Pr. Philippe Maesen)

LIÈGE université
Gembloux
Agro-Bio Tech

Validation of a method for direct determination of glyphosate and AMPA in sugar beet root using hydrophilic interaction liquid chromatography and tandem mass spectrometry.

SALINGROS EDOUARD

TRAVAIL DE FIN D'ÉTUDES PRÉSENTÉ EN VUE DE L'OBTENTION DU DIPLÔME DE MASTER BIOINGÉNIEUR EN CHIMIE ET BIO-INDUSTRIES

ANNÉE ACADÉMIQUE 2019-2020

Promoteur : Philippe MAESEN

Ce travail de fin d'études s'est déroulé au sein du Bureau Environnement et Analyse de Gembloux (BEAGx), Gembloux Agro-Bio Tech Passage des Déportés, 2, B-5030 Gembloux

I. Remerciements

Je remercie l'ensemble de l'équipe du Bureau Environnement et Analyse de Gembloux (BEAGx) pour leur accueil chaleureux et leur aide précieuse. Je remercie tout particulièrement Ir. Stéphanie Lorge et Pr. Philippe Maesen pour leur excellent encadrement et leur disponibilité.

II. Abstract - Résumé

Glyphosate (N-(phosphonomethyl)glycine) is the most used herbicide worldwide. It exhibits all the advantages of the perfect herbicide : it is universal in the way it targets an enzyme present in all plants as well as algae and numerous microorganisms; but not animals, making its acute toxicity very low for human and fauna, its mobility in soil has long been regarded as negligible, it is degraded by UV light (including sunlight) and bacteria commonly found in soils, it allows to limit ploughing and thus to promote soil conservation by reducing erosion; and, above all, it also has the tremendous advantage to spare genetically modified resistant crops, providing a huge financial benefits and allowing to reduce the use of other more toxic herbicides as well as the carbon footprint through reduced use of agricultural machinery.

However, the decades-long debate on its carcinogenicity has been reignited in 2015 when the International Agency for Research on Cancer classified glyphosate as "possibly carcinogenic to humans" (category 2A). The chronic effects of glyphosate and its main metabolite, aminomethylphosphonic acid (AMPA), (i.e. carcinogenicity, mutagenicity, endocrine disruptor potency...) are a real concern knowing that glyphosate is so widely used that the two contaminants, and mostly the more mobile AMPA, has been shown to reach water tables and to become ubiquitous in soils, water streams and sewage. Indeed, the molecule has been shown to be quite persistent in water and soils in a certain number of conditions of composition, weather and bacterial communities. Glyphosate metabolization in plants is vastly recognized as low or negligible, which suggest that genetically modified resistant crops might thus accumulate the herbicide until consumption. Finally, a few studies and even instances of the World Health Organization have been starting to suggest that the negative effects of glyphosate on health -through the studies of bees exposed to the herbicide- could be due to its supposed harmful effect on beneficial intestinal microbiota. All of these considerations make the accurate monitoring of glyphosate and AMPA in the environment, drinking water and food commodities a public health and environmental priority.

The routine analysis of highly polar pesticide has always been challenging in liquid chromatography since these compounds are not compatible with the QuEChERS solid phase extraction associated with reversed phase liquid chromatography, commonly used in multiresidue analysis, nor normal phase liquid chromatography. Yet many popular pesticides fall into this category, including glyphosate and its metabolite, AMPA.

So far, the methods used for quantification of glyphosate and AMPA involved a derivatization step and day-long manipulations that may be regarded as tedious. In this work was a quick, cheap and effective direct determination method for glyphosate and AMPA in sugar beet root using an Hydrophilic Interaction Liquid Chromatography (HILIC) column with a diethylamine stationary phase fit for retention and separation of highly polar anionic compounds; based on the QuPPe-PO extraction method from the European Reference Laboratories for Single Residue Methods (EURL-SRM) and validated in accordance to the requirements in force at the BEAGx and the SANTE/12682/2019 guidelines.

The chosen matrix was sugar beet root. In the E.U., as resistant GM sugar beet are not approved for cultivation, glyphosate is only used for clearing weeds before sowing. However, in the U.S., almost all cultivated sugar beets are GM glyphosate-resistant crops, treated with the herbicide up to three times during cultivation. They are allowed for importation, food and feed use in the E.U., as well as their derived products and by-products. And as European public opinion on glyphosate is deteriorating, countries are progressively removing the active substance from the shelves for domestic users while countries are debating national bans, stakeholder of the sugar industry across Europe are increasingly willing to be able to monitor glyphosate residues in their raw material, products and by-products to prevent any public health crisis or scandal that could be detrimental to their sector.

In this work, a method for the direct determination of glyphosate and AMPA in sugar beet root using a hydrophilic interaction liquid chromatography (HILIC) column with diethylamine stationary phase was successfully validated in the calibration range 0.2–3 mg/kg of sugar beet for both PMG and AMPA, noticeably below the MRL of 15 mg/kg in sugar beet. The method is expected to be adapted for the determination of other anionic polar pesticides such as glufosinate in sugar beet as well as in other matrices of plant origin with minor modifications to the sample preparation, accordingly with the QuPPe-PO method from the EURL-SRM.

The validated method does not require isotope-labelled internal standard and only takes about three to four hours to complete (homogenization of sample, preparation of mobiles phases and system priming included). One run takes only ten minutes. Excluding the cost of the common equipment and the instrumentation, the running cost of the analysis is low as it only requires a few disposable plastic tubes, syringes and syringe-filters and no specific reactants.

Unfortunately, the lockdown implemented between end of March and early May 2020 as a measure to fight the covid-19 pandemic as well as technical issues did not allow to validate methods in water and soil. However, from preliminary testing, it is considered that the quantification of glyphosate and AMPA in soil is most likely more adequate using derivatisation with FMOC-Cl and a phenyl column rather than a diethylamine HILIC column; while a reliable underivatized quantification in environmental water with the used diethylamine HILIC column and MS/MS instrumentation would require a concentration factor of at least 80–100 (using either evaporation or SPE).

****

Le glyphosate (N-(phosphonométhyl)glycine) est l'herbicide le plus utilisé au monde. Il présente tous les avantages de l'herbicide parfait : il est universel dans sa manière de cibler une enzyme présente dans tous les végétaux, les algues et de nombreux microorganismes ; mais pas les animaux, rendant sa toxicité aiguë très faible pour la faune et l'humain, sa mobilité dans les sols a longtemps été considérée négligeable, il est dégradé par la lumière ultraviolette (incluant la lumière solaire) et des bactéries communes dans les sols, il permet de limiter le labour et ainsi de favoriser la conservation des sols en réduisant l'érosion; et, par-dessus tout, il a aussi l'énorme avantage d'épargner les cultures résistantes génétiquement modifiées, fournissant un énorme avantage financier et permettant de réduire l'utilisation d'autres herbicides plus toxiques ainsi que l'empreinte carbone par la réduction de l'utilisation de machines agricoles.

Cependant, le long débat sur sa cancérogénicité a été relancé en 2015 lorsque le Centre international de recherche sur le cancer a classé le glyphosate comme "potentiellement cancérigène pour l'homme" (catégorie 2A). Les effets chroniques du glyphosate et de son principal métabolite, l'acide aminométhylphosphonique (AMPA), (c'est-à-dire sa cancérogénicité, sa mutagénicité, son potentiel en tant que perturbateur endocrinien...) sont une réelle préoccupation sachant que le glyphosate est si largement utilisé qu'il a été démontré que les deux contaminants, et surtout l'AMPA qui est plus mobile, atteignent les nappes phréatiques et deviennent omniprésents dans les sols, les cours d'eau et les eaux usées. En effet, il a été démontré que la molécule est assez persistante dans l'eau et les sols dans un certain nombre de conditions de composition, de temps et de communautés bactériennes. La métabolisation du glyphosate dans les plantes est largement reconnue comme faible ou négligeable, ce qui suggère que les cultures génétiquement modifiées résistantes pourraient ainsi accumuler l'herbicide jusqu'à leur consommation. Enfin, quelques études et même des instances de l'Organisation mondiale de la santé ont commencé à suggérer que les effets négatifs du glyphosate sur la santé - notamment à travers les études sur les abeilles exposées à l'herbicide - pourraient être dus à son effet nocif supposé sur le microbiote intestinal bénéfique. Toutes ces considérations font de la surveillance précise du glyphosate et de l'AMPA dans l'environnement, l'eau potable et les produits alimentaires une priorité de santé publique et environnementale.

L’analyse de routine de pesticides hautement polaires a toujours été difficile en chromatographie liquide compte tenu que ces composés ne sont pas compatibles avec l’extraction en phase solide QuEChERS associée à la chromatographie liquide en phase inverse, couramment utilisée en analyse multi-résidus, ni avec la chromatographie liquide en phase normale. Pourtant, de nombreux pesticides populaires font partie de cette catégorie, y compris le glyphosate et son métabolite, l’AMPA.

Jusqu’à présent, les méthodes utilisées pour la quantification du glyphosate et de l’AMPA, impliquaient une étape de dérivatisation et des manipulations durant une journée entière pouvant être considérée comme fastidieuses. L’objectif de ce travail a été de développer une méthode rapide, peu coûteuse et efficace de détermination directe du glyphosate et de l’AMPA dans la betterave sucrière en utilisant une colonne de Chromatographie Liquide d’Interaction Hydrophile (HILIC) avec une phase stationnaire diéthylamine adaptée à la rétention et à la séparation de composés anioniques hautement polaires; sur la base de la méthode d’extraction QuPPe-PO des Laboratoires Européens de Référence pour les Méthodes monorésidus (EURL-SRM) et validée au regard des exigences en vigueur au BEAGx et dans les directives SANTE/12682/2019.

La matrice choisie a été la betterave sucrière. Dans l'Union européenne, la culture de betteraves sucrières résistantes génétiquement modifiées n’est pas autorisée, le glyphosate est uniquement utilisé pour éliminer les mauvaises herbes avant les semis. Toutefois, aux États-Unis, presque toutes les betteraves sucrières cultivées sont des cultures OGM résistantes au glyphosate, traitées avec cet herbicide jusqu'à trois fois durant leur culture. L’importation, l’utilisation pour l'alimentation humaine et animale de celles-ci est autorisée dans l’U.E., ainsi que leurs produits dérivés et sous-produits. À mesure que l'opinion publique européenne sur le glyphosate se détériore, que les pays retirent progressivement la substances actives des rayons pour l’usage domestique et tandis que les pays débattent des interdictions nationales, les parties prenantes de l'industrie sucrière en Europe sont de plus en plus désireuses de pouvoir surveiller les résidus de glyphosate dans leurs matières premières et leurs produits et sous-produits afin d'éviter toute crise de santé publique ou tout scandale pouvant nuire à leur secteur.

Dans ce travail, une méthode pour la détermination directe du glyphosate et de l'AMPA dans la betterave sucrière à l'aide d'une colonne HILIC (diéthylamine) a été validée avec succès dans la plage d'étalonnage de 0,08-1 mg/L de PMG, 0,073-0,91 mg/L d'AMPA. La méthode devrait être adaptée pour la détermination d'autres pesticides polaires anioniques tels que le glufosinate dans la betterave à sucre ainsi que dans d'autres matrices d'origine végétale, avec des modifications mineures de la préparation de l'échantillon, conformément à la méthode QuPPe-PO de l'EURL-SRM.

La méthode validée ne nécessite pas d'étalon interne marqué aux isotopes et ne prend que trois à quatre heures environ (homogénéisation de l'échantillon, préparation des phases mobiles et amorçage du système inclus). Un seul passage ne prend que dix minutes. Si l'on exclut le coût de l'équipement et des instruments communs, le coût de fonctionnement de l'analyse est faible car elle ne nécessite que quelques tubes en plastique, seringues et seringues-filtres jetables et aucun réactif spécifique.

Malheureusement, le confinement mis en place entre fin mars et début mai 2020 pour lutter contre la pandémie de covid-19 ainsi que d’autres problèmes techniques n'ont pas permis de valider de méthodes dans l'eau et le sol. Toutefois, d'après des essais préliminaires, il est considéré que la quantification du glyphosate et de l’AMPA dans le sol est très probablement plus adéquate en utilisant la dérivation avec le FMOC-Cl et une colonne phényle plutôt qu'une colonne HILIC diéthylamine ; tandis qu'une quantification fiable sans dérivatisation dans une eau environnementale au moyen de la colonne HILIC diéthylamine et l'instrumentation MS/MS utilisée nécessiterait un facteur de concentration d'au moins 80-100 (en utilisant soit l'évaporation soit une SPE).

III. Table of contents

IV. List of figures

V. List of tables

VI. List of annexes

VII. List of abbreviations

ADI	Acceptable daily intake
AGES	Austrian Agency for Health and Food Safety
AMPA	Aminomethylphosphonic acid
AOEL	Acceptable operator exposure level
ARfD	Acute reference dose
CAS	Chemical Abstracts Service
CAC	Codex Alimentarius Commission
CCPR	Codex Committee on Pesticide Residues
DAHP	3-deoxy-D-arabinoheptulosonate 7-phosphate
DCM	Dichloromethane (CH_2Cl_2)
DHQ	3-dehydroquinate
EC	European Commission
EFSA	European Food Safety Authority
ELISA	Enzyme-Linked Immunosorbent Assay
EPA	Environment Protection Agency of United States
EPSP	5-enolpyruvylshikimate-3-phosphate
ESI(-MS)	Electrospray Ionisation (Mass Spectrometry)
EURL	European Union Reference Laboratory
FA	Formic acid (CHOOH)
FAO	Food and Agriculture Organization of the United Nations
FASFC	Federal Agency for the Safety of the Food Chain (Belgium) ("AFSCA" in French)
FDA	Food and Drug Administration of United States
FMOC-Cl	9-fluorenylmethylchloroformate chloride ($C_{15}H_{11}ClO_2$)
GC	Gas Chromatography
GLP	Good Laboratory Practices
GM(O)	Genetically Modified (Organism)
GOX	Glyphosate Oxidoreductase
HILIC	Hydrophilic interaction liquid chromatography
HPLC	High Performance Liquid Chromatography
CI	Confidence interval
IPCS	International Programme on Chemical Safety
IR	Infra-red
ISAAA	International Service for the Acquisition of Agro-Biotech Applications
ISP	Scientific Institute of Public Health (Belgium)
IUPAC	International Union of Pure and Applied Chemistry
JMPR	Joint WHO/FAO Meeting on Pesticide Residues
LC	Liquid chromatography
LIB	Laboratory Information Bulletin
(L)LOD	(Lower) Limit on detection
LOQ	Limit on quantification
MeOH	Methanol (
MRL	Maximum Residue Level
MRM	Multiple Reaction Monitoring
MS	Mass Spectrometry (or Spectrometer)
N-Ac-PMG	N-acetyl-glyphosate
N-Ac-AMPA	N-acetyl-AMPA
NEMI	National Environment Method Index
NHL	Non-Hodgkin lymphoma
PEP	Phosphoenolpyruvate
PPP	Plant protection product
RSD	Relative standard deviation
S3P	Shikimate-3-phosphate
SE	Standard error
SPE	Solid phase extraction
SRM	Single residue method
SS	Sum of squares
NEMI	National Environment Method Index
NWQMC	National Water-Quality Monitoring Council
POE-tallowamine	Polyethoxylated-tallowamine
PPP	Plant Protection Product ; European official name for pesticides
UHPLC	Ultra High Performance Liquid Chromatography
UPLC	Ultra Performance Liquid Chromatography (Waters Corporation trademark)
UV	Ultraviolet
WHO	World Health Organization of the United Nations

1. Glyphosate, or N-(phosphonomethyl)glycine

1.1. Physico-chemical description of PMG and AMPA

Glyphosate (IUPAC name : N-(phosphonomethyl)glycine) (PMG) is a synthetic phosphonomethyl derivative of the amino acid glycine. The compound has a molar mass of 169,07 g/mol and has been introduces as an herbicide active substance in 1974 by Monsanto company. It is also applied prior to the harvest to accelerate plant ripening. Its empirical formula is $C_3H_8NO_5P$ and its CAS number is 1071-83-6.

PMG is a white non-volatile solid with a Henry's law constant of 10^{-12} $Pa.m^3.mol^{-1}$ and a vapor pressure under 10^{-8} kPa at 20 °C (Wollerton and Husband, 1997[2,3] cited by FAO/WHO, 2005[4]). It is heat-stable and decomposes above 200 °C (473 K) (Wollerton and Husband, 1997[2,3] cited by FAO/WHO, 2005[4]). The molecule is stable under sterile conditions and in absence of UV light, at pH 5, 7 and 9 (Wollerton and Husband, 1997[2,3] cited by FAO/WHO, 2005[4]).

The polar organophosphorus compound has three acidic ionizable sites : two on the phosphonic acid moiety (pK_{a0} and pK_{a2}) plus one on the carboxylic acid moiety (pK_{a1}) and one ionizable amine (pK_{a3}). The values of the $pK_{a0,1,2,3}$ are respectively ~0.8, 2.6, 6 and 10.6 (Annex 1) (Figure 2). PMG is thus both amphoteric and zwitterionic between pH 1 and 10.6.

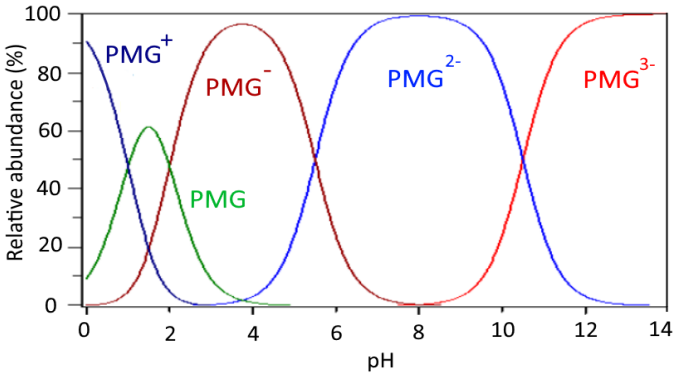

Figure 2 : Relative abundance of PMG ionization states as a function of the pH
Adapted from Kudzin *et al.* (2019).

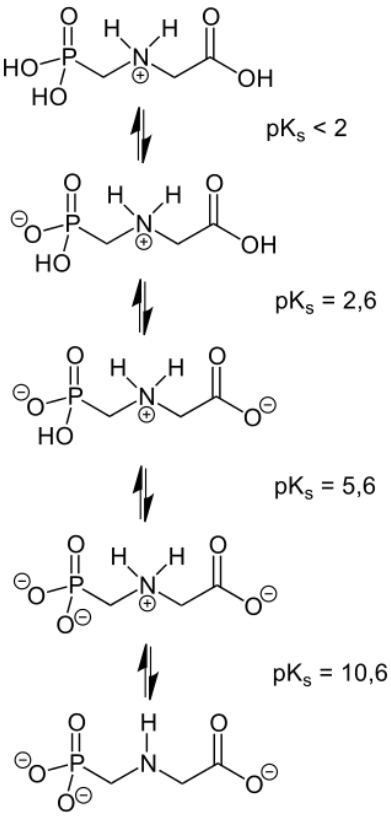

Figure 1 : Ionization states of PMG.
Source : Jü (2011)[5]

PMG solubility in water at ambient temperature ranges from 10,5 g/L (approximately 0.06 M) at pH 1.9 to 157 g/L (approximately 0.92 M) at pH 7.0 (MacBean, 2012[6]). Because of its high polarity, PMG has low solubility in organic solvents (Annex 2) and its reported logarithm of its octanol-water partition coefficient (logP or $logK_{ow}$) values are -1.3 at 20°C (Wollerton and Husband, 1997[2,3] cited by FAO, 2005[4]), -2.8 at 20°C (IPCS 1994) and -3,2 to -3,4 (Sangster, 2006[7] ; Monsanto unpublished

[2] Wollerton C. and Husband R. 1997. Glyphosate acid: Physical and Chemical Properties of Pure Material. Zeneca Agrochemicals, Report RJ2400B. Unpublished.

[3] Wollerton C. and Husband R. 1997a. Glyphosate acid: Physical and Chemical Properties of Technical Material. Zeneca Agrochemicals, Report RJ2401B. Unpublished.

[4] http://www.fao.org/fileadmin/templates/agphome/documents/Pests_Pesticides/JMPR/Evaluation05/2005_Glyphosate1.pdf (27/01/2020)

[5] https://commons.wikimedia.org/wiki/File:Glyphosate_Dissociation_V.1.svg (27/01/2020)

[6] MacBean C, ed; e-Pesticide Manual. 15th ed., ver. 5.1, Alton, UK: British Crop Protection Council. Glyphosate (1071-83-6) (2008-2010)

[7] Sangster J; LOGKOW Database. A databank of evaluated octanol-water partition coefficients (Log P). Available from database query at http://logkow.cisti.nrc.ca/logkow/search.html and cited by https://pubchem.ncbi.nlm.nih.gov/compound/glyphosate (27/01/2020)

study[8] cited by FAO/WHO 2016). PMG and its salts are white odorless solids at ambient temperature. In solution, PMG has many stable conformations, as predicted by Kaliannan (2002) and confirmed by Peixoto *et al.* (2015).

The solubility of PMG salts in water is higher[9] than the solubility of the acidic form. This is the reason why PMG salts are used in formulations rather than pure acidic PMG. The salts used in formulations include PMG-isopropylamine (1:1), PMG-dimethylamine (1:1), sodium PMG (1:1), potassium PMG (1:1), trimethylsulfonium PMG (or trimesium PMG), ammonium PMG (1:1) and diammonium PMG (2:1) (FAO, 2005; Travlos *et al.*, 2017).

Formulations are available in the form of water-soluble solids and liquids containing variable concentrations of (usually) one of the PMG salts listed above. Because they have different molecular mass, the concentration of PMG is expressed in acid equivalent [kg a.e./kg] (Equation 1).

$$(1)\quad Acid\ equivalent\ =\ \frac{Acid\ molecular\ weight - number\ of\ salified\ hydrogen\ atoms}{Salt\ molecular\ weight} \times 100$$

Molecular masses of commonly used PMG salts and conversion factor to acid equivalent are provided in Annex 3. All of the salts mentioned above, excepted trimethylsulfonium, sodium and diammonium salts, are approved in the EU at least until 2022 (Regulation (EU) 2017/2324). The active substance for which an application for approval renewal was made in the EU in 2019 are PMG-isopropylamine, potassium PMG, PMG-dimethylamine and ammonium PMG (1:1)[10,11]. Such products are either ready-to-use (for domestic use) or concentrate available for professional use and aimed to be diluted in large tanks and applied on crops.

Aminomethylphosphonic acid (AMPA[12]) (CAS number : 1066-51-9) is the main decomposition product of PMG through light-catalysed hydrolysis (Lund-Hoie and Friestad, 1986) and glyphosate oxidase activity from bacteria (Sviridov *et al.*, 2015; Huang *et al.*, 2017). The molar mass of AMPA is 111,04 g/mol and its acid decomposition constants are 0.9, 5.6, and 10.2 (Figure 3) (Mogusu *et al.*, 2015), close to those of PMG. AMPA is also heat-resistant and decomposes above 290 °C[13]. Its LogP is around -1.4[14]. Other physical characteristics such as vapor pressure and solubility in common solvents were not retrieved in literature but are expected to be low, similarly to those of PMG.

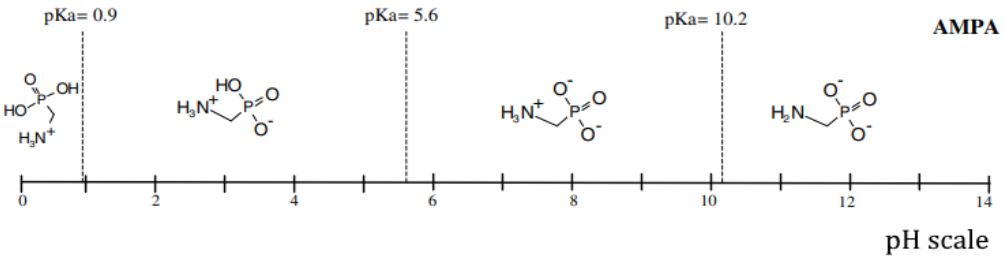

Figure 3 : Ionization states of AMPA as a function of pH.
Source : Mogusu *et al.* (2015)

[8] Octanol/water partition coefficient of Glyphosate and MON 7200. Monsanto Company report no MSL-7241 (amended). GLP, not published

[9] > 1000 g/L for PMG trimesium (MacBean 2012). Solubility data for other salts could not be retrieved in literature. Generally, studies concerning the physicochemical properties of these molecules are carried by the manufacturers and are not published.

[10] https://glyphosate.eu/app/themes/glyphosate/dist/images/pdfs/application-renewal_c7075154.pdf (29/02/2020)

[11] https://glyphosate.eu/app/themes/glyphosate/dist/images/pdfs/application-renewal-20_205f8b2e.pdf (29/02/2020)

[12] The degradation product from PMG commonly called AMPA, should not be confounded with the glutamate ionotropic transmembrane synaptic receptor also shortened by the acronym "AMPA" and belonging to the central nervous system.

[13] http://www.chemspider.com (27/01/2020)

[14] http://www.chemspider.com/Chemical-Structure.13399.html (27/01/2020)

1.2. Industrial production

The two main industrial processes commonly used for PMG synthesis are the glycine-dimethylphosphite (DMP) process (Figure 4) and the iminodiacetic acid (IDA) process (Woodburn, 2000). The two processes leads to the production of an acidic liquor containing ~1.5–2.0 % (w/w) PMG, ~4.5–15.0 % (w/w) NaCl, ~35 % of other organic compounds and ~38–40 % water (Luo *et al*., 2009; Wang *et al*., 2015). Main identified by-products are formaldehyde (2–4 %), formic acid (1–2 %), methyl glyphosate (0.1–0.2 %), AMPA (0.1–0.2 %) and N-phosphonomethyl aminodiacetic acid (0.2–0.3 %) (Xie and Xu, 2010 ; Zhang *et al*., 2011 cited by Shen *et al*., 2014). Formaldehyde and N-nitroso-glyphosate were identified by FAO (2016) as impurities of toxicological concern that should not exceed 1.3 g/kg and 1 mg/kg of technical grade PMG, respectively. In the EU, the minimum purity for PMG used in formulations is 950 g/kg and the tolerated content of formaldehyde and N-nitroso-glyphosate are 1 g/kg and 1 mg/kg respectively (Regulation (EU) 2017/2324).

The obtained acidic liquor is neutralized to pH 1.5–2 with sodium hydroxide (NaOH) in order to obtain conditions of maximum crystallization of PMG (one acidic site ionized) (Woodburn, 2000). Impurities in the remaining waste water can be treated by advanced oxidation, photocatalysis, precipitation or adsorption (Wang *et al*., 2015).

Many articles in literature propose purification techniques of PMG alternatively to neutralization of the acidic liquor, such as diffusion dialysis (Wang *et al*., 2015) (Figure 4), ; or techniques for improved treatment and recovery from waste water resulting from crystallization, such as electro-driven and pressure-driven membrane separation (Shen *et al*., 2014), three-compartment bipolar membrane electrodialysis (Shen *et al*., 2013), interval washing-nanofiltration, direct nanofiltration, diafiltration and dilute-diafiltration (Xie and Xu, 2010).

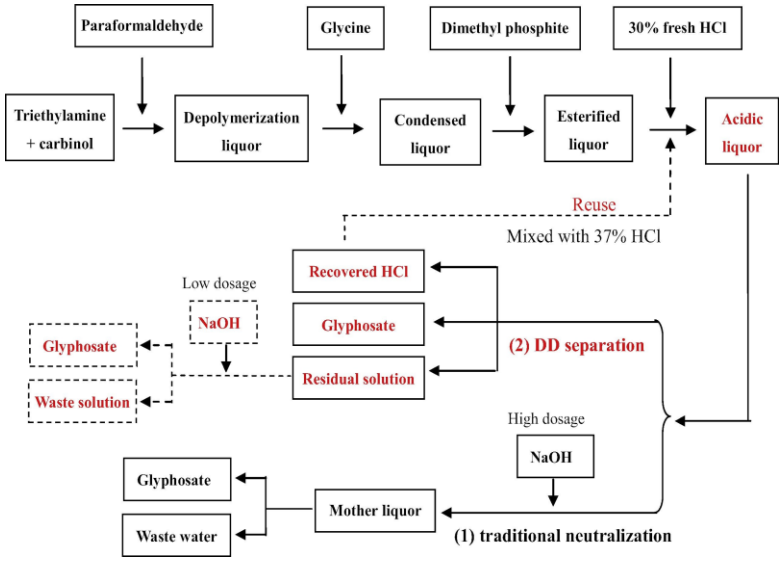

Figure 4 : Flow-chart of the glycine-dimethylphosphite (DMP) process for PMG production. Source : Wang *et al*. (2015)

1.3. Retention, uptake and translocation of PMG in plants.

When formulations are applied on plants, PMG is absorbed through foliage (carbon sources) and is then transported in the phloem to reach all parts of the plant (systemic distribution), accumulating particularly in intense cell division zones such as meristems and storage tissues (sinks) (Sprankle *et al*., 1973, cited by Dill *et al*., 2010). Effectiveness of PMG is thus maximal between sprouting and budding stages. To this regard, PMG is called a post-emergence herbicide, as opposed to pre-emergence herbicides that prevents germination.

Metabolization of PMG in non-resistant plants is low to negligible, with aminomethylphosphonic acid (AMPA) being the only significative metabolite (Duke, 2011; Feng *et al*., 2000; FAO/WHO, 1998). Measured AMPA residues in plant tissue may, at least partially, also come from surface photolysis of PMG outside of the plant and subsequent penetration rather than metabolization inside the plant (Lund-Hoie and Friestad, 1986).

Aside from its toxic chemical mechanism, effectiveness of an herbicide active substance relies on three characteristics of the formulation : spray retention on the leaves (i.e. the part of pesticide effectively landing on the leaves of the plant (foliar interception) that remains after any loss from runoff or rebound), absorption (or uptake) inside the tissues and translocation in the plant. One accurate manner to measure them is by application of a formulation spiked with isotope-labelled analog of the active substance and then by quantifying this analog (and its degradation products) in the washed tissues (leaves and roots) and the washing solution (Feng *et al*., 2000 ; Dill *et al*., 2010).

Many factors affect the uptake of herbicide active substances in plants : droplet size and spread, cuticle thickness and composition, adjuvants, humidity, active substance concentration etc. (Dill *et al*., 2010).

Adjuvants in herbicide formulations (and pesticides in general) include surfactants, stickers, extenders, activators, compatibility agents, buffers and acidifiers, deposition aids, de-foaming agents, thickeners, and dyes (Dill *et al*., 2010). The purposes of adjuvants are to facilitate and/or secure the use of herbicides, enhance their efficiency and stability or for esthetic purpose (dyes) (Dill *et al*., 2010). The functionally most important adjuvants are surfactants as they allow permeation of polar active substances through otherwise impermeable cuticles containing various contents of cutin, cutan and waxes (Nip *et al*., 1986 ; Heredia 2003 ; Hess and Foy, 2000).

Feng *et al*. (2003) showed that bigger droplets induced more PMG absorption in the leaf tissues. Indeed, it was confirmed that bigger droplets, with higher total surfactant content, induced higher levels of pycnosis and cytolysis in vascular, epidermal and mesophyll cells of velvetleaf plants, thus creating breaches facilitating PMG diffusion in the apoplasm (Ryerse *et al*., 2004). From the apoplasm, PMG is passively loaded in the phloem (symplasm), contrary to carbon assimilates that are actively loaded through companion cells, and then further transported passively along with carbon assimilates towards sink tissues (Gougler and Geiger, 1981, cited by Dill *et al*., 2010).

Although bigger droplets allows a better absorption, they are unfavourable for PMG translocation because too high levels of cell damage disrupt the active loading of carbon assimilates in the phloem, subsequently disrupting the flow rate and hampering PMG translocation (Feng *et al*. 1999, 2000 ; Nobel, 2009 ; Ryerse *et al*., 2004). Translocation of PMG is also impeded proportionally to photosynthesis inhibition caused by its own inhibiting effect once it reaches sink tissues (Geiger *et al*., 1986 ; Geiger and Bestman, 1990 cited by Dill *et al*., 2010).

Travlos *et al* (2017) provided a review of the effect of the different salts and adjuvants on their overall efficiency in PMG formulations. Their conclusion was that the effects of salts and adjuvants were species-dependent and that clear conclusions were tricky to draw, as environmental conditions are variable. Ammonium sulphate was however revealed to be a key component in formulations as it increases efficiency in a majority of weed species (Turner *et al*., 1980; Travlos *et al*., 2017).

No study comparing retention, adsorption and translocation of PMG on a wide range of taxa was found. The relevance of comparing different studies is arguable since many environmental factors involved in spray retention, absorption and translocation, such as temperature, weather (sunlight, humidity and rainfall, wind exposure...) as well as application conditions (droplet size of the spray, concentration and composition of the applied mixture, development stage at which formulation is applied...) and physiological state of the plant are either too different for pertinent comparison, not controlled or not reported at all.

The only trend that can be understandably assumed across taxa is that translocation is higher in resistant plants than in their non-resistant analog because of the absence of toxicity and the unaffected phloem flow rate (Hetherington *et al*., 1999).

1.4. Mode of action of PMG as an herbicide

Since the early 1970's, PMG has been known to interfere with the synthesis of the three aromatic amino acids (tryptophan, phenylalanine and tyrosine) in higher plants, algae, bacteria, fungus and protozoans, supporting the hypothesis that PMG targets a metabolic pathway shared by all these taxa, but not by animals (Jaworski, 1972; Gresshoff, 1979). This made PMG a broad-spectrum herbicide active substance of primary interest as it was effective to control potentially all plant species without acute side effects on animals.

It was suggested that PMG was an inhibitor of one of the three enzymes of the shikimate pathway (Figure 5) involved in the synthesis of chorismate (i.e. a key precursor of the three aromatic amino acids and other metabolites, as shown in Annex 4) from shikimate Steinrücken and Amrhein (1980). These enzymes are the shikimate kinase (EC 2.7.1.71), the 5-enolpyruvylshikimate-3-phosphate synthase (EC 2.5.1.19) (EPSP synthase) and the chorismate synthase (EC 4.2.3.5), intervening in that same order in the shikimate pathway.

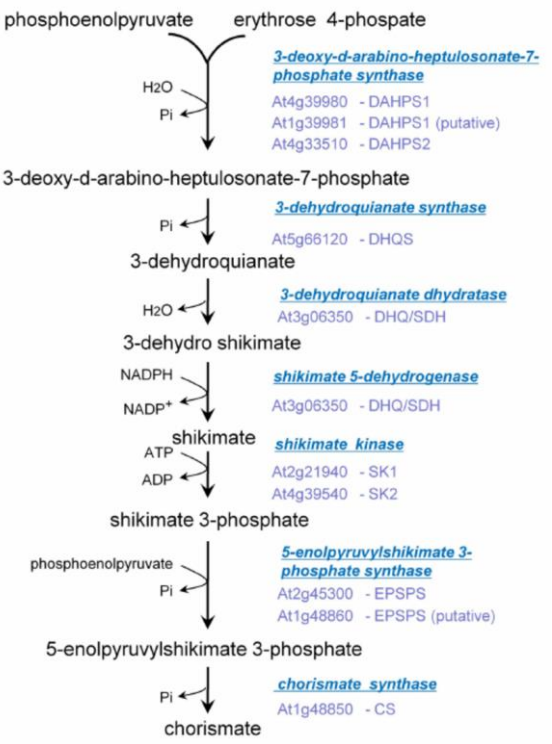

Figure 5 : The shikimate pathway.
Source : Tzin and Galili (2010)

This hypothesis was supported by many observations : the toxic effect of PMG in plant cells was alleviated by an exogenous supply of the three aromatic amino acids (Jaworski, 1972), shikimate labelled with ^{14}C was not incorporated in the three aromatic amino acids in presence of PMG in plant cells (Hollander and Amrhein, 1980; Rubin *et al.*, 1984), increasing contents of PMG were highly correlated with reduction of anthocyanins synthesis from phenylalanine in plants (Amrhein *et al.*, 1980) and accumulation of shikimate-3-phosphate (S3P) was observed in plant cells in presence of PMG (Steinrücken and Amrhein, 1980).

These results indicated that the enzyme inhibited by PMG was the 5-enolpyruvylshikimate-3-phosphate (EPSP) synthase, the enzyme yielding EPSP from S3P. When tested separately only in presence of their respective substrates and PMG, only the EPSP synthase was inhibited (Amrhein *et al.*, 1980).

The reaction inhibited by PMG is shown in Figure 6 : EPSP synthase catalyses the transfer of the enolpyruvyl group (-OC(CH_2)COOH) from phosphoenolpyruvate (PEP) to S3P to produce EPSP and inorganic phosphate (Pi) (Alibhai and Stallings , 2001).

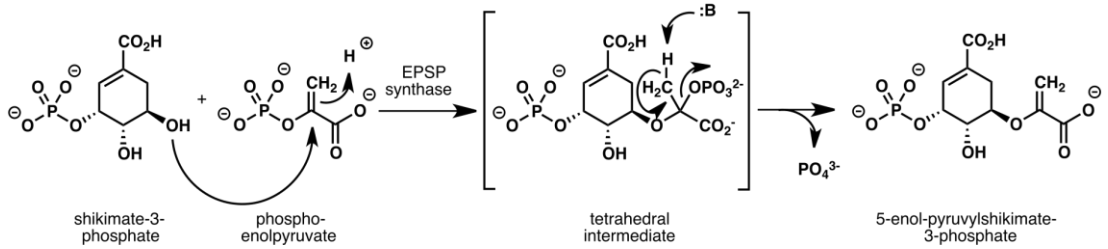

Figure 6 : Reaction inhibited by PMG.
Source : Alibhai and Stallings (2001)

Inhibition of PMG is competitive with regard to PEP (K_i around 1,2 µM) and uncompetitive with regard to shikimate-3-phosphate (K_i around 18,3 µm) (Boocock and Coggins , 1983 ; Rubin *et al.*, 1984). The reaction catalysed by EPSP synthase has a compulsory-order ternary-complex mechanism with S3P being the first substrate binded to EPSPS synthase (Figure 7) (Boocock and Coggins , 1983 ; Rubin *et al.*, 1984 ; Schönbrunn and al , 2001).

$$E + S1 \rightleftarrows E{\cdot}S1 + S2 \rightleftarrows E{\cdot}S1{\cdot}S2 \rightarrow E + P1 + P2$$
$$I \uparrow\downarrow$$
$$E{\cdot}S1{\cdot}I$$

E : EPSP synthase
S1 : S3P
S2 : PEP
I : PMG
P1 : EPSP
P2 : phosphate (P_i)

Figure 7 : Inhibition mechanism of PMG on the reaction catalyzed by EPSP synthase.

The first substrate S3P is responsible for the domain closure that brings together positively charged residues of the enzyme, which attracts the negatively charged second substrate (PEP) and the inhibitor (PMG) (Figure 8) (Schönbrunn *et al.*, 2001).

The binding sites of PEP/PMG and S3P on EPSP synthase are close, although distinct, as the binding of PMG on the enzyme·S3P complex does not alter the affinity of the enzyme for S3P. This explains the fact that PMG is uncompetitive with regards to S3P (Schönbrunn *et al.*, 2001).

This theory is consistent with the previous observation that binding of both S3P and PMG is prevented by the substitution of a residue interacting only with S3P (Shuttleworth *et al.*, 1999).

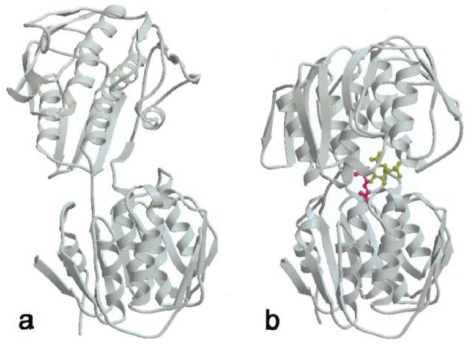

Figure 8 : Open state (a) and closed state (b) of EPSP synthase with S3P in green and PMG in magenta. Source : Schönbrunn *et al.* (2001)

So far, PMG is the only herbicide active substance known to target EPSP synthase.

Besides his inhibiting effect on EPSP synthase, PMG was also reported to have inhibiting properties on other enzymes including enzymes of the shikimate pathway such as 3-deoxy-D-arabinoheptulosonate 7-phosphate synthase (EC 2.5.1.54) (DAHP synthase) as well as 3-dehydroquinate synthase (EC 4.2.3.4) (DHQ synthase) (Boocock and Coggins , 1983) thus reinforcing his overall inhibitor capacity on the shikimate pathway.

However, the fact that these enzymes include trace metals as cofactor (cobalt for DHQ synthase and cadmium for DAHP synthase), along with the fact that the inhibiting activity on these enzymes was only observed for mM concentrations suggest that the inhibition of other enzymes than EPSP synthase is non-specific and induced by the chelation of the metallic cofactors by PMG (Boocock and Coggins , 1983).

Eker *et al.* (2006) showed that PMG efficiency was reduced when cationic content of the sprayed solution increased because of the formation of stable chelation complexes (Figure 9). Conversely, they also showed that application of PMG at 6.0 % of the recommended dose (i.e. 86,4 g a.e./ha) on sunflower (*Helianthus annuus* L.) induced severe chlorosis at shoot tips and at the base of new leaves, significant decrease in shoot and root dry matter, impaired chlorophyll production and significant reduction in iron and manganese translocation to young tissues.

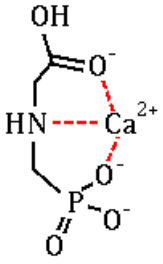

Figure 9 : Chelation complex involving PMG and Ca^{2+}.

1.5. Hormetic effect of PMG on plants

Several studies describing the hormetic effect[15] of PMG on various plant taxa at concentration between 2 and 620 g a.e./ha are reported in the review of Brito *et al*. (2017). Observed effects include increased plant growth (height, dry biomass of leaves, roots and/or shoots), seed production, chlorophyll content and photosynthesis, stomatal opening, shortened life cycle (accelerated ripening). Brito *et al*. (2017) also discuss the fact that hormesis occurs at higher concentrations in resistant plants than in non-resistant plants, possibly contributing to the natural selection of resistant weeds in agricultural environment, in addition with the decline of their non-resistant counterpart.

1.6. PMG-resistant plants and genetically modified (GM) crops in the EU

1.6.1. Genetically modified (GM) plants

Several biological mechanisms can confer PMG resistance to plants. The International Service for the Acquisition of Agro-Biotech Applications (ISAAA) provides a list[16] of all the genes commercially used to provide resistance to PMG in GM plants.

Earlier research investigated increased resistance to PMG in plants through tissue culture and yielded resistance based on overexpression of EPSP synthase (Pline-Srnic, 2006). However, this mechanism only provided limited tolerance (Pline-Srnic, 2006). Currently, two main groups of resistance mechanisms dominate the PMG-resistant GMO market :

The first consists in the introduction of a gene coding for a resistant version of the EPSP synthase. The genes aroA:CP4 (cloned from the common soil bacteria *Rhizobium radiobacter* Young & al., previously *Agrobacterium tumefaciens* Beijerinck & van Delden)), mepsps or 2mepsps belongs to this category. Such resistance is conferred by substituting certain amino acid(s) in the binding site of PEP and PMG in order to reduce the affinity of the site for PMG as much as possible while preserving affinity for PEP, the substrate.

The resistance of the majority of GM crops worldwide and in the EU[17] rely on a resistant version of EPSP synthase. As these genes only provide resistance without improving metabolization, such GM plants may be expected to accumulate PMG in sink tissues and young leaves, which are the parts that are often harvested and consumed.

The second resistance mechanism consist in the introduction of genes coding enzymes that inactivate PMG such as the goxv247 gene, originally cloned from *Ochrobactrum anthropi*, coding for the glyphosate oxidoreductase enzyme that catalyse the oxidation of PMG into AMPA and glyoxalate by converting FAD to $FADH_2$; or the gat4620 and gat4601 genes cloned from *Bacillus licheniformis* and coding for a glyphosate N-acetyltransferase enzyme that catalyse the acetylation of PMG on the amine moiety of the molecule (Figure 10).

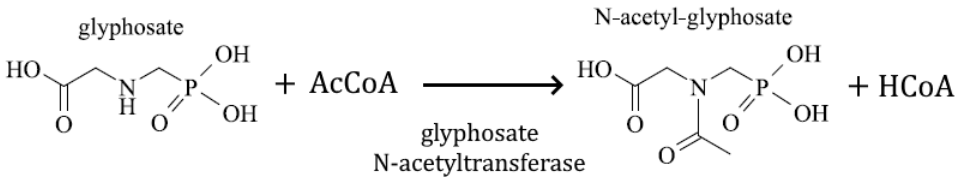

Figure 10 : N-acetylation of PMG by glyphosate N-acetyltransferase (GAT).

[15] a phenomenon in which a substance exhibits adverse effects above a threshold dose and positive effects under this threshold dose

[16] https://www.isaaa.org/gmapprovaldatabase/geneslist/default.asp (30/01/2020)

[17] https://www.isaaa.org/gmapprovaldatabase/approvedeventsin/default.asp?CountryID=EU&Country=European%20Union (29/01/2020)

The two mechanisms are often associated in commercially available GM PMG-resistant crops. By the end of January 2020, the ISAAA listed 221 approved PMG-resistant GM varieties approved in at least one country[18,19], and a total of 100 GM non-ornamental agricultural varieties approved in the EU[20], mainly PMG- and glufosinate-resistant organisms. Three GM sugar beets (*Beta vulgaris* L. subsp. *vulgaris*) varieties are available on the world market : two PMG-resistant (H7-1 and GTSB77) and one glufosinate-resistant (T120-7). The countries where these varieties are approved for cultivation, food and/or feed is provided in Annex 5. Only the GM sugar beet H7-1 KM-ØØØH71-4 [KWS SAAT and Monsanto] with a CP4 resistant EPSP synthase is approved for importation and use in food and feed in the EU with the backing of the EFSA[21] (EFSA, 2006) at least until 2028, but not for cultivation. Allowance is granted for sucrose and by-products from this GM organism as well. In the US, resistant GM sugar beets accounts for 95–100 % of the production of sugar beet (Barker *et al*., 2019).

1.6.2. Naturally arising resistance in weeds

The arising of PMG-resistant weed was first considered unlikely because of the complexity of genetic manipulations required to artificially achieve resistance (Bradshaw *et al*., 1997). However, the first PMG-resistant weeds appeared as soon as 1996 (Heap and Duke, 2017). In February 2020, 48 weed species resistant to PMG were listed the International Survey of Herbicide Resistant Weeds[22]. Several mechanisms have been identified in resistant weeds such as modified leaf angle reducing foliar interception of spray and PMG absorption, reduced translocation of PMG because of vacuole sequestration in the leaves thanks to transporter surexpression, or increased metabolization and increased carbon flow in the shikimate pathway (Sammons and Gaines, 2014).

1.7. Fate of glyphosate in the environment

1.7.1. Mobility of PMG and AMPA in soils

Because of their polarity and phosphate moiety, PMG and AMPA are highly retained in soils either directly on soil particles or indirectly by the mediation of the hydration sphere.

Adsorption of PMG in soils is mainly related to aluminium(III) (oxides, amorphous silicates and edges of clay silicates) and iron (iron(II and III) oxalates and iron(III) oxide-hydroxides) content (Sprankle *et al*., 1975; Piccolo *et al*.,1994), humic substance composition and content (Piccolo and Celano, 1994; Piccolo *et al*., 1996), phosphate ions content (Sprankle *et al*., 1975; Sidoli *et al*., 2016) and pH_{CaCl2} (Sidoli *et al*., 2016). Divalent cations content also influence PMG adsorption at low PMG concentrations (Piccolo *et al*.,1994). Conclusions regarding clay minerals content are sometimes contradictory : Sidoli *et al*., 2016 found no correlation while other studies (Sprankle *et al*., 1975; Piccolo *et al*.,1994) did .

Similarly to phosphates, PMG and AMPA are strongly adsorbed on aluminium hydroxides and iron oxide-hydroxides via their phosphate moiety to form mono or di-functionally bonded inner sphere complexes (Figures 11 and 12) (McBride, 1989; Borggaard *et al*., 2008).

---

18 http://www.isaaa.org/gmapprovaldatabase/gmtrait/default.asp?TraitID=2&GMTrait=Glyphosate%20herbicide%20tolerance (30/01/2020)

19 Alfalfa (*Medicago sativa*, 4 events), Argentine Canola (*Brassica napus*, 15 events), Cotton (*Gossypium hirsutum* L., 23 events),Creeping Bentgrass (*Agrostis stolonifera*, 1 event), Maize (*Zea mays* L., 145 events), Polish canola (*Brassica rapa*, 3 events), Potato (*Solanum tuberosum* L., 4 events), Soybean (*Glycine max* L., 23 events), Sugar Beet (*Beta vulgaris*, 3 events) and Wheat (*Triticum aestivum*, 1 event)

20 http://www.isaaa.org/gmapprovaldatabase/approvedeventsin/default.asp?CountryID=EU&Country=European%20Union (30/01/2020)

21 EFSA states that, beside the presence of the EPSP synthase CP4, the H7-1 GM sugar beet "showed no marked alterations in composition, agronomy and phenotype compared with the control lines and reference lines. The GMO Panel therefore concludes that sugar beet H7-1 is compositionally and phenotypically equivalent to non-genetically modified sugar beet, except for the trait that has been introduced." (EFSA, 2006)

22 http://weedscience.org/summary/moa.aspx?MOAID=12 (02/02/2020)

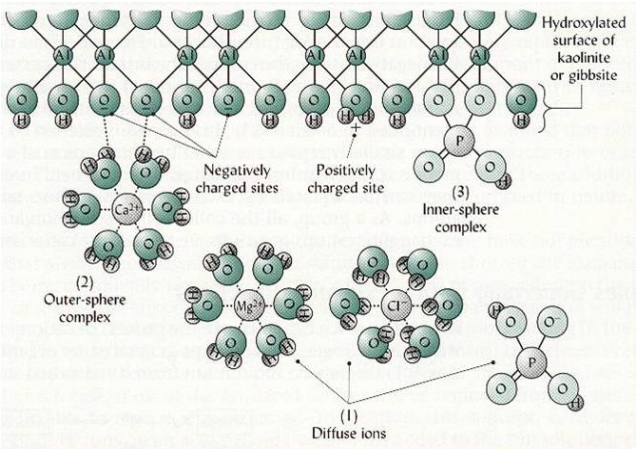

Figure 11 : Adsorption of ions on clay minerals at molecular scale. Source : Brady and Weil (2008)

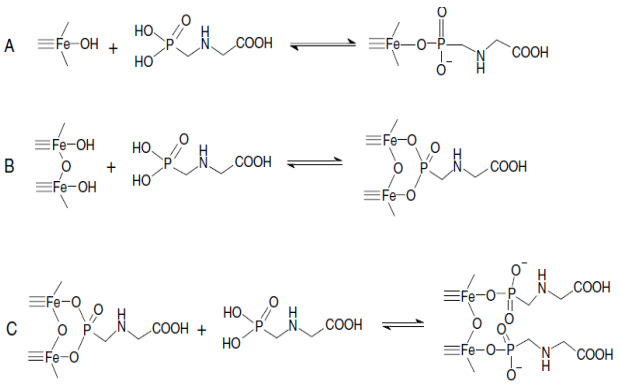

Figure 12 : Putative reactions schemes between PMG and iron hydroxides. Source : Borgaard *et al.* (2008)

Adsorption of PMG on clay minerals is also mediated by interactions with divalent cations involved in outer-sphere complexes (Figure 11), through hydrogen bonding of PMG with water molecules in the hydration sphere of the divalent cations (McBride, 1989). This type of interaction occurs especially in soils with high cation exchange capacity such as 2:1 swelling clay minerals like vermiculite. Such retention mechanism of PMG can be seen as an indirect ion-exchange mechanism in which PMG interacts with the counterion (the cation) and is desorbed along with these cations when the pH increases (Miles and Moye, 1988).

Piccolo *et al*. (1994) showed that, at low concentration, PMG principally interacts with exchangeable divalent cations adsorbed on clay exchange sites; while at higher concentrations, it interacts predominantly with aluminium hydroxides and iron oxide-hydroxides. They also observed that desorption of PMG adsorbed on divalent cations was possible at a concentration of 0.01 M $CaCl_2$, whereas desorption of PMG in outer-sphere complex required higher phosphate concentration. This behavior is most likely attributable to outer-sphere complexes requiring the overcoming of a lower chemical potential barrier than inner-sphere complexes, the first leading to a less stable adsorption than the last.

It was also shown that the addition of copper II ions, a metal known to be readily chelated, resulted in a reduced adsorption and increased desorption of PMG in soils, contrary to calcium and magnesium cations, presumably because interaction with more readily chelated cations in solution resulted in chelation complex rather than outer-sphere complex, preventing adsorption on soil particles (Morillo and Maqueda, 1997).

Adsorption of PMG was shown to be even stronger on humic substances than clay minerals. Piccolo *et al*. (1996) evaluated PMG adsorption on humic substances extracted from peat, volcanic soils, oxidised coal and lignite. They found that the adsorption capacity was more correlated to the molecular size and aliphaticity of the humic substance rather than the abundance of acid groups. The ash content of all humic substances being below 5 %, the immobilisation of PMG on mineral species was not likely to account significantly for the high adsorption capacity measured.

Piccolo and Celano (1994) showed through IR spectroscopy that hydrogen bondings settles between PMG and soluble humic acids via the phosphate moiety, at pH 4 and under. They speculated that this interaction could likely be partly responsible for PMG desorption and leaching, notably because of roots exudates.

Results on PMG and AMPA mobility in literature are very diverse. On the one hand, artificial rainfall experiments showed that 72 % of the applied PMG was retained between 0 and 2 cm depth and less than 0.24 % leached under 15 cm in clay loam, silty clay loam and silty loam soils (Rampazzo *et al*., 2013; Yang *et al*., 2015; Okada *et al*., 2016).

On the other hand, field studies demonstrated that PMG and AMPA leaching is under-estimated with normal rainfall simulations. Indeed, Mamy *et al*. (2008) found AMPA in a clay-loam calcareous Cambisol up to 60–90 cm deep, 192 days after treatment. Similarly, in each of the three consecutive annual lysimeter experiments they carried, Napoli *et al*. (2015) recovered PMG and AMPA at 0.2 % and 0.58 % respectively of the applied concentration, up to 80 cm depth in vineyard silty clay soils. Preferential flows during heavy rainfall and roots exudates are expected to be major contributing factors to PMG and AMPA infiltration in deep layers of the soil (Borgaard and Gimsing, 2008; Mamy *et al*., 2008; Napoli *et al*., 2015).

These results indicate that AMPA is more readily leached than PMG in common soils. However, exceptions should exist as well, as pointed out by Candela *et al*. (2010) who detected PMG up to 1.9 m deep in eroded granite soils with low organic matter content.

One common way to characterise adsorption of a compound in soil is by calculating the coefficients of the empirical Freundlich adsorption equation, describing the adsorption isotherm at a given pressure and temperature (equation 1).

$$(1) \qquad x/m = K_f \, c^{1/n}$$

x/m : adsorbate mass (adsorbed solute) per mass unit of adsorbent
c : concentration of adsorbate in solution at equilibrium.
K : constants characteristic of a couple of adsorbate and adsorbent at a given temperature [mg kg^{-1} (mg L^{-1})$^{-1/n}$]
n : coefficient greater than 1 and characteristic of a couple of adsorbate and adsorbent at a given temperature

The higher the K_f coefficients, the more retained is the considered compound. The 1/n exponent describes how close to saturation is the adsorbent : at high solution concentration, the mass of adsorbate per gram of adsorbent becomes constant and independent of concentration, so 1/n = 1. Conversely, when the concentration is very low, adsorption sites are in great majority free for interactions and adsorption is directly proportional to concentration. Some Freundlich K and n coefficients reported in literature for PMG and AMPA are given in Annex 6. It must be noted that comparison of K values is pointless if 1/n values are not the same (or close). Furthermore, two isotherms can look very similar with different K and 1/n values (Sidoli *et al*., 2016).

Sidoli *et al*. (2016) measured a marked difference in average 1/n values between PMG (0.93 ± 0.06) and AMPA (0.78 ± 0.03). This indicates that despite PMG and AMPA having similar structures, they do not sorb exactly the same way (Sidoli *et al*., 2016). This is presumably related to the fact that between pH 5.4 and 7, AMPA and phosphates ions both have one negative charge (-1), while PMG has two (-2) (i.e. one on the phosphate group and one on the carboxylic group) (Sidoli *et al*., 2016).

Sidoli *et al*. (2016) proposed a non-linear model for prediction of the Freundlich K_f constant of PMG and AMPA with a R^2 of 0.94 and 0.92 respectively. This model is comprised of four variables, tested for independence, which were in order of increasing correlation : pH_{CaCl2}[23], available phosphate[24], amorphous aluminium amount and iron oxide amount (Table 1). Strangely Sidoli *et al*. (2016) claimed that no correlation with organic carbon or clay content was found, contrary to the literature they mention and studies cited above.

[23] The pH of the solution measured after dissolution of calcium chloride ($CaCl_2$) 0.01M.

[24] Determined with the Olsen P method with respect to the ISO 11263:1994.

> "This method estimates the relative bioavailability of inorganic ortho-phosphate (PO_4-P) in soils with neutral to alkaline pH. It is not appropriate for soils which are mild to strongly acidic (pH <6.5). The method is based on the extraction of phosphate from the soil by 0.5 N sodium bicarbonate solution adjusted to pH 8.5. In the process of extraction, hydroxide and bicarbonate competitively desorb phosphate from soil particles and secondary absorption is minimized because of high pH. The orthophosphate ion reacts with ammonium molybdate and antimony potassium tartrate under acidic conditions to form a complex. This complex is reduced with ascorbic acid to form a blue complex which absorbs light at 880 nm. The absorbance is proportional to the concentration of orthophosphate in the sample. The method has shown to be well correlated to crop response to phosphorus fertilization on neutral to alkaline soils. The method has a detection limit of 1.0 ppm (soil basis)."
> Source : https://anlab.ucdavis.edu/analysis/Soils/340 (07/05/2020)

Table 1 : Correlation between observed K_f and measured soil variables. Source : Sidoli *et al*. (2016)

Variables	Correlation coefficient with K_f		Explanation of Sidoli *et al*. (2016)
	PMG	AMPA	
pH_{CaCl2}	-0.83	-0.82	When the pH increases, repulsions between PMG and AMPA increase as their average negative charge also increases.
Available phosphate content[25]	-0.36	-0.67	Available phosphate competes with PMG and AMPA, for adsorption sites.
Al content	0.43	0.68	Aluminium and iron oxides are potential adsorption sites.
Fe oxides content	0.05	0.10	

Sidoli *et al*. (2016) could not validate their model using data from other types of soils because they did not find any study gathering data on the four variables of the model. Furthermore, the performance of models including pH_{water} and pH_{KCl} instead of pH_{CaCl2} were severely reduced ($R^2 \leq 0.65$ for PMG and $R^2 \leq 0.81$ for AMPA), indicating that pH_{CaCl2} is the best indicator for PMG adsorption modelling.

According to Maqueda et al. (2017), the distribution in water sediments is mainly related to the content of iron and aluminium oxides.

1.7.2. Abiotic degradation of PMG in soils, water and sediments

Chemical degradation of PMG under sterile conditions at various pH and temperature was first reported as low or negligible in both soil and water (some half-lives are provided in Annex 7 and 8) (Sprankle *et al*., 1975 ; Rueppel *et al*., 1977; Monsanto unpublished report, 1978, cited by IPCS, 1994[26]; FAO/WHO 1986; unpublished studies cited by FAO, 2012[27,28]). However, in these earlier studies, light exposure conditions were often unclear.

Additional studies confirmed that PMG is not altered under darkness or long-waved light (such as those produced by sodium and tungsten lamps), but significant photolysis was observed under ultraviolet light (254 nm) and sunlight, yielding AMPA as the only significant degradation product (Lund-Hoie and Friestad, 1986; unpublished reports[29] addressed to the US EPA to support glyphosate registration; Assalin *et al*., 2010; Shrikant and Khambete, 2014). AMPA is much more resistant to photolysis than PMG (Lund-Hoie and Friestad, 1986).

---

[25] Measured by the Olsen P method, using a sodium bicarbonate solution.

[26] PTRL Inc. (1989) "Photodegradation of [^{14}C] glyphosate in/on soil by natural sunlight (Project No. 153W). Richmond, Kentucky, Pharmacology and Toxicology Research Laboratory, Inc (Unpublished report submitted by Monsanto Ltd)", cited by IPCS "Environmental health criteria 159 - Glyphosate" (1994) and available at https://apps.who.int/iris/bitstream/handle/10665/40044/9241571594-eng.pdf?sequence=1&isAllowed=y (13/02/2020)

[27] Study number 238500 conducted under the procedure US EPA 161-1 : "Hydrolysis determination of 14C-glyphosate (PMG) at different pH values. report no 238500. GLP, not published" cited in the FAO Specification and Evaluation for Agricultural Pesticides (2012) and available at : http://www.fao.org/fileadmin/templates/agphome/documents/Pests_Pesticides/Specs/Glyphosate_2016_02_10.pdf (13/02/2020)

[28] Study MSL-10575 conducted under the procedure US EPA 161-2 : "Photodegradation of [14C]Glyphosate in a buffered aqueous solution at pH 5, 7 and 9 by natural sunlight. Report no. MSL- 10575/PTRL 233-W-1. GLP, not published" cited in the FAO Specification and Evaluation for Agricultural Pesticides (2012) and available at : http://www.fao.org/fileadmin/templates/agphome/documents/Pests_Pesticides/Specs/Glyphosate_2016_02_10.pdf (13/02/2020)

[29] PTRL Inc. (1996) "Photodegradation of [P-methylene-^{14}C] glyphosate acid: Photodegradation in a buffered [sterile] aqueous solution at pH 5 and 7 by natural light. PTRL project No 546W. Unpublished study performed by PTRL West, Inc.; and submitted by Zeneca Ag Products, Wilmington, DE" , available at https://www3.epa.gov/pesticides/chem_search/cleared_reviews/csr_PC-417300_undated_003.pdf (13/02/2020)

Photolysis is slower in polluted water and water with sediment suspension than in clear deionized water, likely because UV light penetration in polluted water is mitigated (Lund-Hoie and Friestad, 1986 ; IPCS 1994).

PMG photolysis is catalyzed by numerous polyvalent metallic complexes, forming chelation complex with PMG, such as the naturally occuring ferrioxalate ($[Fe(C_2O_4)_2]^-$ and $[Fe(C_2O_4)_3]^{3-}$) (Chen *et al*., 2007a), Fe(III)-pyruvate, Fe(III)-citrate (Chen *et al*., 2007b), goethite and magnetite (Yang *et al*., 2018), MnIV, birnessite (containing MnIII and MnIV) (Li *et al*., 2018), titanium oxide (TiO_2) (Assalin *et al*.,2010) as well as synthetic catalytic complexes such as $BiOBr/Fe_3O_4$ (Cao *et al*., 2019) or synthetic $Fe_3O_4/SiO_2/TiO_2$ (Xu *et al*., 2011).

1.7.3. Biotic degradation of PMG in soils, water and sediments

Many aerobic and anaerobic telluric bacteria genera have been reported to be able to metabolize PMG in soils in both aerobic and anaerobic conditions, either identified taxa (Sviridov *et al*., 2015 ; Huang *et al*., 2017) and unknown taxa (Forlani *et al*., 1998) while metabolization in water was limited (Lund-Hoie and Friestad, 1986). The reviews of Sviridov *et al*. (2015) and Huang *et al*. (2017) described two main biotic degradation pathways.

The first starts with the cleavage of the C-N bond by glyphosate oxidoreductase (GP oxidoreductase or GOX in literature) (EC 1.5.3.23), consuming dioxygen and releasing AMPA and glyoxylic acid. The second starts with the hydrolysis of the C-P bond by a lyase specific to PMG (called "GP-specific C-P lyase" or "CPL" in literature), releasing phosphonic acid and sarcosine. Both pathways are shown in Figure 13.

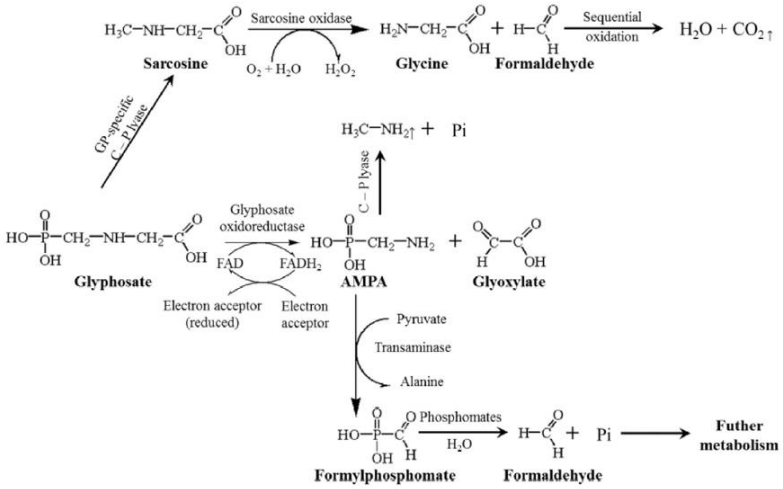

Figure 13 : Major metabolization pathways of PMG by bacteria.
Source : Huang *et al*. (2017)

The final products of these pathways are phosphonic acid, ammonium, carbon dioxide, dioxygen and formaldehyde (Szekacs and Darvas, 2012). Interestingly, Sun *et al*. (2019) detected metabolization of isotope-labelled PMG into glycine, but they did not detect sarcosine, the expected intermediate degradation product between PMG and glycine.

Considering that glycine and sarcosine have comparable half-lives, boths should have been detected. Sun *et al*. (2019) thus suggested the existence of a third pathway involving the cleavage of the C-N bound closer to phosphate moiety and directly yielding glycine and methylphosphonic acid (red path in Figure 14). Such cleavage was also observed through abiotic photolysis catalyzed by MnIV (Li *et al*., 2018).

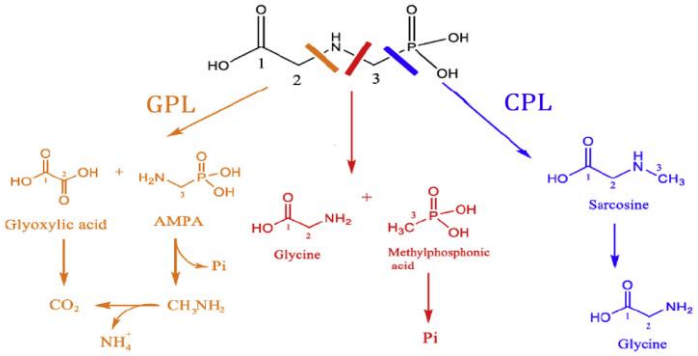

Figure 14 : Metabolization pathways of PMG by bacteria.
Source : Sun *et al*. (2019)

Beside PMG degradation, it is also known since 2004 that the inhibition of EPSP synthase by PMG can be alleviated through N-acetylation by a glyphosate N-acetyltransferase (GAT) (Figure 7) (Castle *et al*., 2004). N-acetyl-glyphosate (N-Ac-PMG) is known to be further metabolized into N-acetyl-AMPA (N-Ac-AMPA) and AMPA (FAO/WHO, 2011).

The rate of biotic degradation in soils depends on pH and temperature (Muskus *et al*., 2019), but also on PMG and AMPA bio-availability, which is decreased when they are strongly adsorbed (i.e. involved in inner-sphere complexes) (Mamy *et al*., 2008; Al-Rajab and Schiavon, 2010). Hence biodegradation of PMG and AMPA is expected to be impaired by high iron and aluminium oxides contents and favoured by higher levels of divalent cations. The influence of phosphate is both : in one hand, high phosphate levels should increase competitivity for adsorption site and bioavailability of PMG and AMPA for soil microorganisms; but on the other hand, compounds with carbon-phosphorus bonds such as PMG and AMPA are not preferential sources of phosphorus for microorganisms because they are less common and requires a specific radical-based C-P lyase to make it usable, in contrast with phosphate ions, phosphate esters and phosphate anhydride that are more easily usable with a larger range of hydrolytic, oxidative and radical based enzymes (Hove-Jensen *et al*., 2014). It seems that, overall, phosphate addition increases biodegradation of PMG (Kanissery *et al*., 2015). Al-Rajab and Schiavon (2010) estimated that the proportion of strongly adsorbed PMG (i.e. non extractable with a serie of extraction with 0.1 M KH_2PO_4) was 18.1 % right after application, 35 % after three days and stable at 30 % 22 days after application and further on sandy loam.

Mercurio *et al*. (2014) measured low metabolization in sea water Some measured half-lives for PMG in water and soil are provided in Annex 7 and 8 respectively. The half-live of AMPA has not been studied as extensively as these of PMG yet, the only estimated half-lives recovered for AMPA were 32 days in a loam soil incubated at 14.3 °C, 50 % of water-holding capacity and aerobic conditions (Simonsen *et al*., 2008); and in the range 139–173 days in an ultisol silt loam soil incubated in the rang, 60 % (w/w) of water and aerobic conditions (Sun *et al*., 2019).

1.7.4. Kinetic of PMG and AMPA dissipation in the environment

It is largely recognized in literature that AMPA is more persistent than PMG in the environment[30] (Mamy *et al*., 2008; Sun *et al*., 2019). Measured half-lives of the two molecules vary widely, depending on many biotic and abiotic factors discussed earlier (see Annex 7 and 8). Degradation of PMG follows a first order kinetic (i.e. directly proportional to its concentration) (Sun *et al*., 2019).

It is very important to notice the fact that the reported half-lives either refer to degradation or dissipation of the compound, depending on the methodology used. In water, dissipation is the sum of degradation and adsorption on solid surfaces, and is measured as the quantity of PMG that is not recovered in the water after a given period of incubation. Degradation is equal to dissipation only when adsorption on surfaces is negligible, i.e. in a plastic container that do not contain any sediment or mineral. In other words, the terminology “dissipation” does not mean “degradation” but only “not measurable anymore in the considered matrix”.

[30] Measured half-lives for AMPA were ~4–6 fold longer than for PMG in the same soil in non-sterile aerobic conditions (Simonsen *et al*., 2008; Sun *et al*., 2019).

1.7.5. Contamination of hydrological settings

With regards to the knowledge on PMG and AMPA mobility and degradation, the risk for groundwater and surface water is generally regarded as low, excepted for surface waters in certain unfavourable application conditions[31] in which surface water could be affected to a contaminated to a limited extend (Piccolo and Celano, 1994; WHO, 1997; Vereecken *et al*., 2005; Borgaard and Gimsing, 2008; EFSA 2015).

However, the studies recovering the two organophosphorus compounds in deep soil layers give rise to concern regarding water table and surface waters contamination. Even though the mobility of PMG and AMPA is low and only a fraction of it reaches hydrological settings, the large quantities of PMG introduced in the environment make this fraction a significant potential contamination. The results of Silva *et al*. (2018) and Battaglin *et al*. (2014) aid to grasp the importance of the issue.

Silva *et al*. (2017, 2018) quantified the presence of 76 pesticides residues in 317 agricultural topsoils samples from 11 EU member states collected in 2015. PMG and AMPA were the main contaminants as they were detected in 21 % and 42 % respectively, with a maximum concentration of 2 mg/kg. Their results indicates that exposure through wind and water erosion represented an alarming potential for secondary contamination for the environment and humans.

Battaglin *et al*. (2014) examined the analysis results of 1,018 quality assurance and 3,732 water and sediment samples from various hydrological types of sites collected in 38 states (USA) in the period 2001-2010 (detailed data provided in Annex 9). To cite but one observation, PMG and AMPA were detected in respectively 5.8 % and 14.3 % of the groundwater samples, all analysed following the USGS method O-2136-01 explained further and including SPE cleanup, derivatization, LC separation and MS detection.

Non-agricultural sources of PMG and AMPA should not be disregarded and are expected to play a significant role in water contamination. Untreated urban sewage[32] (Connor *et al*., 2007; Zgheib *et al*., 2012a; Gasperi *et al.,* 2012) and runoff from treated railways and motorways surroundings (Torstensson *et al*., 2005; Botta *et al*., 2009) were shown to represent a considerable source of non-agricultural herbicides, including PMG and AMPA contamination for surface water at least.

Attention must also be drawn on the fact that AMPA has the potential to be formed from other aminomethyl phosphonate compounds than PMG (Annex 10) (Lesueur *et al*., 2005; Armbruster *et al*., 2019). These compounds are used as laundry and dishwashing detergents in domestic products as well as anti scaling agents, corrosion inhibitor and deflocculating (peptization) agents in industry and water treatment plants. Typically in Drinking water plants only, "1 mL/m^3 to 3 mL/m^3 of an antiscalant product, containing 25% to 50% of active phosphonate, as specified by the manufacturer, is added into the feed water" (Armbruster *et al*., 2019). Therefore, they are present in domestic and industrial sewage as well as water treatment plants effluents. The majority of phosphonate compounds are immobilized in the sludge, with low quantities of AMPA remaining in the treated effluents released in the environment (Nowack, 2003; Lesueur *et al*., 2005). However, these phosphonates are reintroduced in the environment when the sludges are used as fertilizer on fields, with low to moderate biodegradation and high photodegradation in presence of iron III and Mn IV, yielding AMPA and orthophosphates (Nowack, 2003; Lesueur *et al*., 2005, Grandcoin *et al*., 2017). There are currently no regulation concerning phosphonate contents in sludge used as fertilizer. A consistent control of Glyphosate and AMPA levels implies a monitoring of PMG, AMPA and phosphonates levels in sludges prior their use on fields.

The contribution between PMG and other phosphonate compounds to the ubiquitous presence of AMPA in the environment is unknown and highly subject to conflicts of interests from supporters

[31] Such as combined alkalinity, erosion, heavy rainfall and proximity to water streams.

[32] Especially sewer systems devoted to evacuation of rain water and separated from household sewage.

and opponents of PMG. The only national-wide indicative statistic available is that among the 3,732 water samples from various hydrological settings collected in 38 states (USA) in the period 2001-2010, PMG occurence without AMPA was 2.3 % while AMPA occurence without PMG was 17.9 % (Annex 9) (Battaglin *et al*., 2014). More references can be found in the review of Grandcoin *et al*. (2017).

1.8. Regulations and tolerance levels regarding PMG residues

1.8.1. European level

Regulation (EC) N° 1107/2009 amended by Commission Implementing Regulation (EU) No 380/2013 as well as Regulation (EU) No 844/2012 rule the placing on the European market and authorization renewal of active substances intended to be used in plant protection products[33] (PPP). Active substances must first be approved at the European level by the European Commission (EC) before approval of formulated products by member states. The EC's decision is based on the risk assessment provided by the European Food Safety Authority (EFSA).

The risk assessment is carried in three steps. First, the applicant must take charge of safety studies carried in certified (Good Laboratory Practices (GLP)) laboratories according to EU guidance[34] and constitute a dossier with the results along with literature review. Secondly, the dossier is submitted to a Nominated Rapporteur Member State that edit an initial draft assessment report (DAR) or renewal assessment report (RAR). The Rapporteur Member State include the literature review in the draft assessment report with amendments. In the third step, the dossier is submitted to the EFSA for peer reviewing by member states experts, organization of public consultancy and settlement or revision of maximum residue level (MRL) . The applicant can possibly be asked for additional evidences. Then, EFSA submits a Conclusion to the European Commission (EC) which approves the active substance for a period of fifteen years or reject it.

Afterwards, formulated products containing the active substance can be approved by Member States for a (renewable) period of ten years. Applicant shall submit a dossier and request different authorizations for each of the three biogeographical European zones defined by the regulations (North, Center and South).

This regulation is based on the precautionary principle, requiring proof of absence of unacceptable effects on human and animal health, groundwater and environment in general for authorization at the European level.

PMG has been approved for use as an herbicide in all EU countries since 2002 (Commission Directive 2001/99/EC). Its last approval renewal period runs from 16/12/2017 to 15/12/2022 (Regulation (EU) 2017/2324). Companies seeking the renewal of PMG approval in 2022 gathered in a consortium named Glyphosate Renewal Group[35]. On 12/12/2019, this group submitted an application for renewal of all currently approved salts to the EFSA.

Regulation (EC) 396/2005 rules the establishment of maximum residue level (MRL) by EFSA for each PPP used on each crop intended for food and feed, based on the risk assessment. The MRL for PMG in sugar beet is 15 mg/kg. The complete list of MRLs for PMG from Part A of Annex I of Regulation (EC) 396/2005 is provided in Annex 11. Maximum residue levels on plant products are

[33] products "in the form in which they are supplied to the user consisting of or containing active substances [including microorganisms], safeners or synergists" and which are applied to plants with the intend to protect them against pests and diseases, to influence their growth and life process otherwise than as nutrient, to preserve them, to destroy or prevent the growth of undesired plants.

[34] https://ec.europa.eu/food/plant/pesticides/authorisation_of_ppp/application_procedure_en (19/02/2020)

[35] https://glyphosate.eu/ (19/02/2020)

set with respect to the manufacturer recommendations in the least favourable possible conditions[36] of culture.

Directive (EU) 2015/1787/EU fixes quality criteria for water intended for human consumption : the content in any individual pesticide should not exceed 0.1 µg/L, and the total pesticide content should not exceed 0.5 µg/L.

The trimethyl-sulfonium cation from trimesium-PMG is also subject to MRLs in Regulation (EC) 396/2005[37]. A list of EU regulations and directives relevant for PMG is presented in Annex 12.

1.8.2. National level - Belgium

The belgian competent authorities for enforcement of legislation related to PPP are (1) the Federal Agency for the Safety of the Food Chain (FASFC) and (2) the Federal Public Service for Public Health, Food Chain Safety and Environment - DG Plants, Animals and Food , Service Plant Protection Products & Fertilizers. The latter one powers the online platform Phytoweb, hosting resources and database for professional use and public concern. In February 2020, forty-nine PPPs containing PMG or trimesium-PMG were listed on the Phytoweb list of approved PPPs.

1.8.3. United States of America

PMG was registered by the EPA as a pesticide in the United States of America since 1974. The MRLs for PMG in the US is set by the EPA at 10 µg/g in fresh beet tissue and 25 µg/g in pulp (no MRL for molasses) (Code of Federal Regulations, Title 40, Chapter I, Subchapter E, Part 180, Subpart C, §180.364).

1.8.4. International level

The Codex Committee on Pesticide Residues (CCPR) is part of the Codex Alimentarius Commission (CAC), which is itself an instance of the Food and Agriculture Organization of the United States (FAO) and the World Health Organization (WHO). The CCPR is

> "an intergovernmental meeting whose prime objective is to reach agreement between governments on maximum residue limits (MRLs) for pesticides residues in food and feed commodities moving in international trade. The MRL proposals made by [the Joint WHO/FAO Meeting on Pesticide Residues (JMPR)] are considered by the CCPR as part of [a] eight-step procedure which provides opportunity for discussion and comment by national governments and other interested organizations. The MRLs recommended by CCPR are provided to the CAC, for adoption as Codex maximum residue limits"[38].

1.9. Residues in food in the EU

Every year, the EFSA releases its European Union Report on Pesticide Residues in Food synthesizing data from EU member states, Iceland and Norway. The last one was published in june 2019 and reported data from 2017 (EFSA, 2019). In 2017, 95.9 % of the 88,247 analysed samples complied with the legal MRLs (54.1 % below the LOQ and 41.8 % above LOQ and under the MRLs). Annex 13 provides MRL exceedance rates for pesticides with at least 2,000 samples tested and exceeding 0.05 % of MRL.

---

[36] i.e. "those which under the given circumstances produce what would probably be the highest residue situation according to intended use (e.g., maximum (proposed) number of applications, highest prescribed dosage, shortest [preharvest interval]). The trial conditions should also be representative of the main growing regions, influence of varieties, standard application methods and times, spreading of the trials over more than one - usually two - growing seasons." (European Commission, 2017).

[37] https://ec.europa.eu/food/plant/pesticides/eu-pesticides-database/public/?event=pesticide.residue.CurrentMRL&language=EN&pestResidueId=223 (08/03/2020)

[38] http://www.fao.org/agriculture/crops/core-themes/theme/pests/jmpr/en/ (08/03/2020)

In 2017, 8,672 samples (raw and processed products) were tested for PMG residues (among which 71 baby food and 306 samples of animal origin including honey). Of these, 97.5 % were below the LOQ, 2.2 % (191 samples) were above LOQ and under MRL and 0.2 % (21 samples) exceeded MRLs.

The products in which samples exceeded MRLs were honey (7 samples from Germany and 1 frome Austria), rye (1 sample from Italy and 5 samples from unknown origin), buckwheat (1 sample from Poland and 3 of unknown origin), asparagus (1 sample from Italy), pear (1 sample from Poland) and rice (1 sample from France). Honey is the only animal product with samples exhibiting PMG levels above LOQ (24 samples out of 659). Rye is the product of plant origin with the most samples (6 samples out of 339) with PMG above MRL. In rye, PMG is the fourth most detected residue above LOQ (16 samples out of 339). PMG is the 28th and 35th residue with the highest number of samples tested above LOQ in orange and pear respectively. No sample with PMG residues above LOD was reported for other commodities[39].

Supplementary data regarding samples of plant origin tested with PMG residues above LOD are reported in Annex 14 and data regarding pesticides found at or above LOD in animal products are provided in Annex 15.

Similar data were acquired for trimethylsulfonium cation, a residue from PMG trimesium : among 3,596 analysed samples, 97.3 % were below the LOQ, 2.2 % (78 samples), were above LOQ and under MRL and 0.2% (18 samples) exceeded MRLs. Data regarding the trimethyl-sulfonium cation residues in specific food products are reported in Annex 16.

In the report, no specific concern regarding PMG or trimethylsulfonium exposure was expressed. The MRL for sugar beet is set at 15 mg/kg, which is much higher that the MRL of the majority of products (0.1 or 0.05 mg/kg); but still less than other commodities such as soybean, oat, barley, sorghum (20 mg/kg) and wild fungi (50 mg/kg).

1.10. Toxicity, ecotoxicity and public health concern

The toxicity of PMG was assessed many times among the years by several national and international institutions as well as independent studies. The conclusions on which rely the regulation should not be ignored as it impacts public health and access to food as well as global markets and considerable financial stakes. Nevertheless, toxicology and epidemiology are two subjects out of the scope of this study. Hereunder are given some key elements reflecting the position of several important organizations influencing regulations on PMG and AMPA.

In 2015, the International Agency for Research on Cancer (IARC) classified PMG in the category 2A : “probably carcinogenic to humans” which means that there are “limited evidence of carcinogenicity in humans and sufficient evidence of carcinogenicity in experimental animals” in its monograph 112 (IARC, 2015). The evidence included sufficient evidence of cancer in animals exposed to pure PMG and formulations, strong evidence of DNA damage in cells exposed to pure PMG, and Non-Hodgkin lymphoma (NHL) in humans exposed to formulations (evidence found in case-control study[40] and meta-analysis but not in the sole cohort study[41] considered). IARC monographs are based on the review of all the publicly available literature and data.

It must be highlighted that the IARC carry hazardousness assessments, while other institutions usually carry risk assessments, with the risk being proportional to both hazardousness and exposure.

[39] including carrots, cauliflowers, kiwi fruits, onions, potatoes, dry beans, poultry fat and sheep fat.

[40] a study design in which cases two different groups of outcomes (ill and healthy) are considered and causal factors are compared between the two groups.

[41] a study design in which groups with different exposure to causal factor(s) are studied during a given period of time and the rate of outcome is measured.

The Joint WHO/FAO Meeting on Pesticide Residues (JMPR) assessed PMG through meetings in 1986, 1994, 1997, 2004, 2005, 2011, 2013 and 2016[42]; of AMPA as of 1997 and of N-acetyl-PMG (N-Ac-PMG) and N-acetyl-AMPA (N-Ac-AMPA) as of 2011. It has been considered until 2013 that the use of PMG was safe, with low acute toxicity and no sufficient evidence of carcinogenicity, teratogenicity, genotoxicity, neurotoxicity, immunotoxicity and toxicity for reproduction when exposed to residues. PMG was only identified to be eye damaging, to induce basophilic hypertrophy of salivary glands and gastrointestinal irritation (FAO/WHO 2004 and later).

In 2004, the Joint WHO/FAO Meeting on Pesticide Residues (FAO/WHO, 2004) reported data regarding short-term fate of PMG in animals. It was shown in rats that only 30–36 % of ingested PMG in the range 10–1,000 mg/kg body weight was absorbed from the gastrointestinal tract, the 60–70 % remaining being excreted in the faeces. Most of the absorbed PMG was excreted in the urine and less than 0.2 % expired in air. After 168 hours, about 99 % of ingested PMG was cleared from the body, with less than 0.7 % being metabolized in AMPA. The highest tissue concentrations were observed in bone, bone marrow, kidney and liver; no bioaccumulation occured in fat tissues. The acute oral toxicity is low (LD_{50} > 2,000 and 5,000 in mice and rats respectively).

The mechanism by which PMG caused basophilic hypertrophy of salivary glands was qualified as "unclear" in the 2004 JMPR. The JMPR 2016 stated that considering the low pH of the test solution and knowing that ingestion of organic acids can cause similar effects, the symptom was attributed to the moderate acidity of PMG and was not considered of toxicological significance.

In 2016, the JMPR came to conclusions similar to those of IARC in 2015, i.e. "Overall, there is some evidence of a positive association between glyphosate exposure and risk of NHL from the case–control studies and the overall meta-analysis. However, it is notable that the only large cohort study of high quality found no evidence of an association at any exposure level." (FAO/WHO, 2016). Furthermore, JMPR 2016 noted that high doses of PMG were known to affect the gastrointestinal microbiota, with the beneficial bacteria being more sensitive than the pathogenic and that it could be related, and that such perturbation of the microbiota was known to have impact on carcinogenesis. It was stated that even if "the extent to which glyphosate adversely affects the normal functioning of the microbiota in the human gastrointestinal tract or the gastrointestinal tract of mammalian models is unclear" (FAO/WHO, 2016), it was unlikely that carcinogenicity linked to unbalanced microbiota would occur from anticipated exposure to PMG at residual level in the diet.

Genotoxicity was considered unlikely at anticipated levels considering that genotoxicity was not observed in a majority of high oral exposure study in mammals.

No effect attributable to PMG was detected in routine medical surveillance of workers in production and formulation plants, while among workers applying PMG formulations, eye, skin and respiratory tract irritation was reported as well as cases of acute toxicity of PMG formulations in humans, likely attributable to co-formulants, as it was evoked in the study of Bradberry *et al*. (2004).

The acceptable daily intake (ADI) for PMG, AMPA, N-Ac-PMG and N-Ac-AMPA is set at 1 mg/kg body weight since 2004 and no Acute Reference dose (ARfD) was deemed necessary. The MRL in sugar beet was set at 15 mg/kg (PMG alone) (FAO/WHO, 2011). JMPR 2004 considered AMPA "of no greater toxicological concern than its parent compound [PMG]", neither was the case for the other metabolites N-Ac-PMG and N-Ac-AMPA.

On march 2017, the European Chemical Agency (ECHA) re-assessed PMG's hazardousness to revise the labelling of PMG-containing products (under Regulation (EC) No 1272/2008 on the classification, labelling and packaging of substances and mixtures (CLP Regulation)[43]). ECHA

[42] http://www.fao.org/agriculture/crops/thematic-sitemap/theme/pests/lpe/lpe-g/ua/ (19/02/2020)

[43] https://echa.europa.eu/regulations/clp/legislation (23/02/2020)

maintained the previous hazard statements (or "H phrases") : Eye damaging 1 - H318 ("Causes serious eye damage") and Aquatic Chronic 2 - H411 ("Toxic to aquatic life with long-lasting effects"). The risk assessment committee stated that "the available scientific evidence did not meet the criteria in the CLP Regulation to classify glyphosate for specific target organ toxicity, or as a carcinogen, as a mutagen or for reproductive toxicity."[44]. Similarly to IARC, ECHA only provides assessment of the hazard, and not the risk, which is related to exposure. Risk assessment is dependent on formulations and products, and is carried at European level by EFSA.

The process for PMG reapproval in the EU, supervised by the European Food Safety Authority, took place from 2012 (reception of the application dossier by Germany) to 2017 (reapproval by the EC). In February and march 2015, EFSA conducted experts consultations issuing mammalian toxicology, residues, environmental fate, and ecotoxicology, in response to comments on the draft renewal assessment report received in 2014. A supplementary expert consultation on carcinogenicity and mammalian toxicology was carried in September 2015 to discuss the final version of the IARC monograph 112 published in july 2015. The conclusion of the renewal assessment report published in November 2015 lies in the following words :

> "In contrast to the IARC evaluation, the EU peer review experts, with only one exception, concluded that glyphosate is unlikely to pose a carcinogenic hazard to humans and the evidence does not support classification with regard to its carcinogenic potential according to Regulation (EC) No 1272/2008. [...] Based on the representative uses, that were limited to conventional crops only, chronic or acute risks for the consumers have not been identified. [...] Regarding fate and behaviour in the environment, further information is needed to assess the contamination route through runoff [...] and subsequent surface water contamination and bank infiltration to groundwater.
>
> For the section on ecotoxicology, two data gaps were identified to provide an assessment to address the long-term risk for small herbivorous mammals and for insectivorous birds. For aquatic organisms, the risk was considered low [...]. The risk for bees, non-target arthropods, soil macro- and micro-organisms and biological methods for sewage treatment was considered low. The risk to non-target terrestrial plants was considered low, but only when mitigation measures are implemented." (EFSA, 2015a)

Since 2015, the toxicological reference values for PMG are the following : acceptable daily intake (ADI) of 0.5 mg/kg body weight and per day, Acute reference dose (ARfD, i.e. the maximum dose than can be ingested in a short period of time -such as a lunch- without effects on health) of 0.5 mg/kg body weight and an Acceptable Operator Exposure Level (AOEL) of 0.1 mg/kg body weight per day. No ARfD existed prior to 2015.

Further explanation on the process leading to EFSA's conclusions as well as on the conclusion itself regarding carcinogenicity, genotoxicity and co-formulants are provided in a background document published by the EFSA[45] in November 2015. In that document, it is notably stated that :

> "a number of published studies performed with glyphosate-based formulations of unknown composition gave positive results [for genotoxicity and/or endocrine disruption] when tested *in vitro* and *in vivo*. Some of the test systems are not validated and/or of difficult interpretation due to possible confounding effects, such as cytotoxicity, specific organ toxicity or unclear relevance to human health when tested in fish, amphibians or invertebrates according to the current knowledge. POE-tallowamine [(i.e. Polyethoxylated-tallowamine)] is one of the co-formulants that is known to be used in some glyphosate-based formulations. This co-formulant has been shown to be more toxic than the active substance glyphosate on several toxicological endpoints, namely acute, short term, reproductive and developmental toxicity, further to

[44] https://echa.europa.eu/regulations/clp/legislation (23/02/2020)

[45] http://www.efsa.europa.eu/sites/default/files/4302_glyphosate_complementary.pdf (23/02/2020)

> equivocal evidence of DNA damage *in vitro* at high doses (EFSA, 2015c). Although POE-tallowamine is not present in the representative formulation, for which data have been submitted under the European re-approval procedure and which were assessed by EFSA, the peer review concluded that the toxicity of formulations and in particular their genotoxic potential should be further considered and addressed. [...] EFSA has been mandated by the European Commission to assess a co-formulant, POE-tallowamine, that although not present in the representative formulation, is reported as co-formulant for other glyphosate containing PPPs. EFSA does not support the healthbased reference values proposed by the RMS, and considers that the genotoxicity, long term toxicity/carcinogenicity, reproductive/developmental toxicity and endocrine disrupting potential of this co-formulant should be clarified before setting health-based reference values and conducting the risk assessment (EFSA, 2015c)."(EFSA, 2015[46])

The same day, the EFSA also published the document named "Request [of the EC] for the evaluation of the toxicological assessment of the co-formulant POE-tallowamine". In this document, it is stated that :

> "The RMS considered that a toxicological assessment of this surfactant characterised by the CAS no. 61791-26-2 could be necessary at Member State or zonal level for plant protection product authorisations, and therefore a toxicological evaluation including health-based reference values was provided in the RAR. EFSA did not have the possibility to review the original data for most of the endpoints summarised in chapter B.6.13 of the RAR, and some endpoints are not fully addressed, therefore EFSA cannot support the RMS's current assessment and considers that reliable reference values Acceptable Daily Intake (ADI), Acceptable Operator Exposure Level (AOEL), and Acute Reference Dose (ARfD) cannot be established and further data have to be submitted. Therefore, the exposure assessment for operators, workers, bystanders, residents and consumers could not be performed.
>
> Compared to glyphosate, a higher toxicity of the POE-tallowamine was observed on all endpoints investigated. [...] The genotoxicity, long-term toxicity and carcinogenicity, reproductive/developmental toxicity [, environmental fate, dermal absorption, risk assessment for operators, residents and consumers] and endocrine disrupting potential of POE-tallowamine should be further clarified. There is no information regarding the residues in plants and livestock. Therefore, the available data are insufficient to perform a risk assessment in the area of human and animal health for the co-formulant POE-tallowamine." (EFSA, 2015b)

In 2016, following a request from several European parliament members, EFSA announced that the raw data used for the risk assessment of PMG would be shared on request, promoting transparency of the assessment process[47] .

In September 2017, in its peer review of the pesticide risk assessment on the endocrine disrupting properties of PMG, EFSA concluded that PMG was not likely to have significant endocrine disrupting properties (EFSA, 2017b).

In May 2018, based on the MRLs for PMG of the Codex Alimentarius Commission, data on good agricultural practices provided by member states and a consumer risk assessment, EFSA reviewed the MRLs of PMG in plant commodities from conventional crops of various kind and GM crops (EFSA, 2018a). The residue definition for included PMG alone and PMG, AMPA, N-Ac-PMG and N-Ac-AMPA. It was stated that member states should consider implementing mitigation measures according to their good agricultural practices in order to prevent PMG residues on crops on which it is used as a dessicant (EFSA, 2018a).

---

[46] http://www.efsa.europa.eu/sites/default/files/4302_glyphosate_complementary.pdf (23/02/2020)

[47] https://www.efsa.europa.eu/en/press/news/161209 (23/02/2020)

The same day, EFSA published an evaluation of the impact of PMG and its residues in feed on animal health and concluded that "With regard to the assessment of the impact of glyphosate and its residues on animal health, considering the available data, glyphosate is not expected to have a major impact, if any, on animal health." (EFSA, 2018b).

In October 2019, EFSA published a second review of the MRLs for PMG including data that were available during the evaluation but not or not fully taken into account by the rapporteur member state Germany, following Monsanto company claim (EFSA, 2019). This review did not include substantial changes compared to the previous one.

As of march 2020, no other statement concerning POE-tallowamine nor PMG was published by the EFSA.

The US Environmental Protection Agency (EPA) carried risk assessments of PMG in 1985, 1993, 2015 and 2016. In 1985, PMG was considered "Possible Human Carcinogen" by EPA, based on the presence of kidney tumors in male mice. It was however re-evaluated as not significant and PMG was considered "Not Classifiable as to Human Carcinogenicity" by the EPA in 1986, "Evidence of Non-Carcinogenicity for Humans" by the American Carcinogenicity Peer Review Committee in 1991, "Not Likely to be Carcinogenic to Humans" by the EPA in 2015 (EPA, 2016). The 2016 assessment concluded that "The strongest support is for "not likely to be carcinogenic to humans" at doses relevant to human health risk assessment." (EPA, 2016).

1.10.1. Controversy

Although it is out of the scientific scope of this study, it should be noted that the confidence in the conclusions of regulatory agencies concerning PMG is sometimes queried for several reasons. Firstly, contrary to the IARC that only relies on publicly available and supposedly independent studies, regulatory agencies give credit to unpublished studies provided directly by the applicants[48], which constitutes an obvious conflict of interests. Secondly, numerous declassified internal documents and emails (the so-called "Monsanto papers") were cited in media investigations[49] and used as evidences in lawsuits[50,51] against the Monsanto company and court decision. It was revealed from these documents that the Monsanto company exerted intense lobbying campaigns[52,53,54], discredit and intimidation campaigns against IARC[55,56] and U.S. Right To Know[57,58] non-governmental organization and carried disinformation through manipulation of scientific literature -namely "ghost-writing" of studies[59] presented as independent- concluding that PMG is unlikely carcinogenic[60,61]. Severe criticism were also addressed against the conclusions of EFSA and the rapporteur member state Germany[62] notably through the memorandum of Peter

48 http://ec.europa.eu/food/plant/pesticides/eu-pesticides-database/public/?event=activesubstance.ViewReview&id=1200 (24/02/2020)

49 https://www.Europeanpressprize.com/article/monsanto-papers/ (24/02/2020)

50 https://usrtk.org/monsanto-papers/federal-court/ (24/02/2020)

51 https://usrtk.org/monsanto-papers/reporting-and-analysis/(24/02/2020)

52 https://www.documentcloud.org/documents/6306322-69-Internal-Email-Monsanto-Lobbying-Efforts-in.html (24/02/2020)

53 https://usrtk.org/wp-content/uploads/bsk-pdf-manager/2020/01/Monsanto-Let-Nothing-Go-2015-update.pdf (24/02/2020)

54 https://www.globalresearch.ca/monsanto-controls-both-the-white-house-and-the-us-congress/5336422 (24/02/2020)

55 https://usrtk.org/our-investigations/monsanto-relied-on-these-partners-to-attack-top-cancer-scientists/ (24/02/2020)

56 https://usrtk.org/wp-content/uploads/2017/08/72-Document-Details-Monsantos-Strategy-Regarding-IARC.pdf (24/02/2020)

57 an NGO gathering newspaper articles, federal courts documents and state courts documents concerning the trials against Monsanto.

58 https://usrtk.org/our-investigations/monsanto-usrtk-foia/#MonsantoUSRTKdocs (24/02/2020)

59 namely : Williams G.M., Kroes R. & Munro I.C., 2000. Safety evaluation and risk assessment of the herbicide Roundup and its active ingredient, glyphosate, for humans. Regul. Toxicol. Pharmacol. 31(2 I), 117–165. (https://doi.org/10.1006/rtph.1999.1371)

60 https://usrtk.org/monsanto-roundup-trial-tacker/emails-reveal-science-publisher-found-papers-on-herbicide-safety-should-be-retracted-due-to-monsanto-meddling/

61 https://usrtk.org/monsanto-papers/ (24/02/2020)

62 http://icppc.pl/pliki/2015/fakt-glyphosat-bfr-bewertung100.pdf (24/02/2020)

Clausing[63] before the international Monsanto Tribunal (de Hague), and through the article of Portier *et al*. (2016).

In May 2017, following concern on the potential interference of Monsanto Company in EFSA's decision process on PMG assessment, the EFSA published a statement declaring that "there are no grounds to suggest that industry improperly influenced the EU assessment of glyphosate; and that the role of industry and of other actors in the process was carried out according to standard procedures"[64].

Lawsuits, media articles and officials' statements all give different insights on the intricate issue and conflicts of interests surrounding affairs linked to PMG. All the documents and standpoints mentioned above aim at illustrating the issue. Their citation does not constitute any endorsement or position statement.

1.10.2. Further considerations on PMG ecotoxicity

As fungicidal activity of PMG was shown to be low (Dill *et al*. 2010), it is not expected to significantly affect mycorhize in soils.

Although PMG is not expected to directly affect animals since they do not rely on ESPS synthase, indirect impairment may occur through perturbation of gut microbiota. This hypothesis was supported by the observations of Motta *et al*. (2018) : the majority of gut bacteria promoting weight gain and pathogen resistance in honey bees (*Apis mellifera*) were negatively affected when the bees were exposed to concentrations similar to those reported in the environment. This resulted in higher susceptibility to opportunistic pathogens and mortality, especially in young workers. Variability in susceptibility was also correlated to the presence of resistant EPSP synthase in the gut microflora communities. Similar stress may occur in other taxa whose health relies on gut microflora; including human, as it was suggested by the JMPR : "the extent to which glyphosate adversely affects the normal functioning of the microbiota in the human gastrointestinal tract or the gastrointestinal tract of mammalian models is unclear" (JMPR, 2016).

It was also shown by Hawes *et al*. (2003) in farm-scale experiments that the trophic chains were weakened in herbicide-resistant GM crops. With less weeds bordering the crops, less shelter and food resources were available to pollinators and herbivorous invertebrates which declined more than two-fold. The reduction of herbivorous invertebrates in turn induced reduction of carnivorous invertebrates also possibly affecting mammalian and bird populations.

PMG is not included in the list of priority substances to be monitored in waters in Annex II of Directive 2008/105/EC.

1.11. Use and fate of PMG and AMPA in the sugar beet industry

1.11.1. Sugar beet crops

Worldwide, around 80 % of the sugar is produced from sugar cane (*Saccharum* spp.) and 20 % from sugar beet (*Beta vulgaris* L. subsp. *vulgaris*), with 43 countries growing only sugar beet (FAO, 2009). The global production of sugar beet exceeded 275 million of tonnes in 2018, with 43 % from EU (around 120 million of tonnes)[65].

The sugar beet root is composed of 75–83 % of water, 12–21 % of sugar (average : 17–18 %), and about 5 % of pulp (24–32 % pentosans, 24–32 % pectins, 22–30 % cellulose, 3–6 % lignin, 4–5 %

[63] http://www.pan-germany.org/download/Memo_Monsanto-Tribunal_Peter_Clausing_10_2016.pdf (24/02/2020)

[64] https://www.efsa.europa.eu/sites/default/files/170523-efsa-statement-glyphosate.pdf (24/02/2020)

[65] http://www.fao.org/faostat/en/#home (24/02/2020)

proteins and 4–5 % ashes), depending on growth conditions and variety (Draycott, 2006; FAO, 2009). Sugar represents the main extractible value from sugar beet while byproducts are valued to about 10 % of the sugar value (FAO, 2009; Harland *et al*., 2006). The yield of a typical modern crop is between 50 and 100 tons of clean root per hectare, i.e. 8–18 tons of sucrose per hectare) or 130 to 160 kg sugar per ton of beet processed, with an optimal extraction efficiency of 82.5 % in refineries (FAO, 2009).

Sugar beet is cultivated under "temperate humid climate with dry, sunny periods just before the harvest" (FAO, 2009). The plant has a cycle of two years (biennial). Under temperate climate it is sown in spring, it accumulates sugar during summer, it is harvested in autumn or early winter and it blooms after winter (Draycott, 2006; FAO, 2009); while in mediterranean countries, it is grown during winter. Sugar beet is known to be a delicate crop, with many factors influencing yield such as plant density (including competitivity with weeds), harvest date, variety (genotype), nitrogen fertilization, soil type, weather (especially drought), parasites (aphids (*Aphidoidea*)) and diseases (transmitted by aphids) (Draycott, 2006). Optimum conditions for sugar beet culture require moderate nitrogen supply and considerable amounts of potassium (4 kg/t of roots) as well as a soil pH in the range 6.5–8 (Draycott, 2006). As mentioned earlier, alkaline pH is less favorable for PMG and AMPA retention. Sugar beets are mechanically harvested, with machines equipped with mechanic "topper" or "defoliator" followed by a "lifter" (Draycott, 2006; FAO, 2009).

1.11.2. Advantages provided by PMG and PMG-tolerant sugar beet

Sugar beet crops are particularly vulnerable to weed competition, as it is a short crop not exceeding 30 to 60 cm tall at its maximum (May and Wilson, 2006). In Belgium, 27 active substances entries (active substances alone or in combination) are approved for use on sugar beet crops[66]. PMG is not approved for use on sugar beet crops but is approved for green manure termination and intercultural weed control if mechanical means (grinding, ploughing) are ineffective or inappropriate (IRBAB, 2015[67,68], 2016[69,]).

Whereas, in the U.S., PMG it is vastly used on resistant GM sugar beet (nearly 100 % of the sugar beet produced since 2010 (Barker *et al*., 2019)), with two or three applications of PMG-based herbicide during the life cycle of the crop (Barker *et al*., 2019). And, as said earlier, the H7-1 PMG-resistant sugar beet with CP4 resistant EPSP synthase is approved in the EU for importation and use in food and feed.

It was also mentioned above that PMG metabolization in plants is low and the molecule remains in its active form in plant tissues (especially in CP4 GM crops), with AMPA being the only significant metabolite. Root absorption of PMG and AMPA in soil is considered negligible, or at most very limited (FAO/WHO, 1986[70] cited by FAO/WHO, 2005). It was shown that PMG content in H7-1 sugar beet tissues reached 2 to 4 µg/g of fresh tissue in leaves at first, then in the root (Barker *et al*., 2019). However, Barker *et al*. (2019) observed that the PMG content in roots gradually decreased and most of it was dissipated within 15 days after application in laboratory and field experiments. Harvested sugar beets presented PMG residues contents of 1.5 pg/g (one application during culture) and 32 pg/g (two applications during culture) and AMPA was below the LOD. The absence of AMPA suggested that PMG was exuded rather than metabolized (Barker *et al*., 2019), similarly to field horsetail (*Equisetum arvense*) (Coupland and Peabody, 1981) and wheat (*Triticum aestivum*) (Rodrigues *et al*., 1982).

---

66 https://www.irbab-kbivb.be/wp-content/uploads/2019/02/erkende-herbiciden-biet-FR-2019.pdf (21/02/2020)

67 https://www.irbab-kbivb.be/fr/labours-reverdis/ (21/02/2020)

68 https://www.irbab-kbivb.be/fr/destruction-des-couverts-situations-tres-variables/ (21/02/2020)

69 https://www.irbab-kbivb.be/fr/herbicides-non-selectifs-avant-semis/ (21/02/2020)

70 Pesticide residues in food - 1986. Report of the Joint Meeting of the FAO Panel of Experts on Pesticide Residues in Food and the Environment and a WHO Expert Group on Pesticide Residues. FAO Plant Production and Protection Paper 77, Part I, 1986. (not accessed)

The use of PMG on resistant sugar beets provides many advantages : reduced crop injury, reduced total amount of active substance applied, reduced overall ecotoxicity, reduced risk for the handler (low acute toxicity and low volatility), compatibility with conservation tillage practices (reduced erosion and increased soil carbon content), increased yield (land use efficiency), reduced management complexity and workload, reduced cost and reduced fuel consumed (Bennett *et al*., 2005; Märländer, 2005, Morishita, 2017; Barker *et al*., 2019). Sugar beet is said to be one of the most convenient crop for PMG resistance GM technology because "(1) none of the herbicides registered for use in this crop was very effective without risking crop injury; (2) sugar beet cannot be grown in the same field year after year owing to disease concerns and thus requires a 3–4 year rotation; (3) pollen-mediated gene flow is negligible from the sugar beet crop because it is a biennial and harvested before it flowers; (4) the processing of harvested roots to extract the sucrose rapidly degrades the DNA in the extracted raw juice and subsequent refining so that no DNA is present in the finished sugar; (5) studies have shown that processed GR beet sugar is identical to non-GR beet sugar, as well as cane sugar." (Morishita, 2017). Furthermore, unlike PMG-resistant soy and maize, PMG-resistant sugar beet do not suffer from nutrient deficiencies affecting yield or quality as a side-effect of PMG application (Holtschulde *et al*., 2011).

Despite these advantages and the need for competitivity of the sugar industry in the EU since the end of the sugar quotas, the approbation of H7-1 GM sugar beet remains unlikely because of the unpopularity of GMOs alongside concerns about PMG innocuity. Regulation (EC) 1830/2003 has made mandatory the labelling of products containing GM ingredients above 0.9%, even if no protein or DNA remains in the final product (as it is the case for sucrose extracted from sugar beet). This does not include meat from animals fed with GM grains[71].

Currently, GMOs are regulated by the Directive 2001/18/EC and Directive (EU) 2015/412. The last one allows member states to ban GMOs if it is thought that they represent a threat.

1.11.3. Sugar extraction process and effect on PMG

After harvest, sugar beet roots are delivered to the processing plant as soon as possible to limit sugar loss from metabolization. The roots are washed in agitated baths to remove dirt, weeds and stones. The PMG content in the effluent washing water is expected to come mainly from the dirt to be dependent on the time elapsed since the last application, the weather during that period and the composition and quantity of dirt in the bath. Washing is not expected to affect PMG content in the sugar beet root. The MRL for sugar beet is set at 15 mg/kg.

After washing, the roots are sliced in "strips" before extraction. Extraction takes place in a diffuser similar to the one shown in Figure 15. The strips are transported on a sifted conveyor belt and hot water (~72 °C) is aspered at the end of the diffuser, collected, pumped and re-aspersed upstream (countercurrent) in the diffuser so that the sugar concentration of aspersed water is always lower than in the strips aspersed in order to improve extraction from strips to water. Once extracted, strips are called pulps. PMG is expected to be extracted along with sugar, without any alteration.

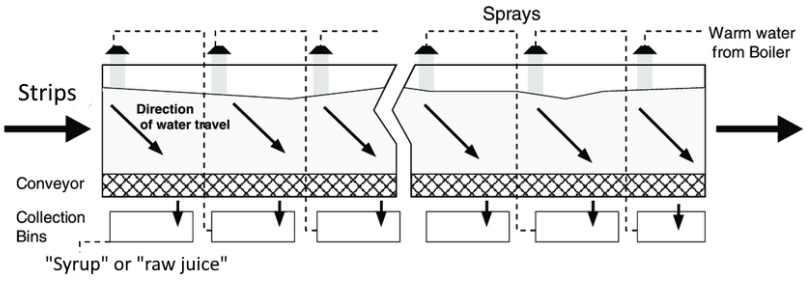

Figure 15 : Industrial sugar diffuser. Source : Hocking and Mitchell (2016)

[71] EU already imports GM soy and maize for feed, and the quantity is expected to increases with international commercial treaty like CETA, TAFTA, MERCOSUR and others (see https://webgate.ec.europa.eu/dyna/gm_register/index_en.cfm)

The raw juice contains variable contents of non-soluble and soluble impurities (more details in Annex 17). Soluble impurities -the most difficult to remove- account for 2 % of the fresh weight of the beet. Some impurities are removed by a carbonation step consisting on addition of limewater (or milk of lime) (i.e. a saturated solution of calcium hydroxide ($Ca(OH)_2$) with solid calcium hydroxide suspension) and injection of carbon dioxide. The carbonation reaction (equation 2) traps solid impurities as calcium carbonate grow on them, trapping them. It also coagulates and removes proteins, absorbs coloured compounds and degrade "molassogenic" monosaccharides because of the alkaline conditions. Carbonated juice is then filtered and cleaned juice (or "thin juice") is obtained. Phosphates and oxalates being removed by carbonation (Annex 17) (Draycott, 2006), PMG and AMPA are also expected to be removed by carbonation along with phosphate and other anionic species. The alkaline conditions of carbonation are optimum for PMG and AMPA ionization and chelation of Ca^{2+}.

$$(2) \qquad Ca(OH)_{2\,(aq)} + CO_{2\,(aq)} \rightleftharpoons CaCO_{3\,(s)} + H_2O_{\,(s)}$$

Clear juice may be neutralized with sodium carbonate (Na_2CO_3 or "soda ash"), sodium hydroxide (NaOH or "caustic soda") or acid in order to avoid sugar hydrolysis (Draycott, 2006). Additionally, sulphate may be added to prevent formation of colouring compounds.

The neutralized clear juice is heated and concentrated in a multiple-effect evaporator to obtain a syrup containing between 65 and 70 % of sucrose (Draycott, 2006). Sucrose crystallization from syrup occurs in a vacuum tank heated at 80°C. Finely ground sucrose crystals are added and serve as nuclei, starting point of sucrose crystal growth. Syrup is gradually added to maintain a weak sursaturation favourable to crystal growth but unfavourable to spontaneous nucleation. Sucrose crystals are recovered with centrifugation. Purification is performed through three consecutive crystallization, the first from clear juice and the two other from impure sucrose crystals recovered in the precedent crystallization step. At the end of the third crystallization, sucrose with a purity above 99.9 % is recovered (Draycott, 2006). The syrup remaining from the last crystallization is called molasses. It still contains ~50 % sugar, but its recovery is not profitable anymore (Draycott, 2006; FAO, 2009).

The by-products of sugar refinery - molasses (~38 kg/ton of sugar beet), wet pulps (500 kg/ton of sugar beet) and beet tops - are used as feed for cattle (FAO, 2009). Pectin can be extracted from pulps while molasses can serve for fermentation (ethanol, rum, yeast and other organic compounds) (FAO, 2009).

1.11.4. Decontamination of water and soils

As mentioned earlier, several studies investigated the decontamination of water effluents through catalyzed photolysis (Assalin *et al*., 2010; Xu *et al*., 2011; Shrikant and Khambete, 2014; Li *et al*., 2018; Cao *et al*., 2019). Wet oxidation in autoclave was also investigated but not likely to be applied at large scale for wastewater or soil (Feng *et al*., 2020). Ozonation seems much more relevant as it is already used in drinking water treatment plants as an alternative to chlorination (Yao and Haag, 1991; Haag and Yao, 1992). Biodegradation is another path for decontamination yet to be investigated. Techniques for removal and concentration prior to destruction include adsorption and ion exchange.

1.12. Review of methods used for PMG and AMPA determination

1.12.1. Incompatibility with QuEChERS extraction and spectrophotometric detection

The original QuEChERS method (quick, easy, cheap, effective, rugged, and safe) developed by Anastassiades *et al*. (2003) and widely used for multiresidue analysis consists in a first single-phase extraction of a 10 g aqueous food sample with 10 mL acetonitrile followed by a liquid-liquid partitioning achieved with the addition of 4 g of anhydrous $MgSO_4$ and 1 g of NaCl. Pesticides are expected to be extracted in the organic phase. Then, dispersive solid-phase extraction is performed on 1 mL of extract with 150 mg anhydrous $MgSO_4$ and 25 mg primary secondary amines in order to remove residual water and polar components such as organic acids, pigments and sugars.

Because of its high polarity, PMG solubility is much higher in water (157 g/L at pH 7) than in acetonitrile (0,8 mg/L). Hence the QuEChERS method is not adapted for PMG and AMPA extraction.

Furthermore, PMG does not absorb nor re-emit specific wavelength and can not be detected with absorption or fluorescence spectrometry without derivatization.

1.12.2. Official methods for PMG determination in United States of America

The methods concerning analysis in environmental samples are listed in the National Environment Method Index[72] (NEMI). The NEMI is powered by three US federal agencies : the US EPA, the United States Geological Survey (USGS) and the National Water-Quality Monitoring Council (NWQMC).

The US EPA method 547 (EPA, 1990) for determination of PMG and AMPA in water consists in a HPLC separation into a cation exchange column by isocratic elution at 65°C followed by a post-column derivatization.

Derivatization is achieved by oxidation of PMG into glycine with calcium hypochlorite at 50°C followed by a reaction of primary amines (including glycine and AMPA) with o-phthalaldehyde-2-mercaptoethanol complex at 38°C in a borate buffer (pH > 9) in order to obtain a fluorophor (1-(2′-hydroxyethylthio)-2- N-alkylisoindole) (Figure 16). Excitation of the fluorophor occur at 340 nm and emission is measured around 455 nm. The initial sample volume is 200 µl filtered water aliquot. Interferences include the amino acid glycine as well as any amine compound with similar retention.

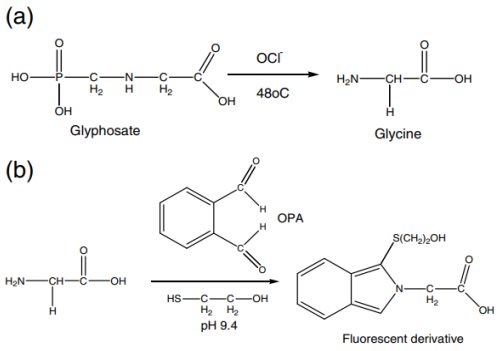

Figure 16 : Oxidative derivation of PMG and AMPA. Source : Colombo *et al*. (2011)

The AOAC International method 991.08[73] (last revision : 1993) is very similar to the EPA method 547. A supplementary concentration step is included prior to derivatization : water samples are evaporated to dryness in a rotary evaporator and the residues are dissolved in EDTA solution. This step allows concentration of PMG and AMPA since they are heat-resistant and not volatile, while EDTA is intended to prevent interaction of PMG and AMPA with cations.

The US EPA method 43265-06-S (last version : 1994) for PMG and AMPA determination in soils consists in a first extraction from a 20 g soil sample with 0.25 M ammonium hydroxide and 0.1 M potassium phosphate under agitation (100 - 120 rpm) for 90 minutes before centrifugation

[72] https://www.nemi.gov/methods/analyte_results/?media_name=&source=&instrumentation=&analyte_name=glyphosate&analyte_name=glyphosate+%28ansi%29&category= (05/02/2020)

[73] Available at https://www.nemi.gov/methods/method_summary/4742/ (10/02/2020)

at 2,000 for 20 min or filtration of 3 mL through 0.45 µm disposable syringe filters. Extracts are then derivatized within four hours with trifluoroacetic anhydride and heptafluorobutanol. Both phosphoric and carboxylic acid moieties are derivatized to form heptafluorobutyl esters while the amine group is derivatized into trifluoroacetyl amide. Excess reagents are evaporated before analysis in GC-MS.

The OSHA PV2067 method from the United States Department of Labor, Occupational Safety and Health Administration (OSHA, 1989) is a method adapted for PMG determination in air. "Samples are collected by drawing known volumes of air through glass fiber filters. Samples are desorbed with 0.025 M borate buffer, derivatized and analyzed by high performance liquid chromatography (HPLC) using an ultraviolet detector (UV)" (OSHA, 1989). Separation, derivatization and detection are similar to the EPA method 547.

The USGS method O-2136-01 (last revision : 2002) for PMG, AMPA and glufosinate determination in water consists in a precolumn derivatization of a 10 mL sample with 9-fluorenylmethyl chloroformate (a protecting group for amines, also known as Fluorenylmethyloxycarbonyl chloride or FMOC-Cl) (Figure 18) in a borate buffer (pH 9). The derivatization is carried in darkness at 40 °C for 24 h and stopped with addition of 2 % phosphoric acid. It is followed by a cleanup and concentration stage performed by solid phase extraction (SPE) on Waters Oasis HLB cartridges before separation in HPLC with (C18 reversed phase; solvent A : 5 mM ammonium acetate in distilled water; solvent B : acetonitrile). Detection is achieved with ESI-MS (negative mode drying gas flow set at 9 L/min. Nebulizer gas pressure set at 1,724 bar ; fragmentor voltage set at 70 V ; drying gas temperature set at 250 °C ; Capillary voltage set at 3500 V).

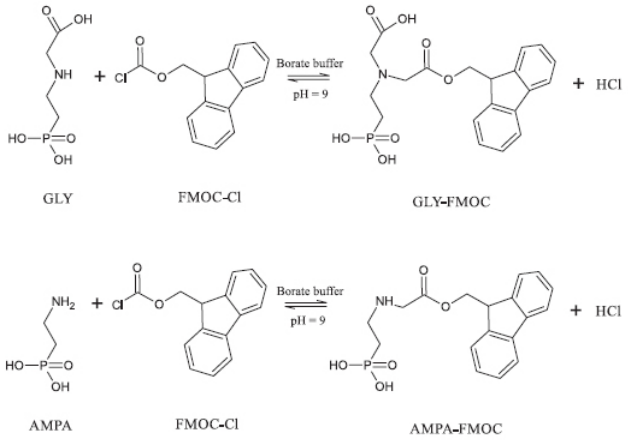

Figure 18 : Derivatization of PMG and AMPA with FMOC-Cl. Source : Catrinck *et al*. (2014)

A calibration method using standard addition and and isotope-labelled analogs internal standards is used for calculation.

This method was updated in 2009 for LC-MS/MS and online SPE and published as USGS method 5-A10. The general principle remains the same. It is stated that "because suspended particulate matter is removed from the samples by filtration, the method only is suitable for analysis of these compounds in the dissolved phase." (USGS, 2009). It was shown that once the derivatization achieved and stopped with phosphoric acid (H_3PO_4), samples can be stored at 4 °C in the dark for at least 60 days.

Two enzyme-linked immunosorbent assays (ELISA) semi-quantitative methods (Abraxis 500081[74] and 500086[75]) produced by the Abraxis corporation (last revision : 2005). The Abraxis 500081 method uses magnetic particles while the Abraxis 500086 method uses a microwell plate. Both methods involve PMG derivatization followed by interaction between PMG and specific antibodies, competition with the PMG enzyme conjugate, washing then revelation with a colouring agent. Intensity of the blue color is inversely proportional to PMG content. These methods are compatible with many matrices, including water, soils, biological fluids and various foods and beverages. Matrices other than water require a variable extraction step prior to the assay. The Abraxis 500086 user guide reports that :

[74] Available at https://www.nemi.gov/methods/method_summary/9244/ (10/02/2020)

[75] Available at https://www.nemi.gov/methods/method_summary/9253/ (10/02/2020)

> "The presence of the following substances up to 10 000 ppm were found to have no significant effect on the Glyphosate ELISA results : nitrate, phosphate, sulphate, sodium fluoride, calcium, magnesium, copper, zinc, iron, and sodium thiosulfate. Manganese up to 100 ppm, humic acid up to 10 ppm, and sodium chloride up to 1M also had no significant effect on the Glyphosate ELISA results." (Abraxis user manual[76], 2005)

The Abraxis ELISA methods are appropriate for routine quality control or preliminary screening but not for accurate quantification. No neutral study comparing this method and chromatographic methods was retrieved in literature. The only article found was carried in collaboration with collaborators of Abraxis corporation (Rubio *et al*., 2003) stating that "no statistically significant differences (95% confidence interval) were found between the ELISA and HPLC analysis" of water samples spiked with PMG.

The FDA SRM methods for glyphosate and AMPA determination in food matrices is directly based on the Laboratory Information Bulletin (LIB) 4604 (FDA,2016), 4595 (FDA,2015a), 4596 (FDA,2015b) and for PMG, AMPA and glufosinate determination in egg, milk and soybean as well as corn, respectively. Contrary to the method previously mentioned, the FDA SRM method is direct (no derivatization required). In these methods, an aliquot of homogenized sample is extracted with 10 mM Na_2EDTA (to prevent interaction of the analytes with cations) and 50 mM acetic acid (to precipitate the majority of proteins). The extract is then centrifuged and the supernatant undergoes SPE through an Oasis HLB cartridge previously conditioned with 2 mL of ethanol and 2 mL of extracting mixture, to retain particles and phospholipids. The cleaned up extra is then directly injected in HPLC equipped with Acclaim Trinity Q1 (3 µm, 100 x 3 mm) column. For MS detection, "two multiple reaction monitoring (MRM) channels were monitored in the method for each target compound to achieve true positive identification. Three isotope-labelled analogs corresponding to each analyte were used as internal standards to counter matrix suppression effects." (FDA, 2015a, 2015b, 2016).

1.12.3. Official methods for PMG determination in Europe and in Belgium

The QuPPe-PO method from the European Union Reference Laboratory - Single residue method (EURL-SRM, 2020) has been designed for the extraction of compounds incompatible with the QuEChERS method in foods of plant origin and honey. This method proposes a matrix-matched calibration. The method include standards steps for fruits and vegetables, and optional steps for dry commodities and pulses and nuts. Only the standard procedure for fruits and vegetables is considered here. The method first consists in cryogenic grinding the sample, adjusting its water content if its below 80 % and spiking with internal standard (isotope-labelled analog). Afterwards, the sample is extracted with 10 mL acidified methanol solution. The extract is preferably frozen before centrifugation for 5 min at ≥ 3,000 g (ideally ≥ 10,000 g) at low temperature. The objective of freezing is to freeze-out as much interferences as possible in order to facilitate sedimentation. A 2 - 3 mL aliquot of supernatant is filtered through a syringe filter (0.2 µm or 0.45 µm followed by 0.2 µm in case of clogging) before injection in LC-MS/MS.

The method for PMG and AMPA determination developed by the Scientific Institute of Public Health[77] (ISP) (Belgium) in collaboration with the AGES (Austria) (hereafter called ISP-AGES method) (ISP, 2010) is recognized by the FASFC in Belgium for official trials. In this method, samples are spiked with internal standard (isotope analog) and added with 10 mL water, 10 mL methanol and 5 mL dichloromethane (liquid-liquid extraction of apolar interferences). The sample is homogenized with a high performance dispersing instrument (Ultra-Turrax®) before centrifugation at 4,000 rpm at 4 °C. A 10 mL aliquot of the aqueous supernatant is isolated and concentrated through evaporation to dryness (55°C, approximately 3 h) and re-dissolved by adding 1 mL of water and soaking in an ultrasound bath. The sample is transferred in a centrifuge tube and

[76] Available at https://www.nemi.gov/methods/method_summary/9253/ (10/02/2020)

[77] Now merged with the Centre for Veterinary and Agrochemical Studies and Research to form Sciensanor

1 mL of borate buffer is added before homogenization. Afterwards, 1 mL of FMOC-Cl is added and the extract is homogenized. After at least 4 hours and maximum four days, derivatization is stopped with 2 mL dichloromethane and the sample is centrifuged 10 minutes at 4 rpm. At this stage, the sample can either be directly injected in LC (500 µL) or further purified in SPE. For that later option, the SPE column (STRATA X, Phenomenex) is first conditioned with 3 mL methanol and equilibrated with 3 mL water. Derivatized sample (1 mL of aqueous phase) is then loaded, washed with 3 mL methanol 5% and eluted with methanol. The eluate is evaporated to dryness, re-dissolved in 1 mL water and injected in LC system (5 µL). Separation conditions are the following : mobile phase A : methanol/water (10:90 v/v), mobile phase B : methanol/water (90:10 v/v), Acquity UPLC BEH C18 (1.7µm 2.1x100mm.

1.12.4. Methods described in literature

Many methods are described in literature, with various principles such as colorimetry, LC, GC etc. Only the methods relevant for comparison with this work will be described.

Guo *et al*. (2016) describe a method for PMG and AMPA direct determination in water consisting in a filtration on 0.45 µm polyethersulfone syringe filters followed by a dilution of 150 µL of sample with 100 µL of formic acid 0.1 % and 50 µL of internal standard (isotope analog). The sample is then directly injected on a Bio-Rad Micro-guard Cation-H+ column (4.6 mm × 30 mm × 9 µm).

Liao *et al*. (2018) extracted PMG and AMPA from food of plant origin with a mixture of Milli-Q water, acidified water, methanol and dichloromethane, with proportion depending on the water content of the sample. After centrifugation, the aqueous extract is derivatized overnight at room temperature with FMOC-Cl at pH 9 (borate buffer). The reaction was stopped with HCl 37 % and the pH adjusted to 1.5. The extracted is cleaned in

Sun *et al*. (2017) extracted PMG from soils and sludges using a solution of 0.03 M sodium phosphate (Na_3PO_4) and 0.01 M trisodium citrate. A cleaning step consisted in adjusting the pH to 9 with HCl 1.0 M, incubating for 10 min before filtration and washing twice with 50 mL n-hexane to remove non-polar interferences. Cleaned extracts were then derivatized with FMOC-Cl at pH 9 (borate buffer) and injected in a HPLC system equipped with a 250mm × 4.6 mm C18 column with 5 µm particles (35 ± 5 °C) and a fluorescence detector. AMPA is not mentioned in the article.

Ibanez *et al*. (2005), Botero-Coy *et al*. (2013) and Sun *et al*. (2019) similarly extracted PMG and AMPA from dried soils with 5–10 mL 0.6 M KOH for 10–30 min under agitation. Extracts were centrifuged at 2275–3500 rpm for 10–30 min. Then, the supernatant was diluted with water and spiked with isotope labelled internal standard (ILIS). The pH of the extract was adjusted to 9 by adding HCl 6 M and/or 0.6 M, before SPE cleaning on a OASIS HLB cartridge (60 mg), previously conditioned with 2 mL methanol and 2 mL water (pH 9). The eluate was derivatized overnight by addition of 120–200 µL FMOC-Cl 12g/L and 120 µL borate buffer 50 g/L (pH 9) before filtration with 0.45 µm nylon disposable syringe filters and injection in LC equipped with a C18 column.

Plastic vessels were used in most methods (USGS, 2002; Guo *et al*., 2016 ; Waters Corporation, 2019[78]; EURL-SRM, 2020) because interaction of PMG and AMPA with glass result in a loss of recovery. Alternatively, glasswork silanization is used in the ISP-AGES method (2010) but this practice is particularly tedious in routine analysis and has no economic advantage.

The most relevant methods mentioned above are compared more completely with regard to sample preparation in Annex 18 and LC separation in Annex 19. The MS/MS detection conditions are not compared because the specificity of each instrument makes comparison difficult and somehow irrelevant.

[78] https://www.waters.com/waters/support.htm?lid=135032660&cid=511442 (13/02/2020)

1.13. Considerations on the instrumentation

1.13.1. Differences between HPLC and UHPLC

Ultra High Performance Liquid Chromatography (UHPLC) is the common name for liquid chromatography with pressure capacity up to 15,000 psi (1030 bar) and particle size under 2 µm, while standard HPLC particle size is in the range 2.5–5 µm and up to 5,000–6,000 psi (350–400 bar).

UPLC (Ultra Performance Liquid Chromatography) is a registered trademark of Waters Corporation, the first to introduce this technology, in 2004. Both designations UPLC and UHPLC are used interchangeably in literature and considered as synonyms, regardless of the manufacturer.

The fundamental theory on chromatography useful to understand the following elements is provided in Annex 20 if necessary. The advantages of UHPLC systems over HPLC systems are the following :

- Eddy diffusion is reduced due to both smaller particles and a better packing of the column;
- Longitudinal diffusion is reduced as the linear velocity is higher;
- On one hand, resistance to mass transfer in the stationary phase is increased proportionally to the flow rate; but on the other hand, it is reduced proportionally to the square of particle size as path length in smaller particle is reduced. Globally, resistance to mass transfer (slope of the C term in Van Deemter equation) is reduced in UHPLC ;
- Resistance to mass transfer in the mobile phase is reduced as the average diameter of the channels formed by interstitial space between particles is reduced along with particle size.
- Optimal linear velocity increases because of the reduced general resistance to mass transfer ;
- Because pressure drop per unit of length increases with the inverse of the square of the particle diameter ($\Delta p \ / \ L \propto 1 \ / \ {d_p}^2$, see Equation 3), a higher operating pressure (up to above 1030 bar for UHPLC against ~400 bar for HPLC) along with a smaller internal column diameter (around 2 mm against 4 mm in HPLC) allows to reach higher optimal linear velocity range.

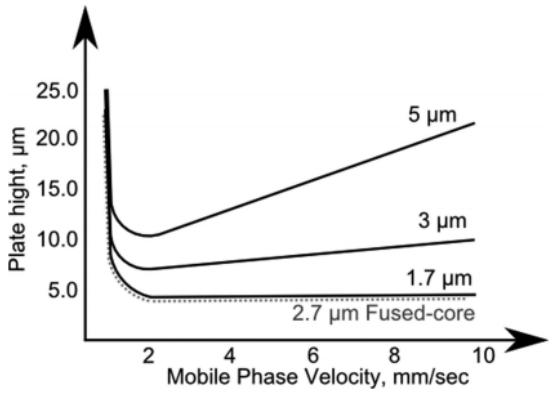

Figure 18 : Typical Van Deemter curves in LC with various particle diameter. Source : Jakimska *et al.*, 2014

As the particle diameter decreases, Van Deemter curve flattens (Figure 18). Higher linear velocity are optimal and plate height is less sensible to linear velocity variations.

$$\Delta P = \frac{\eta \, F \, L}{K^0 \, \pi \, r^2 \, {d_p}^2} \qquad (3)$$

ΔP: pressure loss [N m^{-1}]
η: dynamic viscosity [N s m^{-2}]
F: volumetric flow [mL min^{-1}]
L: length of the column [m]
K^0: specific permeability of the stationary phase
r: column radius [m]
d_p: particles diameter [m]

- As optimum linear velocity increases, analysis time is reduced;
- Reduced internal column diameter and column length allows smaller injection volume, reduced solvent use, reduced extra-column volume and reduces extra-column tubing

diameter, also reducing broadening attributable to physical components of the system others than the column itself (Hong and McConville, 2018[79]).

- Flow rate is also limited by the capacity of the MS detector, the smaller column volume, lower injection volume and lower flow rate in UHPLC allows of flow splitting in UHPLC provides improved ionisation and higher sensitivity with MS detectors.

- The inlet capacity of MS detectors with electrospray ionisation (ESI-MS) being limited by the ionisation efficiency and ion transmission efficiency to the detector itself (Camenzuli *et al.*, 2012), HPLC often requires the use of post-column flow splitters, reducing sensitivity. The use of such splitters may be avoided in some UHPLC systems provided the lower flow rate.

1.13.2. Considerations regarding column chemistry and particles characteristics

The analysis of highly polar compounds such as PMG in liquid chromatography is difficult without derivatization in normal phase or reversed phase. Indeed, they are barely retained on standard reversed phase columns such as C18, and their solubility is very poor in organic solvents used with normal phase in comparison with their affinity for the stationary phase. This situation can be overcome with hydrophilic interaction liquid chromatography.

In hydrophilic interaction liquid chromatography (HILIC), compounds are eluted on a polar stationary phase, such as unbonded silanols, anionic, cationic, zwitterionic or amides. Weak solvents used are typically acetonitrile or acetone, while strong solvents include water, methanol, ethanol or isopropanol, in decreasing order of strength. The mobile phase should contain at least 5 % of strong solvent to maintain the stationary phase wet (solvated).

On a HILIC column, a polar solvent layer is adsorbed on the the polar stationary phase, while the rest of the mobile phase is richer in low-polarity solvent (Figure 19).

Retention of polar and charged analytes occurs via several mechanisms, namely liquid-liquid partitioning between the solvents layers, ion exchange and other hydrophilic interactions (hydrogen bonding, dipole-dipole, induced dipole-dipole...). The mobile phase should contain at least 70 % of weak mobile phase to maintain partitioning.

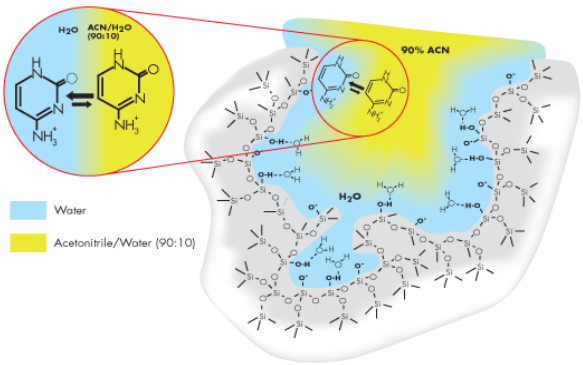

Figure 19 : HILIC mechanism at molecular scale.
Source : Waters Corporation[80]

Many factors should be taken into account in order to optimize a method using a HILIC column. One of the main factor affecting retention is the pH of the mobile phase. It should be selected so that the ionisation of the analytes and thus retention and sensitivity in MS are optimized. For acidic compounds, ionization increases as pH increases. However, the same rule apply to silanols (ionization between pH 5–9) on the surface of the silica particles. Ionized silanols are negatively charged and thus increasing repulsion between the stationary phase and anionic compounds. This problem can be improved by reducing the density of silanols on the particles.

Ethylene bridged hybrid (BEH) particles are particles made of a silica structure with a given proportion of embedded bridged ethanes (Figure 20). The surface of BEH particles is hence less hydrophilic than pure silica because of the bridged ethanes, but it also exhibits less silanols site and is thus less negatively charged at high pH, which reduces repulsion of anionic compounds. In

[79] https://www.waters.com/webassets/cms/library/docs/720005723en.pdf

[80] Comprehensive Guide to HILIC - Hydrophilic Interaction Chromatography

addition, BEH particles are more resistant to high pH degradation than standard silica. Other types of silica (inorganic-organic or type C silica) also reduces influence of silanols.

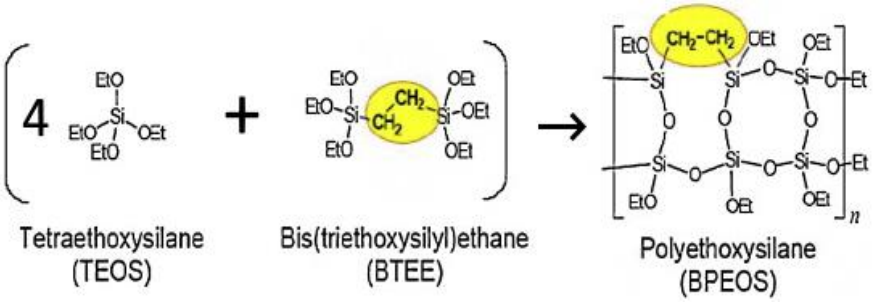

Figure 20 : Synthesis of ethylene bridged hybrid silica (polyethoxysilane). Source : Wang *et al.*, 2012

The high organic solvent content of the mobile phase in HILIC provides two other advantages :

- Increased sensitivity in ESI-MS compared to high water content mobile phase thanks to easier droplet formation, solvent evaporation and ionization.
- Extracts with high organic solvent content obtained from extraction or SPE are compatible with the initial conditions of elution and can therefore be directly injected, without need for evaporation to dryness and reconstitution in water.

However, high organic solvent content also comes with a drawback : direct injection of aqueous samples often results in poor peak shape and retention because of water being a strong eluent. More informations on HILIC separation can be found in the review of Buszewski and Noga (2012) or elsewhere in literature.

In this study, a HILIC column with BEH tri-functionally bonded with diethylamine (DEA) ligands (Waters Corporation, 2019[81]) (Figure 21).

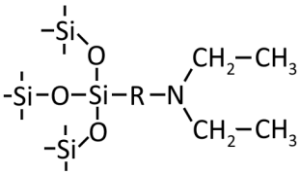

Figure 21 : Tri-functionally bonded silica with diethylamine ligand.

Other stationary phase chemistry has been investigated in literature for determination of polar pesticides. Stationary phase chemistry used in combination with derivatization included C18 reversed phase (Botero-Coy *et al.*, 2013). Stationary phase chemistry used for direct determination (without derivatization) include ion exchange, mixed mode (Guo *et al.*, 2016) containing simultaneously anionic and cationic sites along with alkanes on one or several ligands (Annex 21) and hypercarb (also known as "graphitized carbon" or "porous graphitic carbon") consisting of particles covered with multilayer graphite clusters able to retain polar or ionic compounds through induced dipoles (Debye-like forces) (West *et al.*, 2010).

Superficially porous particles (also known as "core-shell", "pellicular" or "Fused Core™") is often presented by manufacturers as a cheaper alternative to UHPLC. It allows to reach speed and efficiency comparable to UHPLC with pressure twice as low (around 400 to 600 bar), increasing hardware and column lifespan compared to UHPLC, thus making it cheaper. The main inconvenient of superficially porous particles is their lower loading capacity compared to standard fully porous particles (Waters Corporation, 2008[82]). Although presented as opposed alternative to UHPLC, this technology is compatible with UHPLC systems.

Some basic reminders on mass spectrometry are provided in Annex 22.

[81] https://www.waters.com/waters/support.htm?lid=135032660&cid=511442 (18/02/2020)

[82] https://www.waters.com/webassets/cms/library/docs/720002825en.pdf (18/02/2020)

1.14. Factors affecting the chromatographic separation in HILIC

The factors affecting the chromatographic parameters in HILIC are considered in this section. Characteristics of the column (stationary phase ligand and matrix, column dimension, particles size etc.) were already considered previously and were not investigated since these parameters are already fixed.

1.14.1. Ionic strength of the mobile phase

In a reasonable concentration range (typically 5–50 mM), ion strength improves retention and peak shape by acting positively with regards to the two retention mechanisms :

- Ionic strength provides sufficient competitive ions for ion exchange-based retention and prevent tailing;
- Ionic strength further increases the polarity of the aqueous layer and the provide ions that form ion pair with the analyte, increasing its solubility in the aqueous layer and improving retention through partitioning.

In practice, the first effect seems to be predominant as increasing ionic strength do not affect the retentivity of neutral analytes (Craven *et al*., 2019).

In contrast, when ion strength is too high, it competes too strongly with the analyte for ion exchange sites and may have a salting-out effect, negatively affecting both retention mechanisms.

1.14.2. pH of the mobile phase

The pH rules the ionisation state of the analyte(s) (if ionisable), of the stationary phase ligands (if ionisable) and of interferences, strongly affecting retention and sensitivity in MS. Non-ionizable molecules are little or unaffected by the pH.

Optimum pH conditions in HILIC are hard to characterize because of the measured pH being quenched towards neutral pH when the content of aprotic solvent increases because of the different electrochemical properties[83] of the mixture compared to pure water. Furthermore, at a given point in time, composition of the mobile phase (and thus pH) varies gradually from the stationary phase surface (aqueous layer) to the bulk rich in organic solvent. In addition, composition of the whole mobile phase also varies in time depending on the gradient.

The choice of organic the acids (commonly called additives) and salts (commonly called buffers) used to control de pH of the mobile phase is restrained by two properties :

- Solubility in the organic mobile phase, usually acetonitrile ;
- Volatility : only easily nebulized acids and salts should be used in order to avoid mineral deposits inside the spectrometer with electrospray ionisation.

The most commonly used additives and salts in the acidic pH range, with compatibility with ESI-MS, are formic acid /ammonium formate and acetic acid/ammonium acetate.

Heaton *et al*. (2014) studied the effects of formic acid/ammonium formate systems at various concentrations and reported poor peak shape with formic acid only, but ion suppression[84] with ammonium formate in the range 5–50 mM. It is also concluded that "the presence of a reasonable concentration of ammonium ions is likely to encourage [the] formation of the [water] layer as well as masking some of the effects of ionic interactions" (Heaton *et al*., 2014).

[83] junction potential, dielectric constant...

[84] reduced sensitivity in mass spectrometry due to a competition between ionogenic species for ionisation efficiency.

As the composition of the mobile phase changes according to the gradient, it is often advised to buffer both solvents with the same concentration of buffers and additives.

As said earlier, ionization of acidic compounds increases as pH increases. However, the same rule applies to silanols (ionization between pH 5–9) on the surface of the silica particles. Ionized silanols are negatively charged and thus increasing repulsion between the stationary phase and anionic compounds. This phenomenon justifies the use of specific silica with less silanols, such as the BEH particles discussed previously.

1.14.3. Sample solvent

The injection of a solvent mixture that do not match the strength of the mobile phase is a major cause of poor peak shape in HILIC (Waters Corporation, 2014). This is especially the case when injecting samples with high water content, because water is the strong solvent in HILIC. Ideally, the sample solvent should be as close as possible to the initial mobile phase composition (85–90 % acetonitrile). However, in practice, the sample preparation usually does not leave the possibility to comply easily with this prescription[85]. Moreover, polar compounds such as PMG and AMPA usually exhibit very low solubility in mixtures with high acetonitrile content. Sample solvent mixtures with variable content in acetonitrile as well as alternative diluent can be investigated to improve peak shape. Small amounts (0.2 %) of formic acid or ammonium hydroxide may be added to improve solubilization.

1.14.4. Injection volume

Generally, a larger injection volume increases the sensitivity of the method. However, a larger injection volume also results in poor peak shape because of solvent strength mismatch or to overloading.

1.14.5. Mobile phase solvents

Acetonitrile is the most common organic solvent used, however acetone is also proposed by some manufacturers as a substitute (Waters). In case a less abrupt elution is required, methanol, ethanol or isopropanol are weaker alternative to water. However, they should not be used if the sample contains high water content, for the same reasons as previously.

1.14.6. Needle wash solvent

For the same reason, again, the needle wash solvent should be as close as possible to the initial mobile phase composition to avoid contamination of the sample with strong solvent and altered retention and peak shape.

1.14.7. Composition of the equilibration and washing mixtures

Chelating compounds are known for their interaction with metal. Undesirable interaction with metal parts (frit, column walls) may cause tailing. A phosphoric acid wash may be used to displace adsorbed PMG and AMPA.

1.14.8. Elution gradient

Because partitioning is an important mechanism affecting retention, small changes in gradient slope often have important consequences on retention. Reducing the slope increases retention but widen the peaks.

[85] Evaporation of water sample is time-consuming and can not be performed in standard glassware such as the common rotary evaporator, in the case of polar analytes that are readily adsorbed on glass. Evaporation under nitrogen flow should be preferred.

2. Objectives of this work

This work aims at validating methods for the determination of PMG and AMPA in sugar beet root, environmental water and soil using liquid chromatography :

a) preferably without derivatization and using a diethylamine HILIC column (Anionic Polar Pesticide 130 Å, 5 µm, 2.1 mm × 100 mm from Waters Corporation);

b) or, alternatively, using derivatization with FMOC-Cl and a phenyl column (BEH Phenyl 130 Å, 1.7 µm, 2.1 mm × 100 mm from Waters Corporation) when direct determination does not meet the performance requirements.

Prior to the validation, the sample preparation and elution conditions (based on the literature reviewed above and summed up in Annex 18 and 19) will be optimized or adapted if necessary.

3. Materials

3.1. Instrumentation

3.1.1. Chromatographic system and detector

- Chromatographic system : ACQUITY UPLC H-Class PLUS System with Quaternary Solvent Manager (Waters corporation);
- Anionic Polar Pesticide Column, 130 Å, 5 µm, 2.1 mm × 100 mm (Waters corporation) (more details provided in Annex 23);
- Pre-column : Anionic Polar Pesticide VanGuard Cartridge, 130Å, 5µm, 2.1 mm × 5 mm (Waters corporation) (more details provided in Annex 23);
- Xevo TQ-S micro (Waters corporation) equped with electrospray ionization system, Alphagaz 1 N_2 as desolvation gaz and Alphagaz Ar as collision gaz.

3.2. Equipments

- Centrifuge Ohaus Frontier™ 5816R (radius of the rotor : 164.7 mm);
- Blender Robot Coupe R6VV;
- Agitator Edmund Bühler SM 25;
- Analytical balance Kern ALT 310−4 AM;
- Trebuchet Kern PLJ;
- Densimeter Mettler Toledo DA-100M;
- Automatic pipette (1–10 mL; 100–2000 µL; 20–200 µL; 0.5–10 µL);

- Polymethylpentene (PMP) volumetric flasks (10,25, 50 and 100 mL) (Vitlab);
- Polypropylene (PP) vials (12 × 32 mm, screw cap, PTFE/silicon septa, preslit) (Waters);
- Glass (borosilicate, type 1, class A, 33 expansion) vials (12 × 32 mm, Screw cap, PTFE/silicon septa, preslit (Waters);
- Polypropylene (PP) centrifuge tubes (50 and 15 mL, screw cap);
- Polypropylene (PP) tubes (1.5 mL, snap cap);
- Polypropylene centrifuge tubes;
- Hydrophilic polytetrafluoroethylene (H-PTFE) 0.20 µm syringe filters (Macherey-Nagel).

3.3. Reagents

- Glyphosate (N-(phosphonomethyl)glycine), 99.87 % (Dr Ehrenstorfer);
- Isotope-labelled Glyphosate : 1,2-$^{13}C_2$ ^{15}N, 100 mg/L (Dr Ehrenstorfer);
- AMPA (aminomethylphosphonic acid), 91.10 % (Dr Ehrenstorfer);

- Water (H_2O) (mQ);
- Acetonitrile (CH_3CN), ULC/MS grade (Biosolve);
- Ammonium formate ($HCOO^-NH_4^+$) Optima® LC/MS ≥99.0 % (Fisher Scientific);
- Ammonium hydroxide (NH_4OH) 25 % w/w (Merck);
- Disodium ethylenediaminetetraacetate dihydrate ($Na_2EDTA{\cdot}2H2O$), >99 % (Merck);
- Fluorenylmethyloxycarbonyl chloride (FMOC-Cl), 98 % (Acros Organics);
- Formic acid (HCOOH) Optima® LC/MS grade 99.0 % (Fisher Scientific);
- Methanol (CH_3OH, ULC/MS - CC/SFC grade (Biosolve);
- Phosphoric acid (H_3PO_4) 85 % w/w (Acros organics)

3.4. Sample materials

The sugar beet root sample was collected on 26/02/2020 at Florennes, Belgium (50.269086 N, 4.728564 E. The sample was frozen prior to grinding and storage at - 18°C until extraction.

4. Method

4.1. Sample preparation

The method for frozen sugar beet extraction was adapted from the QuPPe-PO method (EURL-SRM, 2019) and is illustrated in Figure 22.

The QuPPe-PO method aims to obtain an extract containing approximately 50:50 v/v water/methanol. The test sample mass and volume of extracting solvent added were scaled down for convenience.

The method was validated using the gradient shown in Table 2 and the settings listed in Table 3.

Table 2 : Gradient used for method validation.

Time (min)	% A	% B	Curve[(a)]
0.0	10	90	-
2.0	85	15	2
6.5	85	15	6
7.0	10	90	1
11.0	10	90	1

(a) : curvature code : 1, immediate transition - 2, gradual transition - 6, linear transition

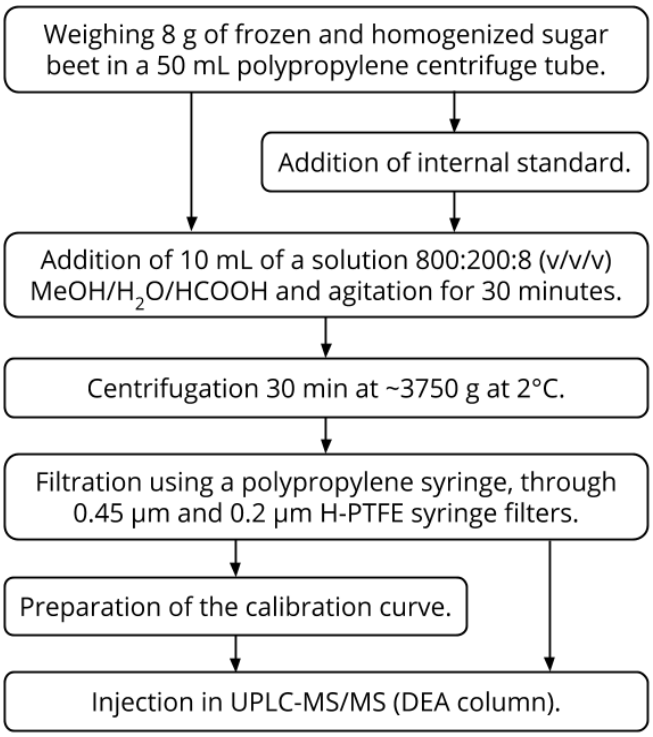

Figure 22 : Flow-chart of the method for frozen sugar beet extraction based on the QuPPe-PO from the EURL-SRM.

Table 3 : Chromatographic settings used for method validation.

Calibration range (mg/L)		Injection volume (µL)	Temperature (°C)		Flow rate (mL/min)	Strong mobile phase (A)	Weak mobile phase (B)	Needle wash
PMG	AMPA		Column	Sample				
0.1–10	0.091–9.1	10	50	10	0.500	mQ water 0.9 % (v/v) HCOOH (~ 236.2 mM), 315 mg/L (~5 mM) $HCOO^-NH_4^+$	acetonitrile 0.9 % (v/v) HCOOH (~ 236.2 mM), 315 mg/L (~5 mM) $HCOO^-NH_4^+$, 5 % water	0.2 % (v/v) H_3PO_4 in 80:20 mQ H2O/MeOH
0.08–1	0.073–0.91	10	50	10	0.500	mQ water 0.9 % (v/v) HCOOH (~ 236.2 mM)	acetonitrile 0.9 % (v/v) HCOOH (~ 236.2 mM)	0.2 % (v/v) H_3PO_4 in 80:20 mQ H2O/MeOH

The conversion between matrix concentration and extract concentration is given in Equation 4 :

$$(4) \qquad Concentration\ (mg/L_{extract}) = \frac{Concentration\ (mg/kg_{matrix}) \times test\ sample\ mass\ (kg_{matrix}) \times Recovery}{Solvent\ volume\ (L_{extract})}$$

4.2. Optimization of the chromatographic settings

The starting chromatographic settings were based on the method for PMG analysis provided by the manufacturer of the column[86] and are shown in Table 4 and 5.

The chromatographic data monitored for optimization were :

- Peak retention time (RT, in minutes)
- Peak area (arbitrary units)
- Peak height (arbitrary units)
- Peak width (peak end time - peak start time, in minutes)
- Peak asymmetry (b/a, dimensionless)
- Peak signal-to-noise ratio (S/N, dimensionless)

Table 4 : Gradient of the initial method for sugar beet analysis.

Time (min)	% A	% B	Curve[(a)]
0.0	10	90	-
2.0	85	15	2
6.5	85	15	6
7.0	10	90	1
11.0	10	90	1

(a) : curvature code :1, immediate transition - 2, gradual transition - 6, linear transition

Table 5 : Chromatographic settings as recommended by the manufacturer of the column.

Temperature (°C)		Flow rate (mL/min)	Strong mobile phase (A)	Weak mobile phase (B)	Injection volume (µL)	Needle wash
Sample	Column					
10	50	0.500	mQ water 0.9 % (v/v) HCOOH (~ 236.2 mM)	acetonitrile 0.9 % (v/v) HCOOH (~ 236.2 mM)	10	0.2 % (v/v) H_3PO_4 in 80:20 mQ H_2O/MeOH

A stepwise optimization was carried out on the gradient and the mobile phase composition with the aim to reduce tailing and shorten analysis time. For this optimization, the same standard solution 10 mg/L PMG and 9.1 mg/L AMPA in 50:50 (v/v) mQ water/methanol was injected (n = 3) after each modification of the method, ensuring that any measured change is attributable to the method and instrument variability.

4.3. Practical considerations

4.3.1. Preparation of the mobile phases

Only volatile additives and buffers should be used with ESI[87]. The chosen additives and buffers for pH and ionic strength regulation were formic acid and ammonium formate. Acetic acid/ammonium acetate may be used as well.

As recommended by the manufacturer of the column (Waters Corporation, 2014), both strong and weak mobile phases used with the Anionic Polar Pesticide HILIC column were prepared with the same concentration of buffer and additives (formic acid/ammonium formate).

When added to acetonitrile, ammonium formate was pre-dissolved in an aliquot of mobile phase A representing 5 % (v/v) of the volume of acetonitrile because the solubility of ammonium formate in acetonitrile alone (< 2 mM) was not sufficient.

The glassware used to contain the mobile phase was systematically cleaned three times with mQ water, then with methanol, then with the solvent it was going to contain. The rinsing with methanol aims to eliminate any bacterial or algal development, which are known to clog the system and increase operating pressure.

Fresh mobile phases were prepared each day.

[86] https://www.waters.com/waters/support.htm?lid=135032660&cid=511442 (20/03/2020)

[87] https://www.waters.com/waters/fr_BE/Solvents-and-Caveats-for-LC-MS/nav.htm? (20/03/2020)

4.3.2. Needle wash

It was observed during preliminary testing that methanol and even mQ water/methanol (80:20 v/v) were not sufficiently strong solvents to completely remove PMG and AMPA from the sample stream line, resulting in a considerable carry-over and even cross contamination of blanks. adsorbed on the stainless steel injection needle, resulting in an important carry-over and even cross-contamination of different vials.

Indeed, it is well known that carry-over arises from undesirable interaction between the polar compounds and stainless steel parts of the chromatographic system, especially the injection needle (Guo *et al*., 2016). A solution 0.2 % phosphoric acid in 80:20 methanol/water (v/v) was used as needle wash to eliminate carry-over, accordingly with the proposition of Guo *et al*. (2016).

4.3.3. Column equilibration and system cleaning

Before the first use, the column was conditioned with 50 column volumes (15 mL) of 50:50 water/acetonitrile at a flow rate of 0.5 mL/min as recommended by the manufacturer[88]. Before any set of injections, the column was equilibrated in the initial conditions (0.5 mL/min, 10:90 A:B, 50°C) for at least 15 minutes (15 empty column volumes). Before each single injection, the column was equilibrated in the initial conditions for at least 3 minutes.

Before any set of sample injection, an elution cycle without injection was performed to ensure that the stationary phases are not contaminated. Afterwards, mQ water followed by blank sample or blank extraction solvent were injected to ensure that the injection line and the extracting solvent were free of detectable residues of analyte. Water was also injected at the end of each set of injections to ensure proper cleaning of the system.

The cone of the mass spectrometer was regularly cleaned, especially after injecting sugar beet extract, because the thermal degradation of the sample with high sucrose content induced heavy soiling.

4.3.4. Containers material

It is well known that interaction between glass and the two polar analytes, PMG and AMPA, result in a loss of recovery, especially at low concentration. This is the reason why most methods use plastic containers and flasks (USGS, 2002; Guo *et al*., 2016; Waters Corporation 2019; EURL-SRM, 2019).

In this study, only polymethylpentene (PMP) volumetric flasks and polypropylene (PP) centrifuge tubes were used. The effect of vials material (glass or polypropylene) was first tested by injecting sugar beet extract spiked at the lowest concentration included in a calibration curve (0.08 mg/L PMG and 0.073 mg/L AMPA) (n = 5) in both glass and polypropylene vials. When not mentioned otherwise, glass vials were used.

4.3.5. Preparation of standard stock solutions

Standards stock solutions of PMG and AMPA are commonly prepared in mQ water since this is the solvent in which their solubility is the highest (Annex 2). For convenience purpose, the stock solutions were prepared in water/methanol 75:25 (v/v) to prevent freezing upon storing at -18°C.

[88] https://www.waters.com/waters/support.htm?lid=135032660&cid=511442 (20/03/2020)

4.3.6. Preparation of calibration curves

Dilutions from the stock solutions were made in 1.5 mL plastic tubes or directly in the vials using automatic pipettes[89].

4.3.7. Peak detection and integration parameters

Peak tailing was ubiquitous because of the high-water content of the sample (Waters Corporation, 2014) and interaction with stainless steel parts of the system. The baseline peak end threshold was set on 5 % to avoid excessive integration of the "tail" causing unreasonable variability in peak width and asymmetry, in addition with biased peak area. The baseline start threshold was set on 1 %.

Even with these settings, the peaks for AMPA sometimes had to be re-integrated manually when the automatic integration was obviously too large, such as the example in Figure 23.

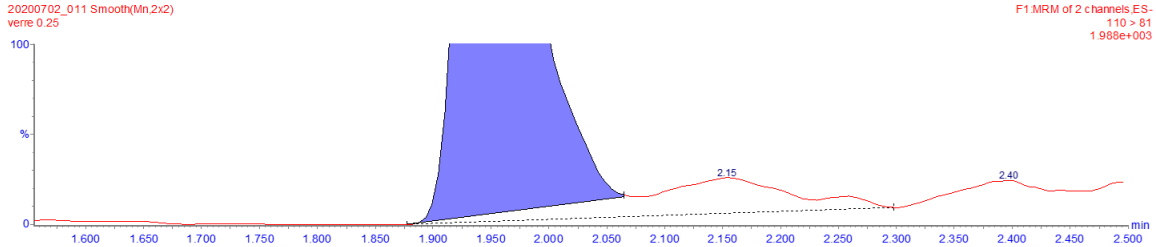

Figure 23 : Example of manual reintegration of chromatogram for AMPA.
(grey dashed line : automatic integration - blue area : manual re-integration)

The area threshold for peak detection was set on 100 (arbitrary units).

4.3.8. Statistical considerations

The significance level (α) was set at 5 %. The statistical treatments were achieved with Excel and R Studio. All the t-tests were performed using the Welch's t-test formula (Equation 5), a generalization of the Student's t-test that takes into account unequal variances and unequal sample size.

(5) $$t = \frac{\overline{X}_a + \overline{X}_b}{\sqrt{\frac{s^2_a}{n_a} + \frac{s^2_b}{n_b}}} \quad \text{with} \quad df = \left(\frac{S_a^2}{n_a} + \frac{S_b^2}{n_b}\right) / \left(\frac{S_a^4}{n_a^2\,(n_a - 1)} + \frac{S_b^4}{n_b^2\,(n_b - 1)}\right)$$

The normality of the samples could usually not be checked because of the low number of replicates and was thus assumed.

4.4. Validation methodology

The different methods were validated in accordance with the procedures in force at the BEAGx and the SANTE/12682/2019 guidelines.

4.4.1. Tuning of MS/MS parameters

The desolvation gas flow was set on 1000 L/Hr, the cone gas flow on 50 L/Hr and the source temperature on 600 °C. The parameters for multiple reaction monitoring (MRM) detection of PMG, AMPA and 1,2-$^{13}C_2$,^{15}N-PMG were optimized both manually and automatically (using IntelliStart software (Waters Corporation)) by infusing a standard solution 10 mg/L PMG and 9.1 mg/L AMPA in water/methanol 80:20 (v/v). Since PMG and AMPA are amphoteric in the pH range of the column

[89] For example, a tenfold dilution was achieved by adding 900 µL of diluent to 100 µL of the solution to be diluted.

(2–7), optimization of the electrospray ionization (ESI) was achieved in both positive and negative mode.

4.4.2. Matrix effect assessment

The matrix effect of frozen sugar beet extract was assessed by injecting (n = 4) blank extraction solvent, blank extract, standards in clean solvent (0.50 mg/L PMG and 0.46 mg/L AMPA) and standards in filtered extract (0.50 mg/L PMG and 0.46 mg/L AMPA). The mobile phases used contained 0.9 % (v/v) formic acid and 315 mg/L ammonium formate.

4.4.3. Linearity assessment

The calibration curves for linearity assessment were prepared in blank sugar beet extract.

In the first place, linearity was assessed in the calibration range was 0.1–10 mg/L for PMG and 0.091–9.1 mg/L for AMPA with mobile phases containing 0.9 % (v/v) formic acid and 315 mg/L ammonium formate. The MRL for sugar beet being 15 mg/kg, the expected extract concentration was ~7 mg/L of extract. Later on, a smaller calibration range (0.08–1 mg/L PMG, 0.073–0.91 mg/L AMPA) with mobile phases containing 0.9 % (v/v) formic acid (no ammonium formate) was investigated to cope with heteroscedasticity of the calibration curves data.

As no peak was detected in the blanks for both PMG and AMPA (area < 100), the area was set to be zero.

The primary criterion for linearity in force at the BEAGx is the non-significance of the nonlinear relationship : $F_{nl} < F_{\alpha = 0.05}$ (with $F_{\alpha = 0.05}$ = 3.23). If not satisfied, the following criteria were evaluated :

- Coefficient of variation (CV) of the calibration points < 15 % at the lowest concentration and < 4 % at higher concentrations ;
- Coefficient of determination (R^2) > 0.996 ;
- Trueness for the set of validation (n = 1) is comprised between 85-115 % at the LOQ and 90-110 % at higher concentrations.

If the three requirements listed above were met, linearity was accepted, even when $F_{nl} < F_{\alpha = 0.05}$. Non-respect of these criteria is highlighted in bold in the results tables.

In addition, the plots of the standardized residuals were systematically checked for homoscedasticity, as it is a primary assumption of least square regression. The results of some Hartley F-tests are provided with these plots when the distinction between hetero- or homoscedasticity was not obvious.

When considering a calibration curve with p concentrations (x), each in n replicates so that the total number of measurements is equal to $N = n \times p$, the observed model is written in Equation 6 and 7 and the corresponding ANOVA table is shown in Table 6.

$$(6) \quad \sum_{i=1}^{p}\sum_{k=1}^{n}(y_{ik}-\overline{y}) = \sum_{i=1}^{p}(y(x_i)-\overline{y}) + \sum_{i=1}^{p}\sum_{k=1}^{n}(\overline{y}_i - y(x_i)) + \sum_{i=1}^{p}\sum_{k=1}^{n}(y_{ik}-\overline{y}_i)$$

$$(7) \quad SS_y = SS_l + SS_{nl} + SS_r$$

with $\underline{y}$: the average peak area of all N observations ; $\underline{y_i}$: the average peak area of a group of replicates of a given concentration ; y_{ik}: observed peak area for concentration i, replicate k ; $y(x_i)$: predicted peak area for concentration i according to the model.

Table 6 : ANOVA table for assessment of the linear and non-linear data relationships.

Variation source	degrees of freedom (df)	Sum of Squares (SS)	Mean Squares (MS)	*F* value
Linear regression	1	SS_l	MS_l	F_l
Nonlinearity	p - 2	SS_{nl}	MS_{nl}	F_{nl}
Residual	N - p	SS_r	MS_r	
Total	N - 1	SS_t		

The SS_r describes the residual variability within the groups of observations of the same concentration that can not explained by the model. It is often mistaken with SS_e(Equation 7) describing the prediction errors, also called the "residuals". It is the SS_e that is minimized by the least squares regression approach.

$$SS_e = \sum (y_i - \hat{y}_i)^2 \quad (12)$$

Linearity was first assessed on ordinary least square (OLS) regression models on untransformed data. Because homoscedasticity was not satisfied, the OLS models on untransformed data could not rigorously be considered reliable. Furthermore, the variability has been observed to increase with the concentration measured. Several options were explored to address the problem :

- Calibrating OLS regression models on transformed data (square root of x and y) ;
- Calibrating weighted least square (WLS) regression models on untransformed data using the following weighting functions :
    - Weight = 1/x (weight inversely proportional to the concentration). This weighting function is the first to come to the mind when considering that the variability of the residuals increases with the concentration, as seen in the plot of the residuals;
    - <Weight = $1/y^2$ (weight inversely proportional to the relative error between each observed area and the predicted area at the corresponding concentration). This weighting function has been suggested by Toffalis (2009) and is equivalent to minimizing the squared relative error rather than the squared "absolute" error (Equation 28).

$$\text{squared relative error} = \sum_i^N \left(\frac{y_i - \widehat{y_i}}{y_i}\right)^2 = \sum_i^N \frac{1}{y_i^2}(y_i - \widehat{y_i})^2 \quad (28)$$

      This weighting function is theoretically more accurate than 1/x because it depends on the observed area and not the concentration which can not be exactly the same among replicates. In that sense, the weighting is specific to each point measured and not to each group of replicates for each concentration.

    - Weight = $1/s_y^2$ (weight inversely proportional to the variance of the observed areas at a given concentration). This weighting function is theoretically optimal when it comes to improving homoscedasticity. The calibration points are considered more informative (i.e. reliable to calibrate the model) when their variance is low.

  Weights of the blanks were set equal to weights of the lower concentration of the curve.
- Calibrating OLS and WLS regression models on data from a reduced calibration range (0.08–1 mg/kg).

The most practical metric to quantify the accuracy of a linear regression model and compare several models is the confidence interval. The most common and conventional confidence interval (and standard error) examined is the standard error on direct prediction ($SE_{\hat{y}}$) (Equation 13), i.e. the standard error of the prediction of y on the basis of x.

$$SE_{\hat{y}} = SE_y\sqrt{1+\frac{1}{n}+\frac{(x-\bar{x})^2}{SS_x}} \quad \text{with} \quad SE_y = \sqrt{\frac{SS_e}{n-2}} \tag{13}$$

But since the purpose of the calibration curve in analytical chemistry is to perform inverse predictions (i.e. the determination of x -the concentration- on the basis of y -the measured peak area-), the standard error for inverse prediction ($SE_{\hat{x}}$) and the associated confidence interval ($CI_{\hat{x}}$) are more relevant.

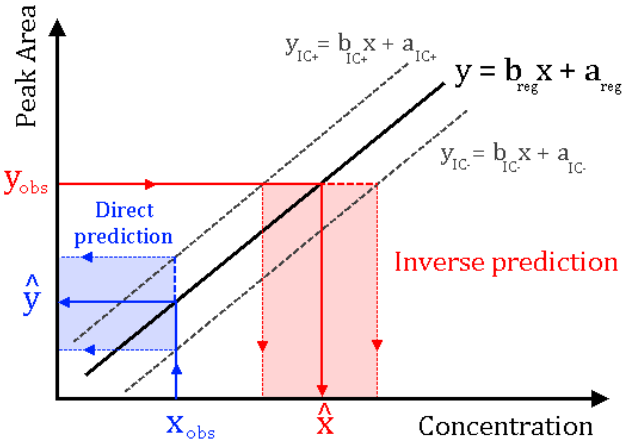

Figure 24 : Illustration of direct and inverse prediction using linear regression.

In their articles, Demidenko *et al.* (2013) and Parker *et al.* (2011) exposed that the determination of $SE_{\hat{x}}$ associated with the prediction of x on the basis of y, the slope (b) and the intercept (a) of the linear regression model (Equation 14) is not trivial because it involves a ratio of two normally distributed random variables (y and $\hat{\beta}$) with $\hat{\beta}$ itself being an estimation of β (the "true" regression coefficient between x and y) with its own confidence interval. Note that the graphical determination remains valid.

$$\hat{x} = \frac{y-a}{b} \tag{14}$$

Expressions of the $SE_{\hat{x}}$ (Equation 15) and the corresponding$CI_{\hat{x}}$ for bilateral hypothesis testing (Equation 16) are given in Equation 15 and 16 (Demidenko *et al.*, 2013; Parker *et al.*, 2011) :

$$SE_{\hat{x}_i} = \sqrt{\frac{1}{n-2}\sum_{i=1}^{n}(\hat{x}_i - x_i)^2} = \sqrt{\frac{1}{n-2}\sum_{i=1}^{n}(\frac{y_i-a}{b} - x_i)^2} = \frac{1}{b}\sqrt{\frac{1}{n-2}\sum_{i=1}^{n}(y_i-\hat{y}_i)^2} = \frac{s_y}{b} \tag{15}$$

$$CI_{\hat{x}_i} = \hat{x}_i \pm t_{1-\alpha/2} \times SE_{\hat{x}_i}\sqrt{1+\frac{1}{n}+\frac{SE_{\hat{x}_i}}{SS_x}} \tag{16}$$

with $t_{1-\alpha/2}$ the $(1-\alpha/2)$th quantile of the Student's t distribution.

The confidence limits for unilateral hypothesis testing are obtained by replacing $t_{1-\alpha/2}$ by $t_{1-\alpha}$.

Parker *et al.* (2011) further compared inverse prediction with reverse prediction (i.e. prediction of x -the concentration- based on y -the signal- but using a regression of x on y rather than y on x; so using the model $x = by + a$ rather than $y = bx + a$). They provided confidence intervals for predictions of both inverse regression (Equation 17, equivalent to Equation 16) and reverse regression (Equation 18).

(17) $$CI_{\widehat{x}I}(\widehat{x}) = \widehat{x}_I \pm t_{1-\alpha/2,(n-2)} \times \frac{s_I}{\widehat{\beta}} \sqrt{1 + \frac{1}{n} + \frac{(\widehat{x}_I - \overline{x})^2}{SS_x}} \quad \text{with} \quad s_I^2 = \frac{1}{n-2} \sum_{i=1}^{n} (y_i - \hat{y}_i)^2$$

(18) $$CI_{\widehat{x}_R}(\widehat{x}, y) = \widehat{x}_R \pm t_{1-\alpha/2,(n-2)} \times s_R \sqrt{1 + \frac{1}{n} + \frac{(y - \overline{y})^2}{SS_y}} \quad \text{with} \quad s_R^2 = \frac{1}{n-2} \sum_{i=1}^{n} (x_i - \hat{x}_i)^2$$

Reverse regression (calibrating the model $x = by + a$ with y -peak area- as the predictor) may be appealing because it simplifies the calculation of predicted concentration and the associated confidence interval. However, one assumption of linear regression is that the error on the regressor (the predictor) must be negligible compared to the error on the dependant variable, or at least inferior. This assumption is usually not verified in chromatography because of the random error of the detector.

In the case of an OLS regression model which assumes homoscedasticity, $SE_{\hat{x}}$ and thus $CI_{\hat{x}}$ are constant all along the curve. In the case of WLS regressions, $SE_{\hat{x}_i}$ and $CI_{\hat{x}_i}$ are variable because s_y (or s_I) and other terms are different for each x. Furthermore, $CI_{\hat{x}_i}$ may even be asymmetric when the data are skewed or when it does not rely on a symmetrical distribution[90].

For a given model, expression of $CI_{\hat{x}_i}$ as a function of y (the peak area) is given in Equation 19 :

(19) $$CI_{\hat{x}}(\widehat{x}) = \left| \frac{y - a_{upr}}{b_{upr}} - \frac{y - a_{lwr}}{b_{lwr}} \right| = \left| y \frac{b_{lwr} - b_{upr}}{b_{lwr}\, b_{upr}} + \frac{a_{lwr}\, b_{upr} - a_{upr}\, b_{lwr}}{b_{lwr}\, b_{upr}} \right|$$

with b_{upr} and a_{upr} the slope and intercept of the upper limit of the confidence interval as a function of y; b_{lwr} and a_{lwr} the slope and intercept of the lower limit of the confidence interval as a function of y.

In order to compare models, the expression of $CI_{\hat{x}_i}$ as a function of the estimate concentration ($\widehat{x}$) is obtained by injecting $y = b_{reg}\widehat{x} + a_{reg}$ in Equation 19, yielding Equation 20 :

(20) $$CI_{\hat{x}}(\widehat{x}) = \left| (b_{reg}\, \widehat{x} + a_{reg}) \frac{b_{lwr} - b_{upr}}{b_{lwr}\, b_{upr}} + \frac{a_{lwr}\, b_{upr} - a_{upr}\, b_{lwr}}{b_{lwr}\, b_{upr}} \right|$$

$$= \left| \widehat{x} \frac{b_{reg}(b_{lwr} - b_{upr})}{b_{lwr}\, b_{upr}} + \frac{a_{reg}(b_{lwr} - b_{upr})}{b_{lwr}\, b_{upr}} + \frac{a_{lwr}\, b_{upr} - a_{upr}\, b_{lwr}}{b_{lwr}\, b_{upr}} \right|$$

with a_{reg} and b_{reg} the intercept and slope of the considered regression model from which $\widehat{x}$ is calculated.

The last expression also having the canonical form of a line with a slope and an intercept. All the coefficients being known, the relation between the predicted concentration ($\widehat{x}$) and its confidence interval was easily compared between models and represented.

4.4.4. Reproducibility assessment

The reproducibility was assessed by replicating the preparation of the calibration curve (n = 4) on the range 0.08–1 mg/L PMG and 0.073–0.091 mg/L AMPA, on four different days, using the same stock solution (500 mg/L PMG and 455.5 mg/L AMPA) and the same frozen sugar beet matrix. Fresh mobile phases (0.9 % formic acid v/v) were prepared each day.

Regression coefficients were compared using the hypothesis testing and confidence interval approach (Equation 21) (Paternoster *et al.* 1998) (i.e. two regression coefficients are considered significantly different when their confidence interval do not overlap).

[90] The mathematical demonstration for such a phenomenon falls beyond the scope of this work.

(21) $$CI_{\hat{b}} = \hat{b} \pm t_{1-\alpha/2} \times SE_{\hat{b}}$$

4.4.5. Recovery assessment

The recovery was calculated by injecting extracts (n = 5) of sugar beet spiked before extraction at 0.21 mg/kg PMG and 0.19 mg/kg AMPA or 2.1 mg/kg and 1.9 mg/kg, along with one calibration curve (n = 1) (range 0.1–10 mg/L PMG and 0.091–9.1 mg/L for AMPA).

According to the SANTE/12682/2019 guidelines, correction for recovery must be applied to the results when the mean recovery is out of the range 80–120 %. The satisfactory criteria for recovery in force at the BEAGx are shown in Table 7.

Table 7 : Satisfactory criteria for recoveries depending on the concentration assessed.

Concentration range	Mean recovery (%)	Recovery RSD (%)
1 µg/kg < C ≤ 0,01 mg/kg	60–120	30
0,01 mg/kg < C ≤ 0,1 mg/kg	70–120	20
0,1 mg/kg < C ≤ 1 mg/kg	70–110	15
C > 1 mg/kg	70–110	10

The recovery was calculated as follows (Equation 22) :

(22) $$Recovery = \frac{Solvent\ volume\ (L_{extract})}{Test\ sample\ mass\ (kg_{matrix})} \times \frac{Concentration\ (mg/L_{extract})}{Concentration\ (mg/kg_{matrix})}$$

Contrary to the usual extraction methods in the field of pesticide residue analysis which involve a liquid-liquid extraction with an exact volume of water-immiscible solvent at some point, the QuPPe-PO extraction method takes place in a single aqueous solvent mixture because polar pesticide has lower solubility in such solvents. As a consequence, recovery calculation is uneasy since the final mass density and volume of the extract -which is assimilated as a ternary mixture containing water, methanol and sucrose in the case of sugar beet- was not known precisely.

The mass density of a pooled filtered sugar beet extract was measured to be 0.961 g/cm^3 using both a densimeter (measurement based on glass-tube oscillation) and a pycnometer (measurement based on the mass-volume ratio).

The dry mass of frozen sugar beet was measured to be 27.2 g/100 g of frozen sugar beet (and hence a water content of 72.8 g/100 g of frozen sugar beet) after drying at 66°C until constant weight (five days) (n = 4). With an estimated pulp content of 5 g/100 g of fresh sugar beet (Draycott, 2006; FAO,2009), the sugar content was thus considered to be 22.2 g/100 g of fresh sugar beet. The mass balance of the extract is shown in Table 8.

It was assumed that all the water and sucrose[91] from the sample contributed to the density and final volume of extract. The volume of extract of each replicate was thus estimated as the total mass of liquid (i.e. mass of extracting solvent mixture added (8.32 g) plus the mass of water and sugar from the sample, which is 95 % of the test sample mass) divided by the measured density of the extract (0.961 g/mL). The final volume of extract was thus ~16.6 mL.

[91] The solubility of sucrose in 55:45 (w/w) water/methanol mixture - i.e. the calculated composition of solvents- was measured to be ~45.5 g/100 g of solvent mixture.

Table 8 : Mass balance of the frozen sugar beet extract.

Source	Water	Methanol	Sucrose	Pulp
Frozen sugar beet (8.0 g)	5.82 g (72.8 %)	0.00 g (0 %)	1.78 g (22.2 %)	0.40 g (5 %)
Added extracting solvent	1.99 g (2 mL, 24°C)	6.33 g (8 mL, 24°C)	0.00 g	0.00 g
Extract (liquid phase only)	7.81 g (49.1)	6.33 g (39.8 %)	1.78 g (11.1 %)	neglected

water mass density at 24°C : 0.997 g/cm³ - methanol mass density at 24°C : 0.791 g/cm³

4.4.6. Limit of detection (LOD) and limit of quantification (LOQ)

The limit of detection (LOD) is the concentration at which the presence of the analyte can be reliably detected (i.e. with a known and reasonable probability of error)[92]. The lower limit of quantification (LOQ or LLOQ) is the lowest concentration at which the analyte can be reliably detected and quantified with a known and acceptable accuracy (defined during the linearity assessment). The LOQ is equal or superior to the LOD. These limits are illustrated on Figure 25.

Both LOD and LOQ are usually calculated on the basis of the standard deviation of the blank (Equations 23 and 24) (the factor multiplying the standard deviation may change depending on the source).

(23) $$LOD = 3.3 \times \sigma_{blank} / slope$$

(24) $$LOQ = 10 \times \sigma_{blank} / slope$$

with σ : the standard deviation at the lowest measured concentration;
slope : the slope of the linear regression curve

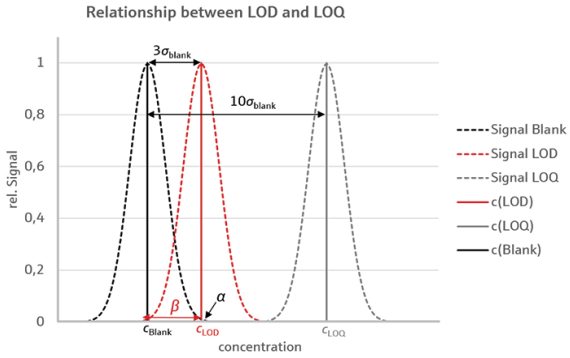

Figure 25 : Representation of LOD and LOQ.
Source : Rene Chemnizer, 2019[93]

However, when no peaks (thus no peak area) are detected in the blanks, LOD and LOQ must be estimated on the basis of solutions with low concentration. In this case, this approximation was reasonable and was only subject to overestimation of the real LOD and LOQ because the standard deviation of the calibration solution was observed to increase with the concentration.

Because the slopes of the calibration curves were significantly different among days, LOD and LOQ were calculated using the data acquired during the linearity and reproducibility assessment.

4.4.7. Stability assessment

The stability of frozen sugar beet extract was assessed by injecting the same calibration curve the day it was prepared, after one day of storage at 5°C and after five days of storage at 5 °C.

The calibration curve tested for stability consisted of three points : 0.08 - 0.5 - 1 mg/L PMG and 0.073 - 0.46 - 0.91 mg/L AMPA, each point prepared by spiking 15 mL of filtered sugar beet extract by either 160 µL of a solution 0.5 mg/L PMG and 0.46 mg/L AMPA, 100 µL of a solution 5 mg/L PMG and 4.6 mg/L AMPA; or 200 µL of a solution 5 mg/L PMG and 4.6 mg/L AMPA respectively. These spiked extracts were then transferred in glass or polypropylene vials and analysed or stored at 5°C.

[92] https://goldbook.iupac.org/terms/view/L03540 (15/05/2020)

[93] http://www.spectroscopyonline.com/strategies-achieving-lowest-possible-detection-limits-icp-ms (15/05/2020)

Since it was shown that the curves were not reproducible, fresh calibration curves were injected along with stored ones, in order to distinguish variation attributable to the detector from variation attributable to the alteration of the calibration curve with time. Replicates of the fresh calibration curves in glass were prepared independently while those in PP are from the same solution (providing information on the variability attributable to automatic pipettes and to the detector).

5. Results and discussion

5.1. Tuning of MS/MS parameter

The desolvation gas flow was set on 1000 L/Hr, the cone gas flow on 50 L/Hr and the source temperature on 600 °C. The optimum settings associated with each MRM transition examined for underivatized PMG and AMPA are shown in Annex 24.

Only one MRM transition was detected for AMPA in positive ionization mode. Since at least one qualifying ion is necessary in addition of the quantifying ion, the negative mode was selected. The retained MRM transitions for PMG and AMPA along with the applied collision energy, capillary voltage and cone voltage are shown in Table 9.

Table 9 : Selected MRM parameters for PMG and AMPA detection in ESI negative.

Compound	Transition (m/z)	Type	Collision energy (V)	Capillary voltage (kV)	Cone voltage (V)
PMG	168 → 150	quantification	8	3.0	30
PMG	168 → 124	qualification	16	3.0	30
PMG	168 → 81	qualification	12	3.0	30
AMPA	110 → 81	quantification	10	3.0	30
AMPA	110 → 63	qualification	14	3.0	30

The transitions and parameters for isotope labelled PMG[94] (or 1,2-$13C_2$,15N-PMG) in ESI- were set correspondingly with those of PMG (Table 9). The selected transition for 1,2-$13C_2$,15N-PMG was 171→153 for quantification and 171→126 and 171→81 for qualification.

5.2. Optimization of chromatographic separation

Chromatographic data acquired by injecting a standard solution 10 mg/L PMG, 9.1 mg/L AMPA (n = 3) using the method given by the manufacturer of the column are shown in Table 10.

Table 10 : Chromatographic data of standard solutions 10 mg/L PMG and AMPA (n = 3) (starting method).

Compound	RT (min)	Area	Height	Width (min)	b/a	S/N
PMG	4.550 ± 0.006	1.15×10^6 ± 2.02×10^4	7.13×10^6 ± 3.71×10^5	0.496 ± 0.032	2.32 ± 0.18	1.31×10^4 ± 8.72×10^1
AMPA	2.102 ± 0.003	4.10×10^5 ± 3.92×10^3	3.81×10^6 ± 2.99×10^4	0.555 ± 0.000	2.50 ± 0.04	1.15×10^4 ± 2.72×10^3

[94] $^{13}COOH^{13}CH_2{}^{15}NHCH_2PO_3$ - CAS number : 1185107-63-4

5.2.1. Optimization of the elution gradient

Considering that PMG and AMPA are eluted relatively early compared to the duration of the starting method, the gradient was compressed as shown in Table 11. in order to shorten analysis time.

Table 11 : Elution gradient compressed in comparison with the starting one.

Time (min)	% A	% B	Curve
0.0	10	90	-
2.0	85	15	2
6.5	85	15	6
7.0	10	90	1
10.0	10	90	1

(a) : curvature code : 1, immediate transition - 2, gradual transition - 6, linear transition

The chromatographic data (n=3) are shown in Table 12. Understandably, retention time significantly decreased for both PMG and AMPA. The retention time of AMPA remains above twice the retention time of the void volume of the column[95], as recommended by the SANTE/12682/2019 guidelines.

Table 12 : Chromatographic data of standard solutions 10 mg/L PMG and AMPA (n = 3) (compressed gradient)

Compound	Gradient	RT (min)	Area	Height	Width (min)	b/a	S/N
PMG	Original	4.550 ± 0.006	1.15×10^6 ± 2.02×10^4	7.13×10^6 ± 3.71×10^5	0.496 ± 0.032	2.32 ± 0.18	1.31×10^4 ± 8.72×10^1
PMG	Compressed	4.241 ± 0.000	1.15×10^6 ± 1.12×10^4	7.48×10^6 ± 2.6×10^4	0.460 ± 0.010	2.16 ± 0.05	1.48×10^4 ± 2.80×10^3
t-test		$P < .001$	$P = .82$	$P = .18$	$P = .15$	$P = .22$	$P = .35$
AMPA	Original	2.102 ± 0.003	4.10×10^5 ± 3.92×10^3	3.81×10^6 ± 2.99×10^4	0.555 ± 0.000	2.50 ± 0.04	1.15×10^4 ± 2.72×10^3
AMPA	Compressed	1.952 ± 0.003	3.75×10^5 ± 1.48×10^4	4.10×10^6 ± 1.29×10^5	0.681 ± 0.003	4.05 ± 0.03	8.88×10^3 ± 1.03×10^3
t-test		$P < .001$	$P = .01$	$P = .02$	$P < .001$	$P < .001$	$P = .20$

The most troubling change is the highly significant rise of peak width and asymmetry for AMPA, although the gradient compression was expected to reduce them.

The effect of gradient compression had different impacts on PMG and AMPA sensitivity : peak area and height of PMG remained stable, while AMPA peak area decreased significantly and peak height increased significantly.

At this point, this gradient was deemed acceptable and allowed to reduce analysis time from 20 to 8 minutes, which was a comfortable advantage in the context of a method optimization where the choice of the following change depends on the results of the previous tests.

With the aim of further reducing tailing for PMG, the maximum elution strength was increased by raising the maximum proportion of aqueous mobile phase A from 85 to 95 % (resulting in the gradient presented in Table 13).

Table 13 : Elution gradient compressed in comparison with the starting one.

Time (min)	% A	% B	Curve
0.0	10	90	-
2.0	95	5	2
6.5	95	5	6
7.0	10	90	1
8.0	10	90	1

(a) : curvature code : 1, immediate transition- 2, gradual transition - 6, linear transition

The chromatographic data (n = 3) are shown in Table 14.

[95] Considering the empty column volume of 0.3 mL and a flow rate of 0.500 mL/min, the void time is approximated to be 1.2 minutes.

Table 14 : Chromatographic data of standard solutions 10 mg/L PMG and AMPA (n = 3) (increased maximum %A).

Compound	Gradient	RT (min)	Area	Height	Width (min)	b/a	S/N
PMG	Compressed max. 85 % A	4.241 ± 0.000	1.15×10^6 ± 1.12×10^4	7.48×10^6 ± 2.6×10^4	0.460 ± 0.010	2.16 ± 0.05	1.48×10^4 ± 2.80×10^3
PMG	Compressed, max. 95 % A	3.833 ± 0.013	9.47×10^5 ± 1.03×10^4	7.19×10^6 ± 7.38×10^4	0.390 ± 0.003	2.02 ± 0.03	8.92×10^3 ± 1.32×10^3
t-test		$P < .001$	$P < .001$	$P = .003$	$P < .001$	$P = .01$	$P = .03$
AMPA	Compressed max. 85 % A	1.952 ± 0.003	3.75×10^5 ± 1.48×10^4	4.10×10^6 ± 1.29×10^5	0.681 ± 0.003	4.05 ± 0.03	8.88×10^3 ± 1.03×10^3
AMPA	Compressed, max. 95 % A	1.906 ± 0.000	3.45×10^5 ± 5.51×10^3	4.12×10^6 ± 5.07×10^4	0.649 ± 0.006	4.33 ± 0.10	9.37×10^3 ± 5.45×10^2
t-test		$P < .001$	$P = .04$	$P = .77$	$P = .001$	$P = .01$	$P = .51$

Increasing the maximum strength (water content) of the gradient resulted in a considerable loss of sensitivity (peak area, height and S/N) for PMG. This loss may be attributed to a too high surface tension of the mobile phase, resulting in an impeded nebulization in ESI. This phenomenon is well known for ESI (Waters Corporation[96]). The improvement in symmetry and peak width is likely a side-effect of the loss of sensitivity. Furthermore, the manufacturer of the column recommends to avoid running with (near) 100 % water for an extended period of time.

This modification of the gradient was rejected and the previous 8-minutes long gradient with a maximum strength at 85 % mobile phase A was retained.

5.2.2. Optimization of pH and ionic strength

Several concentration of formic acid and ammonium formate were tested in order to optimize pH and ionic strength, taking into account the two following constraints :

- The recommended operational pH range of the column is 2–7 ;
- Increasing ionic strength induce a loss of sensitivity (Waters Corporation[97]; Heaton *et al.*, 2014) ;

Three combinations of pH and ionic strength were tested, again by injecting the same standard solution 10 mg/µL PMG and AMPA as previously (n = 3). The results are shown in Table 15 and the p-value of the corresponding t-tests are shown in Table 16.

The main effect observed with increasing content of ammonium formate is the progressive loss of sensitivity (peak area, height and S/N) (due to competition for ionization (Balogh, 2013; Heaton *et al.*, 2014). The addition of ammonium formate apparently reduced peak width and asymmetry. However, this may only be a side-effect of the loss of sensitivity.

[96] https://www.waters.com/waters/fr_BE/Solvents-and-Caveats-for-LC-MS/nav.htm? (20/03/2020)

[97] https://www.waters.com/waters/fr_BE/Solvents-and-Caveats-for-LC-MS/nav.htm? (20/03/2020)

Table 15 : Comparison of the effect of several content of ammonium formate ($HCOO^-NH_4^+$) in the mobile phases used with the Anionic Polar Pesticide HILIC column.

Compound	HCOOH content[a] (% v/v)	$HCOO^-NH_4^+$ content[b] (mg/L)	Mobile phase A pH	RT (min)	Area	Height	Width (min)	b/a	S/N
PMG	0.9	0	2.24	3.834 ± 0.013	9.47×10^5 ± 1.03×10^4	7.19×10^6 ± 7.38×10^4	0.390 ± 0.003	2.02 ± 0.03	8.92×10^3 ± 1.32×10^3
	0.9	158	2.31	3.826 ± 0.003	2.48×10^5 ± 2.16×10^3	2.20×10^6 ± 9.85×10^3	0.315 ± 0.003	1.53 ± 0.03	7.97×10^3 ± 2.13×10^3
	0.9	315	2.36	3.639 ± 0.002	2.12×10^5 ± 1.16×10^4	1.73×10^6 ± 3.07×10^4	0.350 ± 0.017	1.87 ± 0.07	5.43×10^3 ± 1.04×10^3
AMPA	0.9	0	2.24	1.952 ± 0.003	3.75×10^5 ± 1.48×10^4	4.10×10^6 ± 1.29×10^5	0.681 ± 0.003	4.05 ± 0.03	8.88×10^3 ± 1.03×10^3
	0.9	158	2.31	1.881 ± 0.006	1.05×10^5 ± 1.79×10^3	1.29×10^6 ± 1.6×10^4	0.605 ± 0.012	2.42 ± 0.20	8.80×10^3 ± 1.81×10^3
	0.9	315	2.36	1.878 ± 0.000	7.25×10^4 ± 2.81×10^3	8.78×10^5 ± 3.12×10^4	0.619 ± 0.017	2.14 ± 0.28	6.18×10^3 ± 6.49×10^2

a : formic acid 99.0 % is 26.239 M, so 0.9 % v/v formic acid is equal to ~ 236.2 mM.
b : ammonium formate ≥99 % is 63.06 g/mol, so 158 mg/L and 315 mg/L are equal to ~2.5 and ~5 mM respectively.

Table 16 : Effect of ammonium formate content on the chromatographic data.

Compound	Mobile phases compared	RT (min)	Area (a.u.)	Height (a.u.)	Width (min)	b/a	S/N
PMG	0 mg/L $HCOO^-NH_4^+$ vs 158 mg/L $HCOO^-NH_4^+$	$P < .001$	$P < .001$	$P < .001$	$P < .001$	$P < .001$	$P = .03$ 2.7
	158 mg/L $HCOO^-NH_4^+$ vs 315 mg/L $HCOO^-NH_4^+$	$P < .001$	$P = .03$	$P < .001$	$P = .06$	$P = .007$	$P = 0.16$
	0 mg/L $HCOO^-NH_4^+$ vs 315 mg/L $HCOO^-NH_4^+$	$P < .001$	$P < .001$	$P < .001$	$P = .02$	$P < .001$	$P = .02$
AMPA	0 mg/L $HCOO^-NH_4^+$ vs 158 mg/L $HCOO^-NH_4^+$	$P < .001$	$P < .001$	$P < .001$	$P < .001$	$P < .001$	$P = 0.95$
	158 mg/L $HCOO^-NH_4^+$ vs 315 mg/L $HCOO^-NH_4^+$	$P = .42$	$P < .001$	$P < .001$	$P = .30$	$P = .25$	$P = .11$
	0 mg/L $HCOO^-NH_4^+$ vs 315 mg/L $HCOO^-NH_4^+$	$P < .001$	$P < .001$	$P < .001$	$P = .02$	$P = .007$	$P = .03$

a : formic acid 99.0 % is 26.239 M, so 0.9 % v/v formic acid is equal to ~ 236.2 mM.
b : ammonium formate ≥99 % is 63.06 g/mol, so 158 mg/L and 315 mg/L are equal to ~2.5 and ~5 mM respectively.

5.3. Considerations regarding the vial material

The effect of vial material on sensitivity was tested by injecting sugar beet extract spiked at 0.08 mg/L PMG and 0.073 mg/L AMPA (n = 5) in both glass (mean area : 8,097 ± 268 for PMG and 271 ± 13 for AMPA) and polypropylene vials (mean area : 7,929± 64 for PMG and 285 ± 8 for AMPA).

No significant difference in peak area was observed ($P = .19$ for PMG and $P = .051$ for AMPA). Based on this test and for practical reasons, validation was carried on glass vials.

5.4. Method validation for PMG and AMPA analysis in frozen sugar beet

5.4.1. Matrix effect assessment (frozen sugar beet)

Table 17 : Assessment of matrix effect in frozen sugar beet extract.

Compound	Solvent	Concentration (mg/L)	RT (min)	Area (a.u.)
PMG	Clean extraction solvent	0	n.d.	< 100
	Filtered sugar beet extract	0	n.d.	< 100
	Clean extraction solvent	0.5	3.77 ± 0.005	$1.45 \times 10^4 \pm 5.73 \times 10^2$
	Filtered sugar beet extract	0.5	3.80 ± 0.003	$1.29 \times 10^4 \pm 3.76 \times 10^2$
	t-test		*P* < .001	*P* = .004
AMPA	Clean extraction solvent	0	n.d.	< 100
	Filtered sugar beet extract	0	n.d.	< 100
	Clean extraction solvent	0.5	1.911 ± 0.000	$3.64 \times 10^3 \pm 8.89 \times 10^1$
	Filtered sugar beet extract	0.5	1.911 ± 0.000	$2.02 \times 10^3 \pm 9.43 \times 10^1$
	t-test		*P* > .99	*P* < .001

n.d. : no peak detected

The results (Table 17) clearly indicates a significant matrix effect, reducing the sensitivity of both analytes.

Table 18 : Assessment of matrix effect in frozen sugar beet extract with isotope-labelled internal standard.

Compound	Solvent	Concentration (mg/L)	RT (min)	Area ratio analyte/isotpe-labelled PMG
PMG	Clean extraction solvent	0	n.d.	< 100
	Filtered sugar beet extract	0	n.d.	< 100
PMG	Clean extraction solvent	0.1	3.78 ± 0.004	0.112 ± 0.004
	Filtered sugar beet extract	0.1	3.79 ± 0.004	0.119 ± 0.008*
t-test (0.1 mg/L, clean solvent vs extract)			*P* = 0.17	*P* = .16
PMG	Clean extraction solvent	0.5	3.77 ± 0.005	0.508 ± 0.018
	Filtered sugar beet extract	0.5	3.80 ± 0.003	0.513 ± 0.012
t-test (0.5 mg/L, clean solvent vs extract)			*P* = 0.10	*P* = 0.67
AMPA	Clean extraction solvent	0	n.d.	< 100
	Filtered sugar beet extract	0	n.d.	< 100.
AMPA	Clean extraction solvent	0.1	1.911 ± 0.000	0.042 ± 0.002
	Filtered sugar beet extract	0.1	1.911 ± 0.001	0.011 ± 0.000*
t-test (0.1 mg/L, clean solvent vs extract)			*P* 0.06	*P* < .001
AMPA	Clean extraction solvent	0.5	1.911 ± 0.000	0.508 ± 0.018
	Filtered sugar beet extract	0.5	1.911 ± 0.000	0.513 ± 0.012
t-test (0.5mg/L, clean solvent vs extract)*			*P* < 0.001	*P* < .001

n.d. : no peak detected

The matrix effect was tested again (n = 4) at several concentrations with the addition of isotope-labelled PMG (1,2-$^{13}C_2$,^{15}N-PMG) at a fixed concentration of 1 mg/L. The results with isotope-labelled internal standard (reported as the ratios non-isotopic standard / isotope labelled PMG) are reported in Table 18.

As expected, the isotope-labelled internal standard allowed to compensate for the matrix effect for PMG but not for AMPA. Although PMG and AMPA are similar molecules, their retention mechanism is fairly different : AMPA only relies on its phosphate moiety for interaction with the diethylamine stationary phase, while PMG have both phosphate and carboxylic moieties, allowing bidentate and biligand anionic interaction with diethylamine. Considering the high price of isotope-labelled standards, the use of both PMG and AMPA isotope labelled internal standards was excluded suring this work.

Unfortunately, both isotope-labelled standards were only available at 100 mg/L. So once quantitatively transferred and diluted to 10 mg/L in a 10 mL PMP volumetric flask, the concentration of the isotope-labeled internal standard is not sufficient to spike sugar beet extract (~15-20 mL) at 1 mg/L with a negligible volume of internal standard solution.

It was decided to opt for matrix-matched calibration in the first place. The standard addition can be used to compensate for matrix effect and insufficient recovery, but it can be more tedious as it requires one calibration curve in each sample (or at least per pooled sample).

5.4.2. Linearity assessment

Table 19 : Linearity assessment of the calibration data for PMG and AMPA (frozen sugar beet, untransformed data, OLS linear regression models).

Compound	Concentration (mg/L)	Area CV (%)	Calibration trueness[a] (%) (n=3)	Validation trueness[b] (%) (n =1)	F_{nl}[c]	Model		
						slope	intercept	R^2
PMG	0	irr.	irr.	irr.	6.3×10^{-1} $P = .65$	2.827×10^{4} $P < .001$	9.495×10^{2} $P = .36$	0.9991
	0.1	9.9	84.8 ± 0.08	**81.0**				
	0.5	3.2	98.0 ± 0.03	100.0				
	1	2.3	108.9 ± 0.03	108.8				
	5	3.5	98.8 ± 0.04	102.0				
	10	2.5	100.2 ± 0.03	100.5				
AMPA	0	irr.	irr.	irr.	1.5×10^{0} $P = .27$	2.876×10^{3} $P < .001$	5.537×10^{1} $P = .60$	0.9988
	0.09	5.5	98.8 ± 0.06	107.9				
	0.46	2.9	101.1 ± 0.03	105.5				
	0.9	2.6	109.5 ± 0.03	109.4				
	4.6	4.2	97.3 ± 0.04	100.6				
	9.1	2.3	100.6 ± 0.02	99.0				

(a) : calculated concentration / nominal concentration of solutions used for the calibration of the model.
(b) : calculated concentration / nominal concentration of solutions not used for the calibration of the model.
(c) : $F_{\alpha = 0.05} = 3.26$ (with 4 and 12 degrees of freedom).
irr. : irrelevant calculation (impossible to divide by zero).
Non-respect of linearity criteria (see page 41) are highlighted in bold.

The model satisfied all the criteria for linearity in force the BEAGx with a slight exception concerning the recovery of the fourth replicates at 0.1 mg/L for PMG (81.0 % < 85.0 %) (Table 19).

However, this model obviously did not satisfy homoscedasticity (Figure 26), which is an important assumption of linear regression. This model may thus not be considered as fully reliable according to strict theoretical requirements.

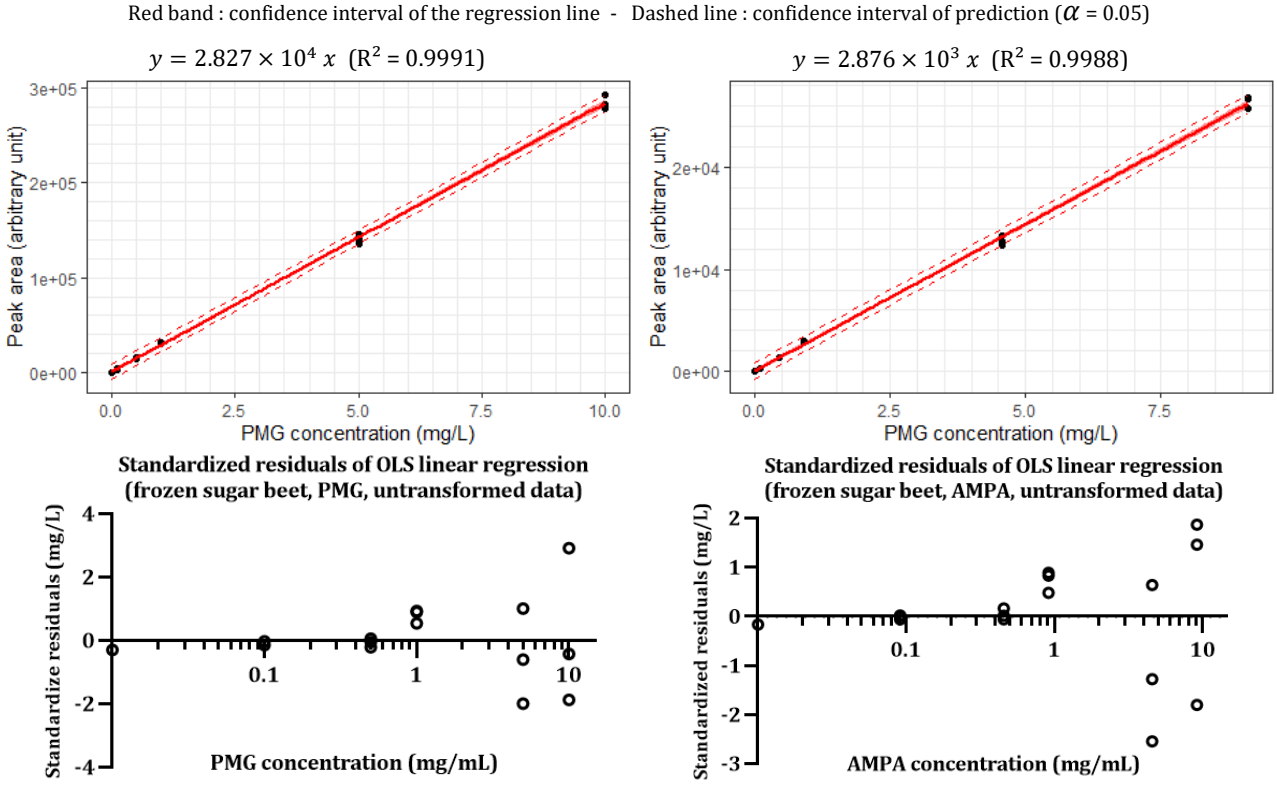

Figure 26 : Linear regression curves and standardized residuals of the OLS models for PMG and AMPA (frozen sugar beet, untransformed data).

Several statistical options were investigated to improve the reliability and relevance of the model.

The first and easiest option was data transformation. In this case, since the linear relationship was already satisfying, both x (concentration) and y (peak area) should be transformed. Data transformation can improve homoscedasticity because the random error is included in the data transformation (Equations 25 and 26). In this case, a data transformation that compresses the error with increasing values of x (such as logarithm and square root) are relevant.

$$y = bx + e \quad (25) \qquad \sqrt{y} = \sqrt{bx + e} \quad (26)$$

The logarithm is not a convenient transformation for calibration curve since the function does not admit $x = 0$ (blanks) in its domain. The square root transformation was applied the results of the calibration and linearity assessment are shown in Table 20 and Figure 27.

Although the non-linear relationship was significant, the remaining criteria were satisfied and the relationship was thus accepted. On major drawback with data transformation is that, when converting back the model in the original units, a bias is introduced because the error is subject to the inverse function (f^{-1}). In the case of square root data transformation, the problem is even worse because even an unbiased model, once expressed in original units, becomes non-linear, as illustrated by Equations 27 and 28.

$$\sqrt{y} = b\sqrt{x} + \epsilon \quad (27)$$

$$y = (b\sqrt{x} + \epsilon)^2 = b^2x + 2b\epsilon\sqrt{x} + \epsilon^2 \quad (28)$$

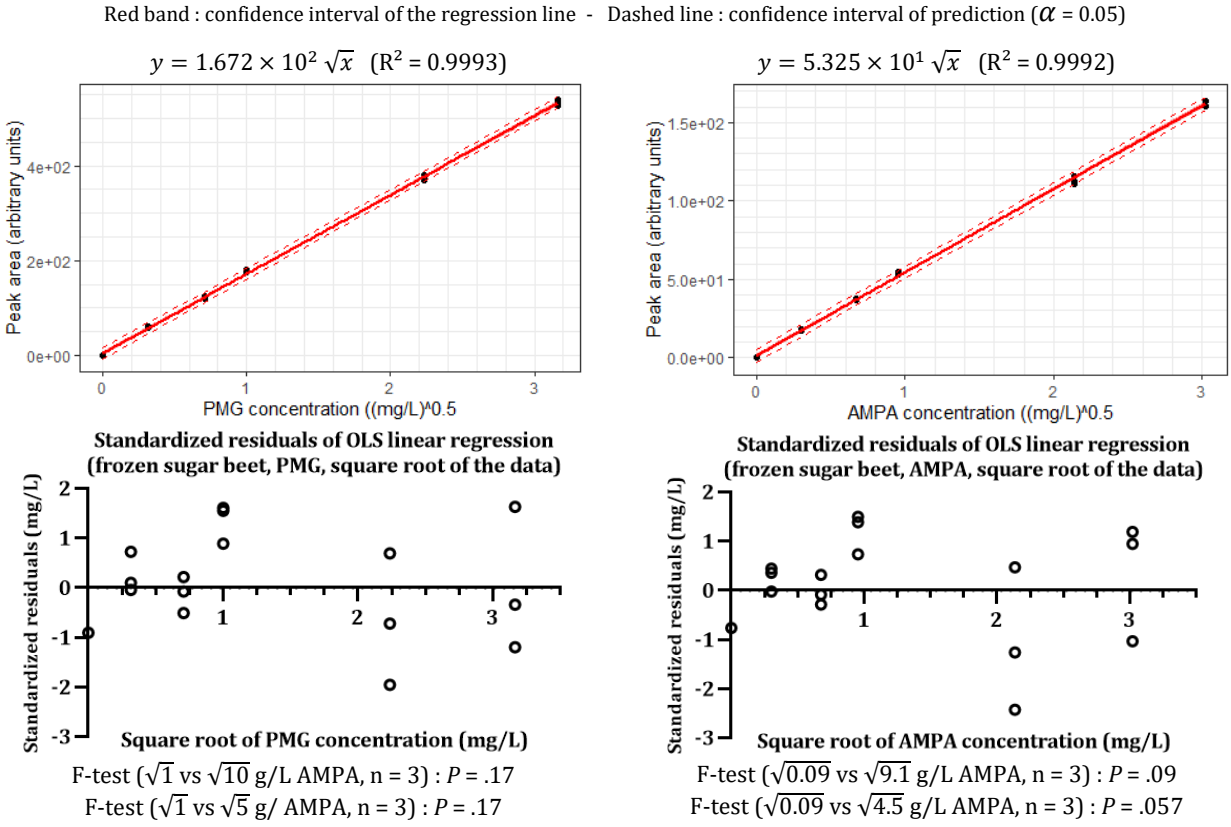

Figure 27 : Linear regression curves and standardized residuals of the OLS models for PMG and AMPA (frozen sugar beet, square root of the data).

Table 20 : Linearity assessment of the calibration data for PMG and AMPA (frozen sugar beet, square root of the data, OLS linear regression models).

Compound	Square root of the concentration (mg/L)	Area CV (%)	Calibration trueness[a] (%) (n=3)	Validation trueness[b] (%) (n =1)	F_{nl}[c]	Model		
						Slope	Intercept	R^2
PMG	0	irr.	irr.	irr.	**5.1 x 10¹** *P* < .001	1.672 x 10² *P* < .001	4.399 x 10⁰ *P* = .03	0.9993
	0.32	4.2	91.4 ± 0.04	89.7				
	0.71	1.6	95.5 ± 0.02	96.5				
	1	1.2	101.9 ± 0.01	101.8				
	2.24	1.8	99.1 ± 0.02	100.8				
	3.16	1.3	100.6 ± 0.01	100.7				
AMPA	0	irr.	irr.	irr.	**4.1 x 10¹** *P* < .001	5.325 x 10¹ *P* < .001	1.229 x 10⁰ *P* = .06	0.9992
	0.30	2.5	102.7 ± 0.03	106.7				
	0.67	1.4	99.9 ± 0.01	102.1				
	0.95	1.3	104.0 ± 0.01	103.9				
	2.13	2.1	98.5 ± 0.02	100.1				
	3.02	1.2	100.4 ± 0.01	99.5				

(a) : calculated concentration / nominal concentration of solutions used for the calibration of the model.
(b) : calculated concentration / nominal concentration of solutions not used for the calibration of the model.
(c) : $F_{\alpha = 0.05}$ = 3.26 (with 4 and 12 degrees of freedom).
irr. : irrelevant calculation (impossible to divide by zero).
Non-respect of linearity criteria (see page 41) are highlighted in bold.

The second option investigated to improve the reliability and relevance of the regression model was to calibrate weighted lean square models (WLS) (also called weighted linear regressions) instead of OLS models. Such models are a common manner to compensate for heteroscedasticity and possibly extend the linear range. In a nutshell, instead of minimizing the error sum of squares (Equation 12), these models tends to minimize the weighted error sum of squares (Equation 27) using a weighting function (w).

$$\text{weighted } SS_e = \sum w\,(y_i - \hat{y}_i)^2 \tag{27}$$

The introduction of weight is equivalent to considering some data points more informative than others. The OLS model is a specific case of WLS where all the weights are equals and all the points considered equally informative in the determination of the regression coefficient and intercept.

The assumption of homoscedasticity and equally informative points in OLS models results in a constant standard error all along the linear range (i.e. the dashed lines in Figures 26 and 27 are parallel to the regression curve).

However, in many cases in chemistry, the variability and so the "unreliability" of the calibration solutions increases with the concentration; and so should the standard error of the model. This is easily understandable : a given volumetric error occurring when preparing the calibration induces an error directly proportional to the concentration and the volume transferred.

Weighted least squares models allow a lower standard error than OLS models at lower concentration points of the curve, which is especially convenient in analytical chemistry because the MRL is usually among the lowest points of the calibration curve.

Several weighting functions were tested :

- Weight = 1/x (weight inversely proportional to the concentration). This weighting function is the first to come to the mind when considering that the variability of the residuals increases with the concentration, as seen in the plot of the residuals;

- Weight = $1/y^2$ (weight inversely proportional to the relative error between each observed area and the predicted area at the corresponding concentration). This weighting function has been suggested by Toffalis (2009) and is equivalent to minimizing the squared relative error rather than the squared "absolute" error (Equation 28).

$$\text{squared relative error} = \sum_i^N \left(\frac{y_i - \widehat{y_i}}{y_i}\right)^2 = \sum_i^N \frac{1}{y_i^2}(y_i - \widehat{y_i})^2 \tag{28}$$

  This weighting function is theoretically more accurate than 1/x because it depends on the observed area and not the concentration which can not be exactly the same among replicates. In that sense, the weighting is specific to each point measured and not to each group of replicates for each concentration.

- Weight = $1/s_y^2$ (weight inversely proportional to the variance of the observed areas at a given concentration). This weighting function is theoretically optimal when it comes to improving homoscedasticity. The calibration points are considered more informative (i.e. reliable to calibrate the model) when their variance is low.

weighting = 1/x, untransformed data

weighting = 1/x, untransformed data

C = 2.848 x 10^4 area + 4.299 x 10^2 (R^2 = 0.9985)

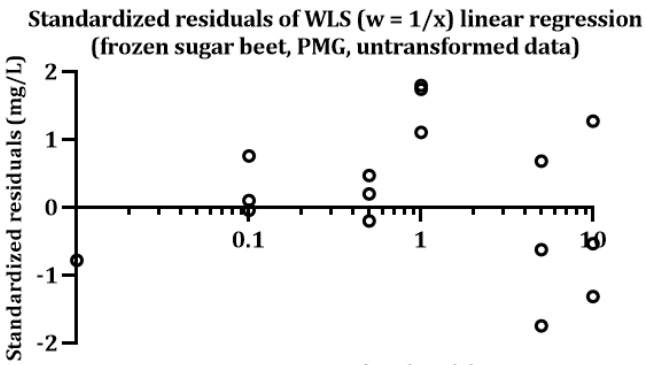

F-test (0.1 vs 10 mg/L PMG, n = 3) : *P* = .14

C = 2.885 x 10^3 area + 3.789 x 10^1 (R^2 = 0.9983)

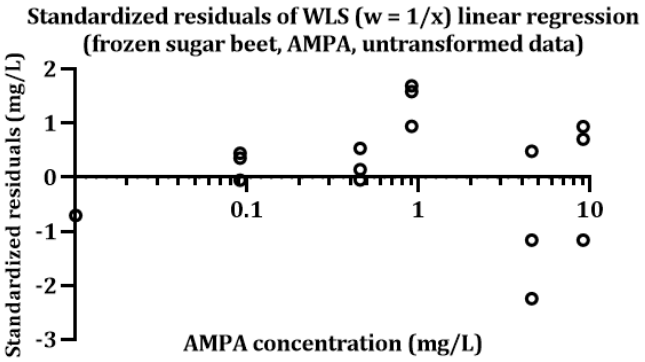

F-test (0.091 vs 9.1 mg/L AMPA, n = 3) : *P* = .12
F-test (0.091 vs 4.6 mg/L AMPA, n = 3) : *P* = .11

weighting = $1/y^2$, untransformed data

C = 3.011 x 10^4 area + 3.437 x 10^{-5} (R^2 = 0.9939)

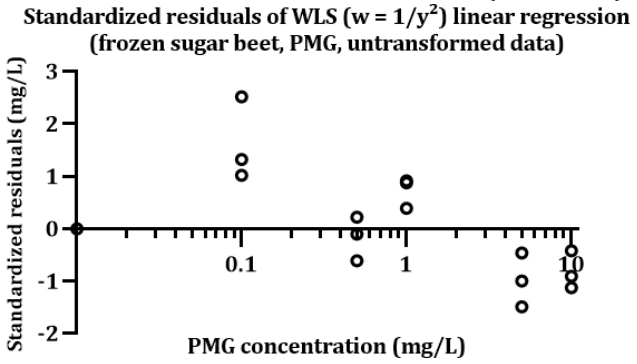

weighting = $1/y^2$, untransformed data

C = 3.042 x 10^3 area + 3.735 x 10^{-4} (R^2 = 0.9941)

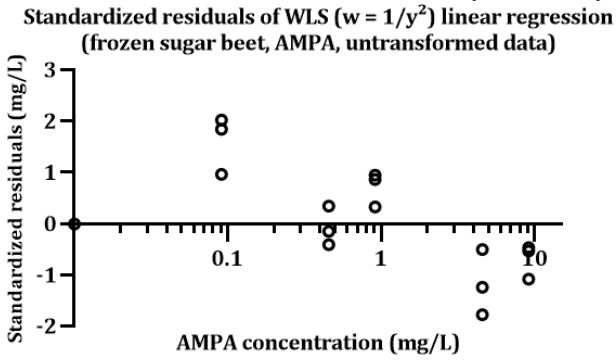

weighting = $1/s_y^2$, untransformed data

C = 2.984 x 10^4 area + 3.093 x 10^2 (R^2 = 0.9961)

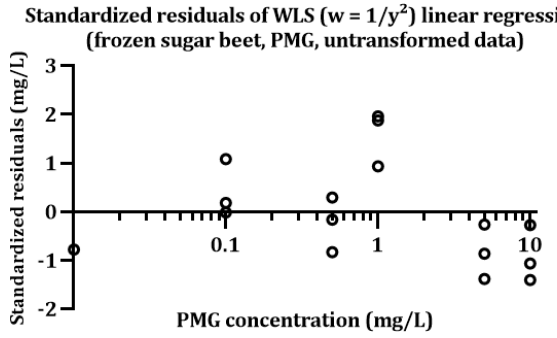

weighting = $1/s_y^2$, untransformed data

C = 2.991 x 10^3 area + 2.317 x 10^{-6} (R^2 = 0.9964)

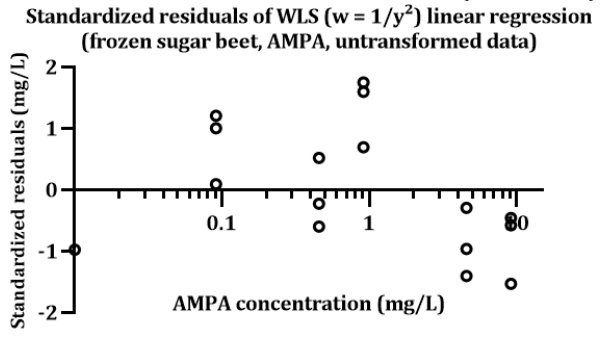

Figure 28 : Standardized residuals of the WLS regression curves (weight = 1/x, $1/s_y^2$ and $1/y^2$) for PMG and AMPA (frozen sugar beet, untransformed data).

The WLS model with the weighting function 1/x barely satisfied homoscedasticity while the WLS models with the weighting $1/s_y^2$ and $1/y^2$ fully satisfied homoscedasticity and may be regarded as more robust and reliable.

Red band : confidence interval of the regression line - Dashed line : confidence interval of prediction (α = 0.05)

weighting = 1/x, untransformed data

weighting = 1/x, untransformed data

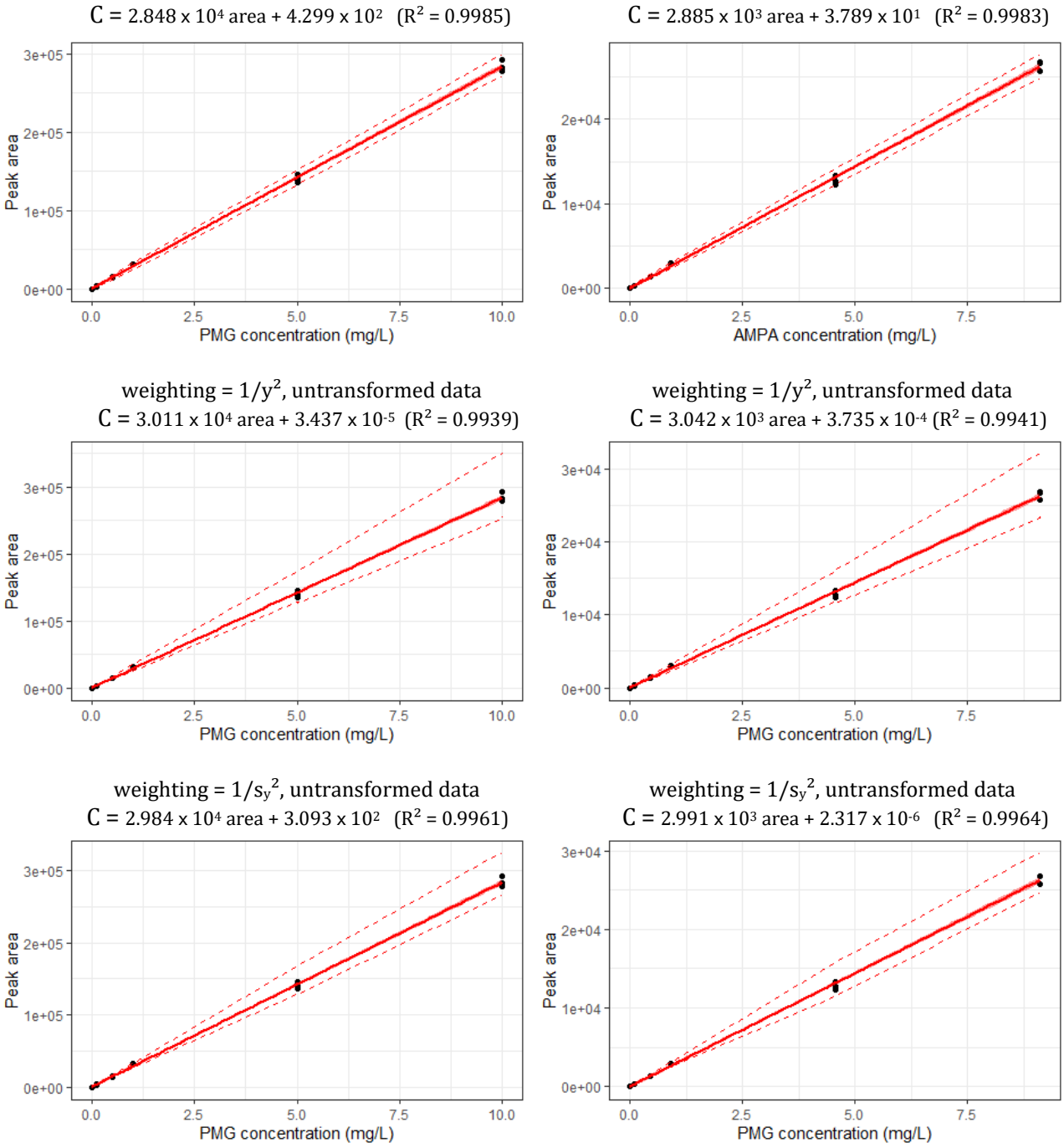

Figure 29 : WLS linear regression curves (weight = 1/x, $1/s_y^2$ and $1/y^2$) for PMG and AMPA (frozen sugar beet, untransformed data).

The WLS models are less biased (smaller intercept) than the OLS models calibrated on untransformed data.

Table 21 : Linearity assessment of the calibration data for PMG and AMPA
(frozen sugar beet, untransformed data, WLS linear regression models (weight = 1/x, $1/y^2$, $1/s_y^2$).

Weight	Compound	Concentration (mg/L)	Area CV (%)	Calibration trueness[a] (%) (n=3)	Validation trueness[b] (%) (n =1)	F_{nl}[d]	Model		
							Slope	Intercept	R^2
1/x	PMG	0	irr.	irr.	irr.	8.9×10^{-1} $P = 0.50$	2.848×10^{4} $P < .001$	4.299×10^{2} $P = .09$	0.9985
		0.1	7.9	105.4 ± 8.3	101.6				
		0.5	3.1	101.5 ± 3.1	103.4				
		1	2.3	110.2 ± 2.3	110.0				
		5	3.5	98.4 ± 3.4	101.7				
		10	2.5	99.6 ± 2.5	99.9				
	AMPA	0	irr.	irr.	irr.	7.1×10^{-6} P > .99	2.885×10^{3} $P < .001$	3.789×10^{1} $P = .12$	0.9983
		0.09	5.2	105.2 ± 5.5	114.2				
		0.46	2.8	102.1± 2.9	106.5				
		0.9	2.6	109.8 ± 2.8	109.7				
		4.6	**4.2**	97.1 ± 4.1	100.4				
		9.1	2.3	100.3 ± 2.3	98.7				
$1/y^2$	PMG	0	irr.	irr.	irr.	**2.3×10^{1}** ***P* < .001**	3.011×10^{4} $P < .001$	3.437×10^{-5} $P > .99$	**0.9939**
		0.1	6.9	114.0 ± 7.9	110.4				
		0.5	3.0	98.9 ± 3.0	100.7				
		1	2.2	105.7 ± 2.4	105.6				
		5	3.5	93.4 ± 3.2	96.5				
		10	2.5	94.4 ± 2.4	94.7				
	AMPA	0	irr.	irr.	irr.	**1.9×10^{1}** ***P* < .001**	3.042×10^{3} $P < .001$	3.735×10^{-4} $P > .99$	**0.9941**
		0.09	4.6	113.4 ± 5.2	**122.1**				
		0.46	2.8	99.5 ± 2.8	103.5				
		0.9	2.5	105.5 ± 2.7	105.3				
		4.6	**4.2**	92.4 ± 3.9	95.5				
		9.1	2.3	95.3 ± 2.2	93.8				
$1/s_y^2$	PMG	0	irr.	irr.	irr.	**1.1×10^{1}** ***P* < .001**	2.984×10^{4} $P < .001$	3.093×10^{2} $P = .10$	0.9961
		0.1	6.9	115.0 ± 8.0	111.4				
		0.5	3.0	99.8 ± 3.0	101.6				
		1	2.2	106.7 ± 2.4	106.5				
		5	3.5	94.3 ± 3.3	97.4				
		10	2.5	95.3 ± 2.4	95.5				
	AMPA	0	irr.	irr.	irr.	**1.0×10^{1}** ***P* < .001**	2.991×10^{3} $P < .001$	2.317×10^{-6} $P = .05$	0.9964
		0.09	4.6	119.0 ± 5.4	**122.0**				
		0.46	2.8	104.5 ± 2.9	103.8				
		0.9	2.5	110.7 ± 2.8	105.4				
		4.6	**4.2**	96.9 ± 4.1	95.5				
		9.1	2.3	100.0 ± 2.3	93.8				

(a) : calculated concentration / nominal concentration of solutions used for the calibration of the model.
(b) : calculated concentration / nominal concentration of solutions not used for the calibration of the model.
(c) : $F_{\alpha = 0.05} = 3.26$ (with 4 and 12 degrees of freedom).
irr. : irrelevant calculation (impossible to divide by zero).
Non-respect of linearity criteria (see page 41) are highlighted in bold.

The model with the weighting 1/x satisfied all the requirements for linearity with a slight exception (non-respect of the requirements are highlighted in bold). It also seemed to provide the smallest error on prediction, especially at low concentration (Figure 29); but again, it may not be the most reliable of all because it does not have the most homoscedastic residuals.

The linearity of the models with the weighting $1/y^2$ was rejected because of the significant nonlinear relationships, insufficient R^2 and other irregularities.

The models with the weighting $1/s_y^2$ exhibited significant nonlinear relationships and slight irregularities, but with sufficient R^2.

The third option investigated to satisfy homoscedasticity was to reduce the range of the calibration curve (0.08–0.1–0.25–0.75–1 mg/L for PMG and 0.073–0.091–0.23–0.68–0.91 mg/L for AMPA) so that the difference in variability between the highest and lower concentrations of the curve is lessen.

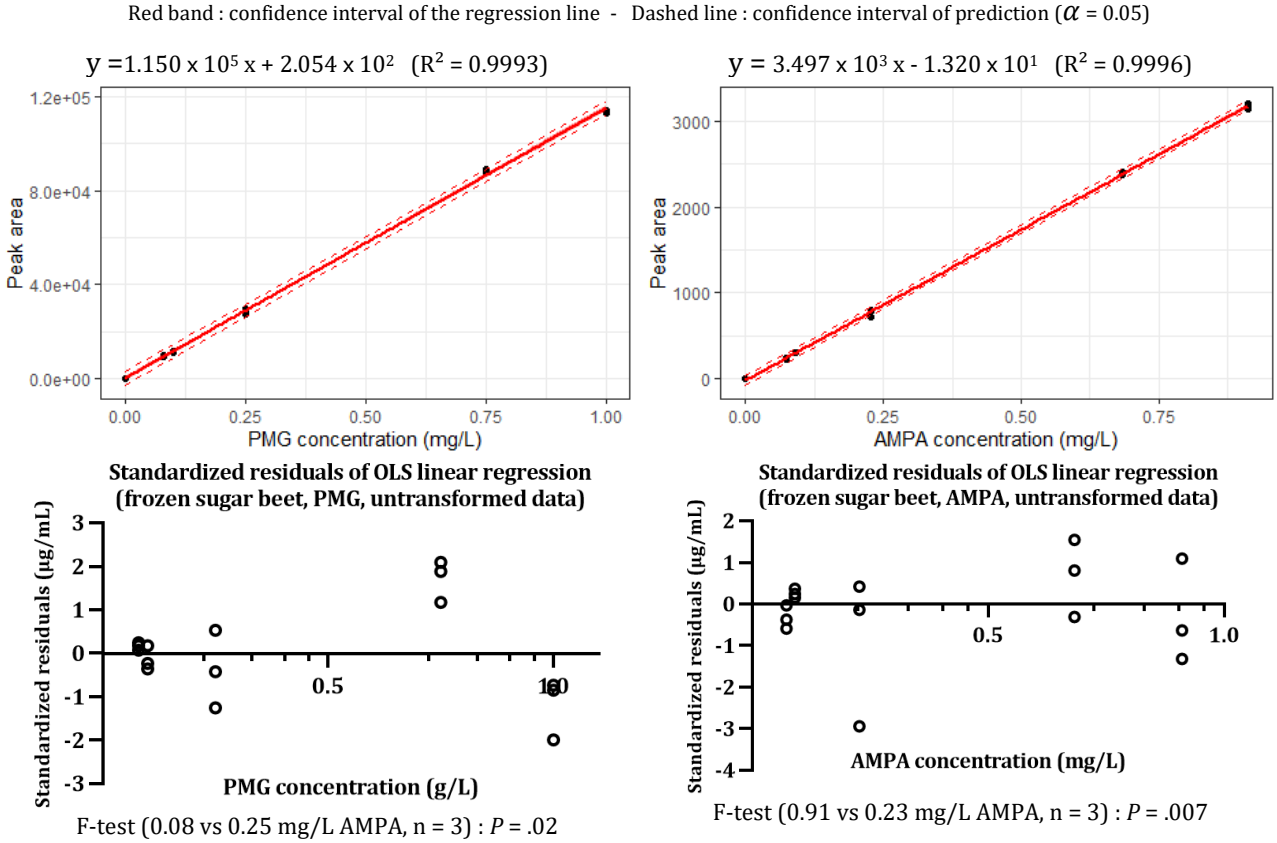

Figure 30 : Linear regression curves and standardized residuals of the OLS models for PMG and AMPA (frozen sugar beet, untransformed data, reduced range (0.08-1 mg/L)).

Omitting one outlier data point observed at 0.23 mg/L AMPA (Figure 30), reducing the calibration range allowed to attain homoscedasticity for OLS regression on untransformed data. The prediction error was also remarkably lower.

Table 22 : Linearity assessment of the matrix-matched linear calibration of frozen sugar beet extract (reduced calibration range).

Compound	Concentration (mg/L)	Area CV (%)	Calibration trueness[a] (%) (n=3)	Validation trueness[b] (%) (n =1)	F_{nl}[c]	Model		
						Slope	Intercept	R^2
PMG	0	irr.	irr.	irr.	1.55 P = .25	1.150×10^5 *P* < .001	2.054×10^2 *P* = .62	0.9993
	0.08	1.1	102.2 ± 0.01	106.6				
	0.1	3.0	98.5 ± 0.03	103.7				
	0.25	3.8	98.4 ± 0.04	96.1				
	0.75	0.7	102.4 ± 0.01	96.2				
	1	0.7	98.7 ± 0.01	95.3				
AMPA	0	irr.	irr.	irr.	1.43 P = .28	3.497×10^3 *P* < .001	-1.320×10^1 *P* = .11	0.9996
	0.07	2.7	97± 0.03	113.1				
	0.09	0.8	101.9 ± 0.01	**110.2**				
	0.23	**5.4**	97.4 ± 0.05	101.2				
	0.68	0.9	100.7 ± 0.01	99.9				
	0.91	0.9	99.8 ± 0.01	98.8				

(a) : calculated concentration / nominal concentration of solutions used for the calibration of the model
(b) : calculated concentration / nominal concentration of solutions not used for the calibration of the model
(c) : $F_{\alpha = 0.05} = 3.26$ (with 4 and 12 degrees of freedom)
irr. : irrelevant calculation (impossible to divide by zero)
Non-respect of linearity criteria (see page 41) are highlighted in bold.

As found in Table 22, the linearity requirements were satisfied.

The computed $CI_{\hat{x}_i}$ as a function of the estimated concentration ($\hat{x}$) for the accepted models are represented in Figure 30 (detailed values in Annex 25). The values of the different coefficients used in the calculation appear in Annex 26. The model with square root data transformation was excluded because the other models were more straightforward and reliable.

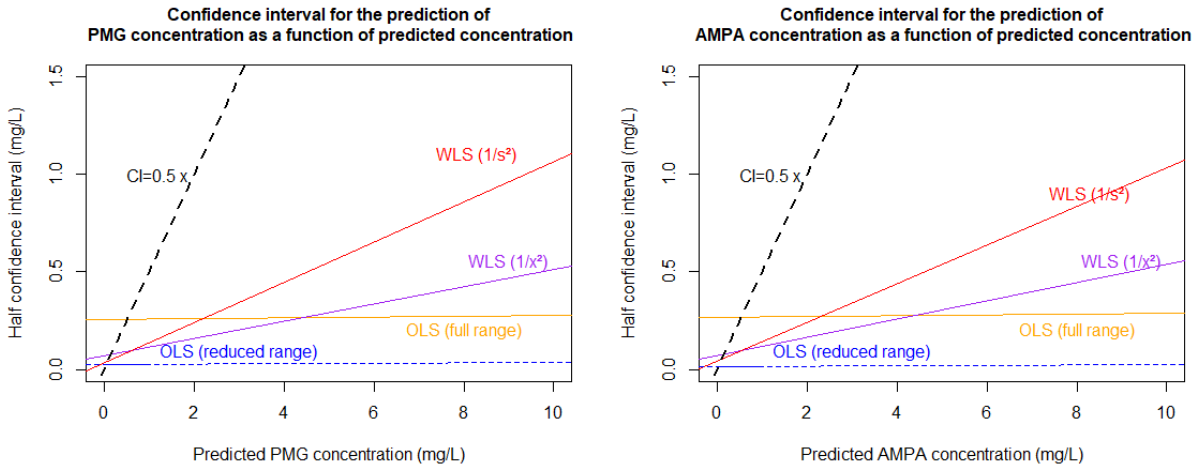

Figure 30 : Value of the half confidence intervals for inverse prediction for the discussed least squares models.

The confidence interval of all models lies below the maximum expanded uncertainty of 50 % recommended in SANTE/12682/2019 guidelines.

As intended, the accuracy of each WLS model increases when the concentration decreases. As said earlier, the more weight is given to lower concentration, the less biased the model is (i.e. the smaller is the intercept).

The model calibrated on the reduced range (0.08–1 mg/L) was the most accurate and least biased of all. Even though it does not cover the MRL of sugar beet (15 mg/kg or ~7 mg/$L_{extract}$), the sample can easily be diluted with blank sugar beet extract.

Although the confidence interval of the WLS model with the weight $1/s_y^2$ is narrower than the one of the WLS model with the weight $1/y^2$, this last one does not require any replicate to be calibrated, contrary to the first which needs at least three replicates in order to calculate s_y^2.

5.4.3. Reproducibility

As it can be seen in Figure 31, the regression coefficient of calibration curves prepared and measured independently on different days are significantly different. It can also be noted that, when compared to each other, interday variations of PMG and AMPA are not related. This indicate that these variations are not likely attributable to mishandling during the preparation of calibration curves or mobile phases.

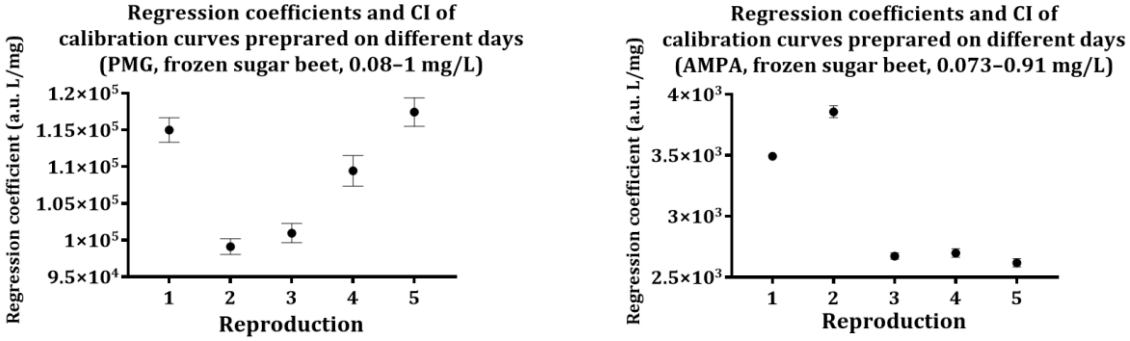

Figure 31 : Regression coefficients and confidence interval of calibration curves for PMG and AMPA prepared on different days.

These results also point out that a given calibration curve can not reliably be used to quantify samples analysed on a different day, i.e. samples must always be analysed along with a calibration curve.

5.4.4. Recovery assessment

Table 23 : Recovery of PMG and AMPA in frozen sugar beet extract.

Sample mass (g)	Compound	Spiked concentration (mg/kg)	Calculated recovery (%)[a]		
			OLS PMG : $y = 1.264 \times 10^4\ x$ AMPA : $y = 2.552 \times 10^3\ x$	**WLS 1/x** PMG : $y = 1.208 \times 10^4\ x$ AMPA : $y = 2.581 \times 10^3\ x$	**WLS $1/s^2$** PMG : $y = 1.237 \times 10^4\ x$ AMPA : $y = 2.992 \times 10^3\ x$
7.984 ± 0.04	PMG	0.21	68.7 ± 13.1	67.8 ± 14.1	70.2 ± 13.4
	AMPA	0.19	63.0 ± 13.7	62.3 ± 13.5	65.5 ± 14.2
7.984 ± 0.04	PMG	2.1	73.4 ± 12.9	72.5 ± 14.0	75.0 ± 13.2
	AMPA	1.9	79.7 ± 12.5	78.8 ± 12.4	82.8 ± 13.0

(a) : none of the intercept of the regression curves were significant ($P > .80$) and were thus not included in the calculation of recovery.

Although the relative standard deviation is below 15 % for both analytes, their mean recoveries at the lowest concentration of the calibration curve (0.1 mg/L PMG and 0.091 mg/L AMPA) are slightly below the acceptable recovery range of 70–110 %. At ten times the lowest concentration of the calibration curve (1 mg/L PMG and 0.91 mg/L AMPA), the mean recoveries and relative standard deviations are acceptable.

Accordingly to the SANTE/12682/2019 guidelines, a correction for recovery should be applied to the results obtained with this method. Ideally, the recovery on each point of the calibration curve should be measured in order to determine whether it significantly vary across the calibration range.

5.4.5. LOD and LOQ calculation

Table 24 : Calculated LODs and LOQ for PMG and AMPA in Frozen sugar beet (OLS, untransformed data only).

Data origin	PMG (n = 3)			AMPA (n = 3)		
	Slope (mg/kg a.u)	LOD (mg/L)	LOQ (mg/L)	Slope (mg/kg a.u)	LOD (mg/kg)	LOQ (mg/kg)
Linearity assessment (0.1–10 mg/L)	2.83×10^4	0.09	0.2	2.88×10^3	0.07	0.2
Reproducibility (day 1)	1.15×10^5	0.01	0.03	3.49×10^3	0.02	0.07
Reproducibility (day 2)	9.91×10^4	0.03	0.09	3.86×10^3	0.03	0.1
Reproducibility (day 3)	1.01×10^5	0.02	0.06	2.67×10^3	0.7	2
Reproducibility (day 4)	1.09×10^5	0.03	0.09	2.70×10^3	0.07	0.2
Reproducibility (day 5)	1.17×10^5	0.03	0.09	2.62×10^3	0.03	0.1

Table 24 gives the LODs and LOQs in mg/kg sugar beet root calculated using the slope and recovery (at the lower concentration) of the OLS model (untransformed data). The LODs and LOQs expressed in mg/L extract are shown in Annex 27 for information. The LOQs are much below the MRL of PMG and AMPA in sugar beet (15 mg/kg of PMG equivalent), allowing a reliable verification of the compliance with the MRL.

5.4.6. Stability assessment

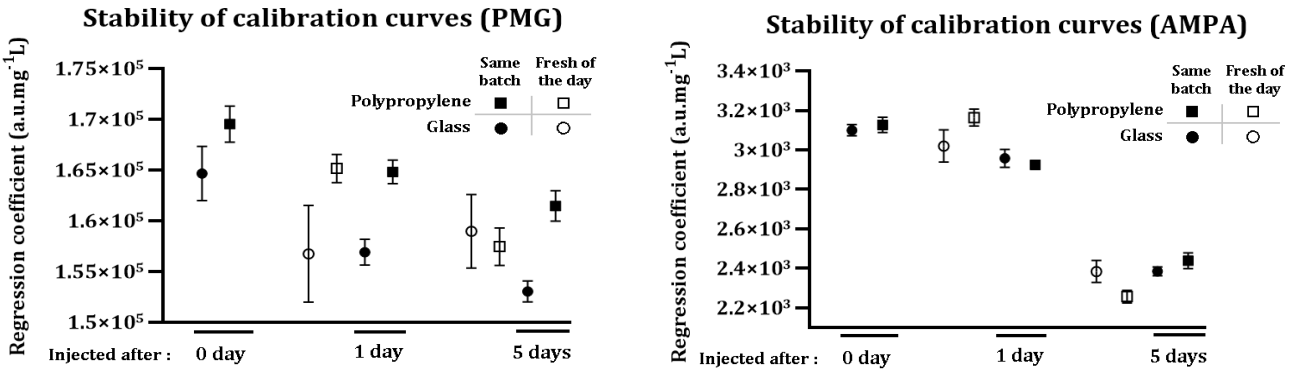

Figure 32 : Stability assessment of calibration curves after one and five days of storage at 5°C (whiskers represent 95 % confidence intervals).

Before any interpretation, it must be reminded that only the replicates of the fresh calibration curve in glass (white dots) were prepared independently. Other replicates are the same exact solution measured from different vials. This gives a rough estimation of the variability attributable to the instrument on consecutive measurement of the same solution and variability attributable to automatic pipettes.

Interestingly and accordingly with the precedent test, the effect of vial material was not unanimously significant. It is hypothesized that vial material do have an impact, but too low to be unequivocally confirmed. Also, when looking at the wider confidence interval of regression coefficient from curves calibrated from replicates prepared independently (white dots), it can be assumed that the variability between glass and polypropylene (PP) vials (variability between groups) is comparable to the variability attributable to the automatic pipettes arising when preparing replicates of the curves independently (at least during the first 24 hours in the vial).

The evolution of the regression coefficient with time is unclear : for PMG, it decreased in glass vials and increased in PP vials; while for AMPA, it was unchanged in glass vials and also increased in PP vials (although it was lower the day before). It is hypothesized that several phenomena such as evaporation and adsorption on glass are simultaneously at stake through time.

From these results, it can be assumed that the calibration curve can be stored at 5°C during at least one day without practically impairing the trueness of the measurement. It can also be mentioned that the extract contains enough methanol to prevent freezing at -18°C, thus stability may be improved by storing the calibration solutions at -18°C.

5.5. Considerations on PMG and AMPA determination in soil and water

Initially, the validation of a method for the determination of PMG and AMPA in soil and water using a BEH phenyl column (130 Å, 1.7 µm, 2.1 mm × 100 mm, more details in Annex 23) and based on the derivatization procedure proposed by the manufacturer[98] was intended. Unfortunately, due to independent circumstances[99] and technical issues (system overpressure), this could not be achieved in time.

However, it was learned from different preliminary testing (results not shown) that :

- Accordingly with the literature reviewed (Annex 18), alkaline conditions and free phosphate ions allow to desorb the analytes from soil by reducing outer-sphere interaction and through ion exchange (competition for adsorption sites) respectively. It was found that trisodium or tripotassium phosphate (K_3PO_4 (pk_a = 12.4) and Na_3PO_4 (pk_a = 11.77)) were also effective.

- Due to the harsh alkalinity required for soil extraction, the Anionic Polar Pesticide column was unfit for PMG and AMPA analysis from soil (maximum operating pH : 7). Instead, the derivatization method using FMOC-Cl proposed with the BEH phenyl column is performed in borate buffer (pH = 9) and the column is able to operate in the pH range 1–12, which better suits the extraction conditions and also allow to reach higher sensitivity, but at the expense of cost and time.

- The Anionic Polar Pesticide column did not allow to reach sufficient sensitivity to quantify PMG and AMPA at the MRL in drinking water (0.1 µg/L) or environmental water (i.e. Environmental quality standards set as part of the Water Framework Directive in force in United Kingdom (196 µg/L), France and Germany (28 µg/L)). However, it was estimated that a near-hundredfold concentration of the sample along with an increased injection volume should allow to reach a sufficient sensitivity to include the MRL of 0.1 µg/L in the lowest points of a calibration curve. Such a concentration could be achieved using rotary evaporator with a silanised flask or solid phase extraction. Despite their low throughput, these solutions are cheap and suited for occasional analysis of PMG and AMPA in water.

These elements give several clues on potential uses of the BEH phenyl column.

---

[98] Waters corporation, available at https://www.waters.com/webassets/cms/library/docs/720006246en.pdf (15/07/2020)

[99] Namely, the national-wide confinement imposed as a measure to fight the covid-19 pandemic

6. Conclusions and recommendations

This work successfully established a validated method for the direct determination of PMG and AMPA in sugar beet root using the HILIC Anionic Polar Pesticide (diethylamine) column, in the calibration range 0.2–3 mg/kg of sugar beet for both PMG and AMPA, noticeably below the MRL of 15 mg/kg in sugar beet. The method is expected to be adapted for the determination of other anionic polar pesticides such as glufosinate in sugar beet as well as in other matrices of plant origin with minor modifications to the sample preparation, accordingly with the QuPPe-PO method from the EURL-SRM.

The validated method does not require isotope-labelled internal standard and only takes about three to four hours to complete (homogenization of sample, preparation of mobiles phases and system priming included). One run takes only ten minutes. Excluding the cost of the common equipment and the instrumentation, the running cost of the analysis is low as it only requires a few disposable plastic tubes, syringes and syringe-filters and no specific reactants.

It was shown that isotope labelled PMG (1,2-$^{13}C_2$ ^{15}N-PMG) used as internal standard successfully compensate for matrix effect (and presumably recovery) for PMG but not for AMPA. Isotope labelled AMPA must also be used if one wants to use the isotope labelled internal standard approach, which was unnecessary for sugar beet mut might be required for other oleaginous or proteaginous matrices with low water content such as soy and maize.

As it is often the case in liquid chromatography, the reproducibility assessment indicated that the calibration curves are not valid for quantification of samples injected a different day, supposedly because of the detector random interday variations. Calibration must thus be performed along with each analysed set of samples. Still, calibration solutions were demonstrated to be stable for at least one day at 5°C. Further testing is required to verify stability beyond two days of storage at 5°C. The stability may be extended by storing at -18°C, as the extract contain enough methanol to prevent freezing.

The different effects of glass and polypropylene vials in the validated calibration range were unclear. Nevertheless, the potential difference between the two vial materials was deemed negligible in the validated calibration range and was estimated to be comparable to the variation between independent replicates in repeatability conditions. It may be more important at lower concentrations. Anyhow, the current method satisfied validation requirements using glass vials.

Unfortunately, the lockdown implemented between end of March and early May 2020 as a measure to fight the covid-19 pandemic as well as technical issues did not allow to validate methods in water and soil. However, from preliminary testing, it is considered that the quantification of glyphosate and AMPA in soil is most likely more adequate using derivatisation with FMOC-Cl and a phenyl column rather than a diethylamine HILIC column; while a reliable underivatized quantification in environmental water with the used diethylamine HILIC column and MS/MS instrumentation would require a concentration factor of at least 80–100 (using either evaporation or SPE).

7. References

Alibhai M.F. & Stallings W.C., 2001. Closing down on glyphosate inhibition - With a new structure for drug discovery. Proc. Natl. Acad. Sci. U. S. A. 98(6), 2944–2946.

Al-Rajab A.J. & Schiavon M., 2010. Degradation of 14C-glyphosate and aminomethylphosphonic acid (AMPA) in three agricultural soils. J. Environ. Sci. 22(9), 1374–1380.

Amrhein N., Schab J. & Steinrücken H.C., 1980. The mode of action of the herbicide glyphosate. Naturwissenschaften 67(7), 356–357.

Anastassiades M., Lehotay S.J. & Stajnbaher D., 2003. Quick, Easy, Cheap, Effective, Rugged, and Safe (QuEChERS) approach for the determination of pesticide residues. 18th Annu. Waste Test. Qual. Assur. Symp. WTQA 2002 - Proc. (January), 231–241.

AOAC International, 1998. Official Methods of Analysis of AOAC International, 16th Edition, 4th Revision, Volume I.

Armbruster D., Müller U. & Happel O., 2019. Characterization of phosphonate-based antiscalants used in drinking water treatment plants by anion-exchange chromatography coupled to electrospray ionization time-of-flight mass spectrometry and inductively coupled plasma mass spectrometry. J. Chromatogr. A 1601, 189–204.

Assalin M.R., de Moraes S.G., Queiroz S.C.N., Ferracini V.L. & Duran N., 2010. Studies on degradation of glyphosate by several oxidative chemical processes: Ozonation, photolysis and heterogeneous photocatalysis. J. Environ. Sci. Heal. - Part B Pestic. Food Contam. Agric. Wastes 45(1), 89–94.

Barja B.C. & Dos Santos Afonso M., 1998. An ATR-FTIR study of glyphosate and its Fe(III) complex in aqueous solution. Environ. Sci. Technol. 32(21), 3331–3335.

Barker A.L. & Dayan F.E., 2019. Fate of Glyphosate during Production and Processing of Glyphosate-Resistant Sugar Beet (Beta vulgaris). J. Agric. Food Chem. 67(7), 2061–2065.

Battaglin W.A., Meyer M.T., Kuivila K.M. & Dietze J.E., 2014. Glyphosate and its degradation product AMPA occur frequently and widely in U.S. soils, surface water, groundwater, and precipitation. J. Am. Water Resour. Assoc. 50(2), 275–290.

Bennett R.M., Phipps R.H. & Strange A.M., 2006. An Application of Life-Cycle Assessment for environmental planning and management: The potential environmental and human health impacts of growing genetically-modified herbicide-tolerant sugar beet. J. Environ. Plan. Manag. 49(1), 59–74.

Bergström L., Börjesson E. & Stenström J., 2011. Laboratory and Lysimeter Studies of Glyphosate and Aminomethylphosphonic Acid in a Sand and a Clay Soil. J. Environ. Qual. 40(1), 98–108.

Boocock M.R. & Coggins J.R., 1983. Kinetics of 5-enolpyruvylshikimate-3-phosphate synthase inhibition by glyphosate. FEBS Lett. 154(1), 127–133.

Borggaard O.K. & Gimsing A.L., 2008. Fate of glyphosate in soil and the possibility of leaching to ground and surface waters: a review. Pest Manag. Sci. 63(11), 1100–1106.

Botero-Coy A.M., Ibáñez M., Sancho J. V. & Hernández F., 2013. Improvements in the analytical methodology for the residue determination of the herbicide glyphosate in soils by liquid chromatography coupled to mass spectrometry. J. Chromatogr. A 1292, 132–141.

Botta F., Lavison G., Couturier G., Alliot F., Moreau-Guigon E., Fauchon N., Guery B., Chevreuil M. & Blanchoud H., 2009. Transfer of glyphosate and its degradate AMPA to surface waters through urban sewerage systems. Chemosphere 77(1), 133–139.

Bradberry S.M., Proudfoot A.T. & Vale J.A., 2004. Glyphosate poisoning. Toxicol. Rev. 23(3), 159–167.

Bradshaw L.D., Padgette S.R., Kimball S.L. & Wells B.H., 2013. Mini-Review / Commentary Perspectives on Glyphosate Resistance ’. Weed Sci. Soc. Am. 11(1), 189–198.

Brady N.C., Weil R.R, 2008. Nature and Properties of Soils The, 14th Edition. 14th ed. Upper Saddle River, N.J., Pearson/Prentice Hall.

Brito I.P.F.S., Tropaldi L., Carbonari C.A. & Velini E.D., 2018. Hormetic effects of glyphosate on plants. Pest Manag. Sci. 74(5), 1064–1070.

Buszewski B. & Noga S., 2012. Hydrophilic interaction liquid chromatography (HILIC)-a powerful separation technique. Anal. Bioanal. Chem. 402(1), 231–247.

Camenzuli M., Goodie T.A., Bassanese D.N., Francis P.S., Barnett N.W., Ritchie H., Ladine J., Shalliker R.A. & Conlan X.A., 2012. The use of parallel segmented outlet flow columns for enhanced mass spectral sensitivity at high chromatographic flow rates. Rapid Commun. Mass Spectrom. 26(8), 943–949.

Candela L., Caballero J. & Ronen D., 2010. Glyphosate transport through weathered granite soils under irrigated and non-irrigated conditions - Barcelona, Spain. Sci. Total Environ. 408(12), 2509–2516.

Cao L., Ma D., Zhou Z., Xu C., Cao C., Zhao P. & Huang Q., 2019. Efficient photocatalytic degradation of herbicide glyphosate in water by magnetically separable and recyclable BiOBr/Fe3O4 nanocomposites under visible light irradiation. Chem. Eng. J. 368, 212–222.

Castle L.A., Siehl D.L., Gorton R., Patten P.A., Chen Y.H., Bertain S., Cho H.J., Duck N., Wong J., Liu D. & Lassner M.W., 2004. Discovery and directed evolution of a glyphosate tolerance gene. Science (80-.). 304(5674), 1151–1154.

Catrinck T.C.P.G., Dias A., Aguiar M.C.S., Silvério F.O., Fidêncio P.H. & Pinho G.P., 2014. A simple and efficient method for derivatization of glyphosate and AMPA using 9-fluorenylmethyl chloroformate and spectrophotometric analysis. J. Braz. Chem. Soc. 25(7), 1194–1199.

Chamberlain K., Evans A.A. & Bromilow R.H., 1996. 1-Octanol/Water Partition Coefficient (K ow) and pK a for Ionisable Pesticides Measured by apH-Metric Method . Pestic. Sci. 47(3), 265–271.

Chamkasem N. & Harmon T., 2016. Direct determination of glyphosate, glufosinate, and AMPA in soybean and corn by liquid chromatography/tandem mass spectrometry. Anal. Bioanal. Chem. 408(18), 4995–5004.

Chen Y., Wu F., Lin Y., Deng N., Bazhin N. & Glebov E., 2007a. Photodegradation of glyphosate in the ferrioxalate system. J. Hazard. Mater. 148(1–2), 360–365.

Chen Y., Wu F., Zhang X., Deng N., Bazhin N. & Glebov E., 2007b. Fe(III)-pyruvate and Fe(III)-citrate induced photodegradation of glyphosate in aqueous solutions. J. Coord. Chem. 60(22), 2431–2439.

Colombo S. de M. & Masini J.C., 2011. Developing a fluorimetric sequential injection methodology to study adsorption/desorption of glyphosate on soil and sediment samples. Microchem. J. 98(2), 260–266.

Coupland D. & Peabody D. V, 2016. Absorption , Translocation , and Exudation of Glyphosate , Fosamine , and Amitrole in Field Horsetail (Equisetum arvense) l. Weed Sci. Soc. Am. 29(5), 556–560.

Craven C.B., Joyce C.W. & Lucy C.A., 2019. Effect of nature of electrolytes on retention and selectivity in hydrophilic interaction liquid chromatography. J. Chromatogr. A 1584, 80–86.

Demidenko E., Williams B.B., Flood A.B. & Swartz H.M., 2013. Relationship : Approximate and Exact Statistical Inference. Stat Med 32(12), 2048–2061.

Dill G.M., Sammons R.D., Feng P.C.C., Kohn F., Kretzmer K., Mehrsheikh A., Bleeke M. Honegger J.L., Farmer D., Wright D. Haupfear E.A., 2010. Glyphosate: Discovery, Development, Applications, and Properties. In : Nandula V.K., ed., Glyphosate Resistance in Crops and Weeds: History, Development, and Management, 1st ed., John Wiley & Sons, Inc. pp. 1-33.

Draycott A.P.,, 2006. Weeds and Weed Control. In: Draycott A.P., ed., Sugar Beet, 1st ed. Oxford, UK: Blackwell Publishing Ltd. pp. 1-8.

Duke S.O., 2011. Glyphosate degradation in glyphosate-resistant and -susceptible crops and weeds. J. Agric. Food Chem. 59(11), 5835–5841.

Eker S., Ozturk L., Yazici A., Erenoglu B., Romheld V. & Cakmak I., 2006. Foliar-applied glyphosate substantially reduced uptake and transport of iron and manganese in sunflower (Helianthus annuus L.) plants. J. Agric. Food Chem. 54(26), 10019–10025.

Erban T., Stehlik M., Sopko B., Markovic M., Seifrtova M., Halesova T. & Kovaricek P., 2018. The different behaviors of glyphosate and AMPA in compost-amended soil. Chemosphere 207, 78–83.

European Union Reference Laboratories for Residues of Pesticides - Single Residue Method, 2020. Quick Method for the Analysis of Numerous Highly Polar Pesticides in Food Involving Extraction with Acidified Methanol and LC MS/MS Measurement - I. Food of Plant Origin (QuPPe PO Method). By Anastassiades M., Kolberg D. I., Eichhorn E., Wachtler A.-K., Benkenstein A., Zechmann S., Mack D., Wildgrube C., Barth A., Sigalov I., Görlich S., Dörk D., Cerchia G.

European Commission, 2017. Commission Implementing Regulation (EU) 2017/2324 of 12 December 2017 renewing the approval of the active substance glyphosate in accordance with Regulation (EC) No 1107/2009 of the European Parliament and of the Council concerning the placing of plant protection products on the market, and amending the Annex to Commission Implementing Regulation (EU) No 540/2011 (Text with EEA relevance.). Official journal of the European Union. NoL 333, 15.12.2017, p. 10–16.

European Commission, Directorate-General for Health and Food Safety, 2020. Analytical quality control and method validation procedures for pesticide residues analysis in food and feed.

European Commission, 2000. Directive 2000/60/EC of the European Parliament and of the Council of 23 October 2000 establishing a framework for Community action in the field of water policy. Official journal of the European Union. No L 327, 22.12.2000, p. 1–73, as last amended by Commission Directive 2014/101/EU.

European Commission, 2001. Commission Directive 2001/99/EC of 20 November 2001 amending Annex I to Council Directive 91/414/EEC concerning the placing of plant protection products on the market to include glyphosate and thifensulfuron-methyl as active substances. Official journal of the European Union. No L 304, 21.11.2001, p. 14–16

European Commission, 2017. Commission Implementing Regulation (EU) 2017/2324 of 12 December 2017 renewing the approval of the active substance glyphosate in accordance with Regulation (EC) No 1107/2009 of the European Parliament and of the Council concerning the placing of plant protection products on the market, and amending the Annex to Commission Implementing Regulation (EU) No 540/2011. Official journal of the European Union. No L 333, 15.12.2017, p. 10–16.

European Food Safety Authority (EFSA), 2006. Opinion of the Scientific Panel on Genetically Modified Organisms on an application (reference EFSA-GMO-UK-2004-08) for the placing on the market of products produced from glyphosate-tolerant genetically modified sugar beet H7-1, for food and feed uses, under Regulation 9EC) No1829/2003 from KWS SAAT and Monsanto, The EFSA Journal (2006) 431, 1-18.

European Food Safety Authority (EFSA), 2015a. Conclusion on the peer review of the pesticide risk assessment of the active substance glyphosate. EFSA Journal 2015;13(11):4302, 107 pp.

European Food Safety Authority (EFSA), 2015b. Statement of EFSA on the request for the evaluation of the toxicological assessment of the co-formulant POE-tallowamine. EFSA Journal 2015;13(11):4303, 13 pp.

European Food Safety Authority (EFSA), 2017. Conclusion on the peer review of the pesticide risk assessment of the potential endocrine disrupting properties of glyphosate. EFSA Journal 2017;15(9):4979, 20 pp.

European Food Safety Authority (EFSA), 2018a. Reasoned Opinion on the review of the existing maximum residue levels for glyphosate according to Article 12 of Regulation (EC) No 396/2005. EFSA Journal 2018;16(5):5263, 230 pp.

European Food Safety Authority (EFSA), 2018. Scientific Report on evaluation of the impact of glyphosate and its residues in feed on animal health. EFSA Journal 2018;16(5):5283, 22 pp.

European Food Safety Authority (EFSA), 2019. Review of the existing maximum residue levels for glyphosate according to Article 12 of Regulation (EC) No 396/2005 – revised version to take into account omitted data. EFSA Journal 2019;17(10):5862, 211 pp.

Feng D., Malleret L., Soric A. & Boutin O., 2020. Kinetic study of glyphosate degradation in wet air oxidation conditions. Chemosphere 247, 125930.

Feng P.C.C., Ryerse J.S., Jones C.R. & Sammons R.D., 1999. Analysis of surfactant leaf damage using microscopy and its relation to glyphosate or deuterium oxide uptake in velvetleaf (Abutilon theophrasti) . Pestic. Sci. 55(3), 385–386.

Feng P.C.C., Chiu T., Sammons R.D. & Ryerse J.S., 2003. Droplet size affects glyphosate retention, absorption, and translocation in corn. Weed Sci. 51(3), 443–448.

Feng P.C.C., Sandbrink J.J. & Sammons R.D., 2000. Retention, Uptake, and Translocation of 14 C-Glyphosate from Track-Spray Applications and Correlation to Rainfastness in Velvetleaf (Abutilon theophrasti) 1 . Weed Technol. 14(1), 127–132.

Food and Agriculture Organization of the United Nations, 2009. Agribusiness handbook : Sugar beet, White Sugar.

Food and Agriculture Organization of the United Nations, 2016. FAO specifications and evaluations for agricultural pesticides - Glyphosate - N-(phosphonomethyl)glycine

Food and Agriculture Organization of the United Nations, World Health Organisation, 1986. Pesticide residues in food - 1986. Report of the Joint Meeting of the FAO Panel of Experts on Pesticide Residues in Food and the Environment and a WHO Expert Group on Pesticide Residues. FAO Plant Production and Protection Paper 77, 1986.

Food and Agriculture Organization of the United Nations, World Health Organisation, 1997. Pesticide residues in food - 1996. Report of the Joint Meeting of the FAO Panel of Experts on Pesticide Residues in Food and the Environment and the WHO Core Assessment Group. FAO Plant Production and Protection Paper, 140, 1997.

Food and Agriculture Organization of the United States, World Health Organization, 2004. Pesticide residues in food - 2004. Report of the Joint Meeting of the FAO Panel of Experts on Pesticide Residues in Food and the Environment and the WHO Core Assessment Group. FAO Plant Production and Protection Paper, 178, 2004.

Food and Agriculture Organization of the United Nations, World Health Organisation, 2005.Pesticide residues in food - 2005. Report of the Joint Meeting of the FAO Panel of Experts on Pesticide Residues in Food and the Environment and the WHO Core Assessment Group. FAO Plant Production and Protection Paper, 183, 2005.

Food and Agriculture Organization of the United States, World Health Organization, 2011. Pesticide residues in food - 2011. Report of the Joint Meeting of the FAO Panel of Experts on Pesticide Residues in Food and the Environment and the WHO Core Assessment Group. FAO Plant Production and Protection Paper, 211, 2011.

Food and Agriculture Organization of the United States, World Health Organization, 2016. Pesticide residues in food - 2016. Report of the Joint Meeting of the FAO Panel of Experts on Pesticide Residues in Food and the Environment and the WHO Core Assessment Group.FAO Plant Production and Protection Paper, 227, 2016.

Forlani G., Mangiagalli A., Nielsen E. & Suardi C.M., 1999. Degradation of the phosphonate herbicide glyphosate in soil: Evidence for a possible involvement of unculturable microorganisms. Soil Biol. Biochem. 31(7), 991–997.

Gasperi J., Zgheib S., Cladière M., Rocher V., Moilleron R. & Chebbo G., 2012. Priority pollutants in urban stormwater: Part 2 - Case of combined sewers. Water Res. 46(20), 6693–6703.

Geiger D.R., Kapitan S.W. & Tucci M.A., 1986. Glyphosate Inhibits Photosynthesis and Allocation of Carbon to Starch in Sugar Beet Leaves. Plant Physiol. 82(2), 468–472.

Ghassemi M., Fargo L., Painter P., Quinlivan S., Scofield R. & Takata A., 1981. Environmental Fates and impacts of major forest use pesticides, Environmental Protection Agency, 501.

Grandcoin A., Piel S. & Baurès E., 2017. AminoMethylPhosphonic acid (AMPA) in natural waters: Its sources, behavior and environmental fate. Water Res. 117, 187–197.

Gresshoff P., 1979. Growth Inhibition by Glyphosate and Reversal of Its Action by Phenylalanine and Tyrosine. Funct. Plant Biol. 6(2), 177.

Guo H., Riter L.S., Wujcik C.E. & Armstrong D.W., 2016. Direct and sensitive determination of glyphosate and aminomethylphosphonic acid in environmental water samples by high performance liquid chromatography coupled to electrospray tandem mass spectrometry. J. Chromatogr. A 1443, 93–100.

Haag W.R. & Yao D.C.C., 1992. Rate Constants for Reaction of Hydroxyl Radicals with Several Drinking Water Contaminants. Environ. Sci. Technol. 26(5), 1005–1013.

Harland J.I., Jones C.K., Hufford C., 2006. Weeds and Weed Control. In: Draycott A.P., ed., Sugar Beet, 1st ed. Oxford, UK: Blackwell Publishing Ltd. pp. 443-463.

Hawes C., Haughton A.J., Osborne J.L., Roy D.B., Clark S.J., Perry J.N., Rothery P., Bohan D.A., Brooks D.R., Champion G.T., Dewar A.M., Heard M.S., Woiwod I.P., Daniels R.E., Young M.W., Parish A.M., Scott R.J., Firbank L.G. & Squire G.R., 2003. Responses of plants and invertebrate trophic groups to contrasting herbicide regimes in the Farm Scale Evaluations of genetically modified herbicide-tolerant crops. Philos. Trans. R. Soc. B Biol. Sci. 358(1439), 1899–1913.

Heap I. & Duke S.O., 2018. Overview of glyphosate-resistant weeds worldwide. Pest Manag. Sci. 74(5), 1040–1049.

Heaton J.C., Russell J.J., Underwood T., Boughtflower R. & McCalley D. V., 2014. Comparison of peak shape in hydrophilic interaction chromatography using acidic salt buffers and simple acid solutions. J. Chromatogr. A 1347, 39–48.

Heredia A., 2003. Biophysical and biochemical characteristics of cutin, a plant barrier biopolymer. Biochim. Biophys. Acta - Gen. Subj. 1620(1–3), 1–7.

Hess F.D. & Foy C.L., 2000. Interaction of Surfactants with Plant Cuticles 1 . Weed Technol. 14(4), 807–813.

Hetherington P.R., Reynolds T.L., Marshall G. & Kirkwood R.C., 1999. The absorption, translocation and distribution of the herbicide glyphosate in maize expressing the CP-4 transgene. J. Exp. Bot. 50(339), 1567–1576.

Holländer H. & Amrhein N., 1980. The Site of the Inhibition of the Shikimate Pathway by Glyphosate. Plant Physiol. 66(5), 823–829.

Holtschulte B., Korbel G. & Miller M., 2011. Nutrient deficiencies in glyphosate-resistant sugar beets.

Hove-Jensen B., Zechel D.L. & Jochimsen B., 2014. Utilization of Glyphosate as Phosphate Source: Biochemistry and Genetics of Bacterial Carbon-Phosphorus Lyase. Microbiol. Mol. Biol. Rev. 78(1), 176–197.

Huang X., He J., Yan X., Hong Q., Chen K., He Q., Zhang L., Liu X., Chuang S., Li S. & Jiang J., 2017. Microbial catabolism of chemical herbicides: Microbial resources, metabolic pathways and catabolic genes. Pestic. Biochem. Physiol. 143(October 2019), 272–297.

Ibáñez M., Pozo Ó.J., Sancho J. V., López F.J. & Hernández F., 2005. Residue determination of glyphosate, glufosinate and aminomethylphosphonic acid in water and soil samples by liquid chromatography coupled to electrospray tandem mass spectrometry. J. Chromatogr. A 1081(2), 145–155.

Institut de Santé Publique (ISP), 2010. Dosage quantitatif du glyphosate et de son métabolite dans les aliments d'origine végétale par UPLC-MS/MS. SOP 22/F/1251. Belgium.

International Agency for Research on Cancer (IARC) of the World Health Organization, 2015. IARC Monographs Volume 112: some organophosphate insecticides and herbicides. IARC monographs on the evaluation of carcinogenic risks to humans, 112, 2015.

International Program on Chemical Safety of the Whorld Health Organization, 1994. Environmental Health criteria 159 - Glyphosate.

Jakimska A., Kot-Wasik A. & Namieśnik J., 2014. The Current State-of-the-Art in the Determination of Pharmaceutical Residues in Environmental Matrices Using Hyphenated Techniques. Crit. Rev. Anal. Chem. 44(3), 277–298.

Jaworski E.G., 1972. Mode of Action of N-Phosphonomethylglycine: Inhibition of Aromatic Amino Acid Biosynthesis. J. Agric. Food Chem. 20(6), 1195–1198.

Kaliannan P., Mohamed Naseer Ali M., Seethalakshmi T. & Venuvanalingam P., 2002. Electronic structure and conformation of glyphosate: An ab initio MO study. J. Mol. Struct. THEOCHEM 618(1–2), 117–125.

Kanissery R.G., Welsh A. & Sims G.K., 2015. Effect of Soil Aeration and Phosphate Addition on the Microbial Bioavailability of Carbon-14-Glyphosate. J. Environ. Qual. 44(1), 137–144.

Kudzin M.H., Zylla R., Mrozinska Z. & Urbaniak P., 2019. 31 P NMR investigations on roundup degradation by AOP procedures. Water (Switzerland) 11(2).

Lesueur C., Pfeffer M. & Fuerhacker M., 2005. Photodegradation of phosphonates in water. Chemosphere 59(5), 685–691.

Li H., Wallace A.F., Sun M., Reardon P. & Jaisi D.P., 2018. Degradation of Glyphosate by Mn-Oxide May Bypass Sarcosine and Form Glycine Directly after C-N Bond Cleavage. Environ. Sci. Technol. 52(3), 1109–1117.

Liao Y., Berthion J.M., Colet I., Merlo M., Nougadère A. & Hu R., 2018. Validation and application of analytical method for glyphosate and glufosinate in foods by liquid chromatography-tandem mass spectrometry. J. Chromatogr. A 1549, 31–38.

Lund-HØie K. & Friestad H.O., 1986. Photodegradation of the herbicide glyphosate in water. Bull. Environ. Contam. Toxicol. 36(1), 723–729.

Luo J., Wei S., Su Y., Chen X. & Wan Y., 2009. Desalination and recovery of iminodiacetic acid (IDA) from its sodium chloride mixtures by nanofiltration. J. Memb. Sci. 342(1–2), 35–41.

Maqueda C., Undabeytia T., Villaverde J. & Morillo E., 2017. Behaviour of glyphosate in a reservoir and the surrounding agricultural soils. Sci. Total Environ. 593–594, 787–795.

May M.J. & Wilson R.G., 2006. Weeds and Weed Control. In: Draycott A.P., ed., Sugar Beet, 1st ed. Oxford, UK: Blackwell Publishing Ltd. pp. 359-386.

Mercurio P., Flores F., Mueller J.F., Carter S. & Negri A.P., 2014. Glyphosate persistence in seawater. Mar. Pollut. Bull. 85(2), 385–390.

Miles C.J. & Anson Moye H., 1988. Extraction of Glyphosate Herbicide from Soil and Clay Minerals and Determination of Residues in Soils. J. Agric. Food Chem. 36(3), 486–491.

Mogusu E.O., Wolbert J.B., Kujawinski D.M., Jochmann M.A. & Elsner M., 2015. Dual element (15N/14N, 13C/12C) isotope analysis of glyphosate and AMPA by derivatization-gas chromatography isotope ratio mass spectrometry (GC/IRMS) combined with LC/IRMS. Anal. Bioanal. Chem. 407(18), 5249–5260.

Morillo E., Maqueda C. & Recursos I. De, 1997. Adsorption of Glyphosate on the Clay Mineral Montmorillonite: Effect of Cu(II) in Solution and Adsorbed on the Mineral 31(12), 3588–3592.

Morishita D.W., 2018. Impact of glyphosate-resistant sugar beet. Pest Manag. Sci. 74(5), 1050–1053.

Motta E.V.S., Raymann K. & Moran N.A., 2018. Glyphosate perturbs the gut microbiota of honey bees. Proc. Natl. Acad. Sci. U. S. A. 115(41), 10305–10310.

Muskus A.M., Krauss M., Miltner A., Hamer U. & Nowak K.M., 2019. Effect of temperature, pH and total organic carbon variations on microbial turnover of 13C315N-glyphosate in agricultural soil. Sci. Total Environ. 658, 697–707.

Napoli M., Cecchi S., Zanchi C.A. & Orlandini S., 2015. Leaching of Glyphosate and Aminomethylphosphonic Acid through Silty Clay Soil Columns under Outdoor Conditions. J. Environ. Qual. 44(5), 1667–1673.

Nip M., Tegelaar E.W., de Leeuw J.W. & Schenck P.A., 1986. A New Non-saponifiable Highly Aliphatic and Resistant Biopolymer in. Naturwlssenschaften (73), 579 585.

Nobel P.S., 2009. Plants and Fluxes. Physicochem. Environ. Plant Physiol. 438–505.

Nowack B., 2003. Environmental chemistry of phosphonates. Water Res. 37(11), 2533–2546.

Okada E., Costa J.L. & Bedmar F., 2016. Adsorption and mobility of glyphosate in different soils under no-till and conventional tillage. Geoderma 263, 78–85.

Parker P.A., Wilson G.G.V., Sara R.W., Szarka III J.L. & Johnson N.G., n.d. The Prediction Properties of Inverse and Reverse Regression for the Simple Linear Calibration Problem, 21.

Paternoster R., Brame R., Mazerolle P. & Piquero A., 1998. Using the correct statistical test for the equality of regression coefficients. Criminology 36(4), 859–866.

Peixoto M.M., Bauerfeldt G.F., Herbst M.H., Pereira M.S. & Da Silva C.O., 2015. Study of the stepwise deprotonation reactions of glyphosate and the corresponding p K a values in aqueous solution. J. Phys. Chem. A 119(21), 5241–5249.

Piccolo A.; Celano G., 1994. Hydrogen-Bonding Interactions Between the Herbicide. Environ. Toxicol. Chem. 13(11), 1737–1741.

Piccolo A., Celano G. & Conte P., 1996. Adsorption of Glyphosate by Humic Substances. J. Agric. Food Chem. 44(8), 2442–2446.

Piccolo A., Celano G. & Pietramellara G., 1992. Adsorption of the herbicide glyphosate on a metal-humic acid complex. Sci. Total Environ. 123–124(C), 77–82.

Piccolo A., Celano G. & Arienzo M., 2008. Journal of Environmental Science and Health , Part B : Pesticides , Food Contaminants , and Agricultural Wastes Adsorption and desorption of glyphosate in some European soils (August 2013), 1105–1115.

Pline-Srnic W., 2006. Physiological Mechanisms of Glyphosate Resistance. Weed Technol. 20(2), 290–300.

Portier C.J., Armstrong B.K., Baguley B.C., Baur X., Belyaev I., Bellé R., Belpoggi F., Biggeri A., Bosland M.C., Bruzzi P., Budnik L.T., Bugge M.D., Burns K., Calaf G.M., Carpenter D.O., Carpenter H.M., López-Carrillo L., Clapp R., Cocco P., Consonni D., Comba P., Craft E., Dalvie M.A., Davis D., Demers P.A., De Roos A.J., DeWitt J., Forastiere F., Freedman J.H., Fritschi L., Gaus C., Gohlke J.M., Goldberg M., Greiser E., Hansen J., Hardell L., Hauptmann M., Huang W., Huff J., James M.O., Jameson C.W., Kortenkamp A., Kopp-Schneider A., Kromhout H., Larramendy M.L., Landrigan P.J., Lash L.H., Leszczynski D., Lynch C.F., Magnani C., Mandrioli D., Martin F.L., Merler E., Michelozzi P., Miligi L., Miller A.B., Mirabelli D., Mirer F.E., Naidoo S., Perry M.J., Petronio M.G., Pirastu R., Portier R.J., Ramos K.S., Robertson L.W., Rodriguez T., Röösli M., Ross M.K., Roy D., Rusyn I., Saldiva P., Sass J., Savolainen K., Scheepers P.T.J., Sergi C., Silbergeld E.K., Smith M.T., Stewart B.W., Sutton P., Tateo F., Terracini B., Thielmann H.W., Thomas D.B., Vainio H., Vena J.E., Vineis P., Weiderpass E., Weisenburger D.D., Woodruff T.J., Yorifuji T., Yu I.J., Zambon P., Zeeb H. & Zhou S.F., 2016. Differences in the carcinogenic evaluation of glyphosate between the international agency for research on cancer (IARC) and the european food safety authority (EFSA). J. Epidemiol. Community Health 70(8), 741–745.

Rampazzo N., Todorovic G.R., Mentler A. & Blum W.E.H., 2013. Adsorption of glyphosate and aminomethylphosphonic acid in soils. Int. Agrophysics 27(2), 203–209.

Rodrigues J.J. V., Worsham A.D. & Corbin F.T., 2017. Exudation of Glyphosate from Wheat (Triticum aestivum) Plants and Its Effects on Interplanted Com (Zea mays) and Soybeans (Glycine max). Weed Sci. 30, 316–320.

Rubin J.L., Gaines C.G. & Jensen R.A., 1984. Glyphosate Inhibition of 5-Enolpyruvylshikimate 3-Phosphate Synthase from Suspension-Cultured Cells of Nicotiana silvestris . Plant Physiol. 75(3), 839–845.

Rubio F., Veldhuis L.J., Clegg B.S., Fleeker J.R. & Hall J.C., 2003. Comparison of a direct ELISA and an HPLC method for glyphosate determinations in water. J. Agric. Food Chem. 51(3), 691–696.

Rueppel M.L., Brightwell B.B., Schaefer J. & Marvel J.T., 1977. Metabolism and Degradation of Glyphosate in Soil and Water. J. Agric. Food Chem. 25(3), 517–528.

Ryerse J.S., Downer R.A., Sammons R.D. & Feng P.C.C., 2004. Effect of glyphosate spray droplets on leaf cytology in velvetleaf (Abutilon theophrasti) . Weed Sci. 52(2), 302–309.

Sammons R.D. & Gaines T.A., 2014. Glyphosate resistance: State of knowledge. Pest Manag. Sci. 70(9), 1367–1377.

Schönbrunn E., Eschenburg S., Shuttleworth W.A., Schloss J. V., Amrhein N., Evans J.N.S. & Kabsch W., 2001. Interaction of the herbicide glyphosate with its target enzyme 5-enolpyruvylshikimate 3-phosphate synthase in atomic detail. Proc. Natl. Acad. Sci. U. S. A. 98(4), 1376–1380.

Shen J., Huang J., Liu L., Ye W., Lin J. & Van der Bruggen B., 2013. The use of BMED for glyphosate recovery from glyphosate neutralization liquor in view of zero discharge. J. Hazard. Mater. 260, 660–667.

Shen J., Huang J., Ruan H., Wang J. & Van der Bruggen B., 2014. Techno-economic analysis of resource recovery of glyphosate liquor by membrane technology. Desalination 342, 118–125.

Shrikant B.R. & Khambete A.K., 2014. Case Studies for Organophosphate Pesticides Treatment. Int. Res. J. Eng. Technol. 2(3), 1596–1599.

Shuttleworth W.A., Pohl M.E., Helms G.L., Jakeman D.L. & Evans J.N.S., 1999. Site-directed mutagenesis of putative active site residues of 5- enolpyruvylshikimate-3-phosphate synthase. Biochemistry 38(1), 296–302.

Sidoli P., Baran N. & Angulo-Jaramillo R., 2016. Glyphosate and AMPA adsorption in soils: laboratory experiments and pedotransfer rules. Environ. Sci. Pollut. Res. 23(6), 5733–5742.

Silva V., Mol H.G.J., Zomer P., Tienstra M., Ritsema C.J. & Geissen V., 2019. Pesticide residues in European agricultural soils – A hidden reality unfolded. Sci. Total Environ. 653(November), 1532–1545.

Silva V., Montanarella L., Jones A., Fernández-Ugalde O., Mol H.G.J., Ritsema C.J. & Geissen V., 2018. Distribution of glyphosate and aminomethylphosphonic acid (AMPA) in agricultural topsoils of the European Union. Sci. Total Environ. 621, 1352–1359.

Simonsen L., Fomsgaard I.S., Svensmark B. & Spliid N.H., 2008. Fate and availability of glyphosate and AMPA in agricultural soil. J. Environ. Sci. Heal. - Part B Pestic. Food Contam. Agric. Wastes 43(5), 365–375.

Sprankle P., Meggit W.F. & Penner D., 1975. Adsorption, mobility, and microbial degradation of glyphosate in the soil. Weed Sci. v. 23(3), 229–234.

Steinrucken H.C. & Amrhein, N. 1980. The herbicide glyphosate is a potent inhibitor of 5- enolpyruvylshikimic acid-3-phosphate synthase. Biochem. Biophys. Res. Commun. 94, 1207– 1212.

Sun L., Kong D., Gu W., Guo X., Tao W., Shan Z., Wang Y. & Wang N., 2017. Determination of glyphosate in soil/sludge by high performance liquid chromatography. J. Chromatogr. A 1502, 8–13.

Sun M., Li H. & Jaisi D.P., 2019. Degradation of glyphosate and bioavailability of phosphorus derived from glyphosate in a soil-water system. Water Res. 163, 114840.

Sun M., Li H. & Jaisi D.P., 2019. Degradation of glyphosate and bioavailability of phosphorus derived from glyphosate in a soil-water system. Water Res. 163, 114840.

Sviridov A. V., Shushkova T. V., Ermakova I.T., Ivanova E. V., Epiktetov D.O. & Leontievsky A.A., 2015. Microbial degradation of glyphosate herbicides (review). Appl. Biochem. Microbiol. 51(2), 188–195.

Székács A. & Darvas B. (2012) Forty years with glyphosate. In: Herbicides – Properties, Synthesis and Control of Weeds (Hasaneen, M. N. A. E.-G., Ed.), InTech, Rijeka, Croatia, pp. 247-284.

Tofallis C., 2011. Least Squares Percentage Regression. SSRN Electron. J. (May 2009).

Torstensson L., Börjesson E. & Stenström J., 2005. Efficacy and fate of glyphosate on Swedish railway embankments. Pest Manag. Sci. 61(9), 881–886.

Travlos I., Cheimona N. & Bilalis D., 2017. Glyphosate efficacy of different salt formulations and adjuvant additives on various weeds. Agronomy 7(3).

Turner D.J. & Loader M.P.C., 1980. Effect of ammonium sulphate and other additives upon the phytotoxicity of glyphosate to Agropyron repens (L.) Beauv. Weed Res. 20(3), 139–146.

Tzin V. & Galili G., 2010. The Biosynthetic Pathways for Shikimate and Aromatic Amino Acids in Arabidopsis thaliana . Arab. B. 8(May 2014), e0132.

U.S. Department of Labor, Occupational Safety and Health Administration, 1989. Glyphosate, sampling and analytical method [PV2067].

U.S. Environmental Protection Agency, 1990. Determination of glyphosate in drinking water by direct-aqueous injection hplc, post-column derivatization, and fluorescence detection.

U.S. Environmental Protection Agency, 1994. TOUCHDOWN® : Determination of GLYPHOSATE and AMINOMETHYLPHOSPHONIC ACID in Soil by Gas Chromatography and Mass Selective Detection. By P.L. Alferness.

U.S. Environmental Protection Agency, Office of Pesticide Programs, 2016. Glyphosate Issue Paper: Evaluation of Carcinogenic Potential. Avilable at

U.S. Food and Drug Administration, 2016. Direct Determination of Glyphosate, Glufosinate, and AMPA in milk by Liquid chromatography/tandem mass spectrometry. By Chamkasem N., Morris C. & Hargrove K.L. Laboratory Information Bulletin 4595.

U.S. Food and Drug Administration, 2016. Direct Determination of Glyphosate, Glufosinate, and AMPA in Soybean and Corn by Liquid chromatography/tandem mass spectrometry. By Chamkasem N., Morris C. & Hargrove K.L. Laboratory Information Bulletin 4596.

U.S. Food and Drug Administration, 2016. Direct determination of glyphosate, glufosinate, and aminomethylphosphonic acid (AMPA) in egg by liquid chromatography/tandem mass spectrometry. By Chamkasem N., Morris C. & Hargrove K.L. Laboratory Information Bulletin 4604.

U.S. Geological Survey Organic Geochemistry Research Group, 2001. Methods of Analysis by the U.S.G.S. Organic Geochemistry Research Group:Determination of Glyphosate, Aminomethylphosphonic Acid, and Glufosinate in Water Using Online Solid-Phase Extraction and High-P. By Lee, E.A., Strahan, A.P., and Thurman, E.M.

Vereecken H., 2005. Mobility and leaching of glyphosate: A review. Pest Manag. Sci. 61(12), 1139–1151.

Wang P., Zhang G. & Wu Y., 2015. Diffusion dialysis for separating acidic HCl/glyphosate liquor. Sep. Purif. Technol. 141, 387–393.

Wang Y., Ai F., Ng S.C. & Tan T.T.Y., 2012. Sub-2μm porous silica materials for enhanced separation performance in liquid chromatography. J. Chromatogr. A 1228, 99–109.

Waters corporation, 2010. Comprehensive Guide to HILIC: Hydrophilic Interaction Chromatography. By Grumbach E.S. and Fountain K.J. Milford, Mass : Waters Corportaion,

West C., Elfakir C. & Lafosse M., 2010. Porous graphitic carbon: A versatile stationary phase for liquid chromatography. J. Chromatogr. A 1217(19), 3201–3216.

Williams G.M., Kroes R. & Munro I.C., 2000. Safety evaluation and risk assessment of the herbicide Roundup and its active ingredient, glyphosate, for humans. Regul. Toxicol. Pharmacol. 31(2 I), 117–165.

Woodburn A.T., 2000. Glyphosate: Production, pricing and use worldwide. Pest Manag. Sci. 56(4), 309–312.

Xie M. & Xu Y., 2011. Partial desalination and concentration of glyphosate liquor by nanofiltration. J. Hazard. Mater. 186(1), 960–964.

Xu X., Ji F., Fan Z. & He L., 2011. Degradation of glyphosate in soil photocatalyzed by Fe3O4/SiO2/TiO2 under solar light. Int. J. Environ. Res. Public Health 8(4), 1258–1270.

Yang X., Wang F., Bento C.P.M., Xue S., Gai L., van Dam R., Mol H., Ritsema C.J. & Geissen V., 2015. Short-term transport of glyphosate with erosion in Chinese loess soil - A flume experiment. Sci. Total Environ. 512–513, 406–414.

Yang Y., Deng Q., Yan W., Jing C. & Zhang Y., 2018. Comparative study of glyphosate removal on goethite and magnetite: Adsorption and photo-degradation. Chem. Eng. J. 352, 581–589.

Yao D.C.C. & Haag W.R., 1991. Rate constants for direct reactions of ozone with several drinking water contaminants. Water Res. 25(7), 761–773.

Zgheib S., Moilleron R. & Chebbo G., 2012. Priority pollutants in urban stormwater: Part 1 - Case of separate storm sewers. Water Res. 46(20), 6683–6692.